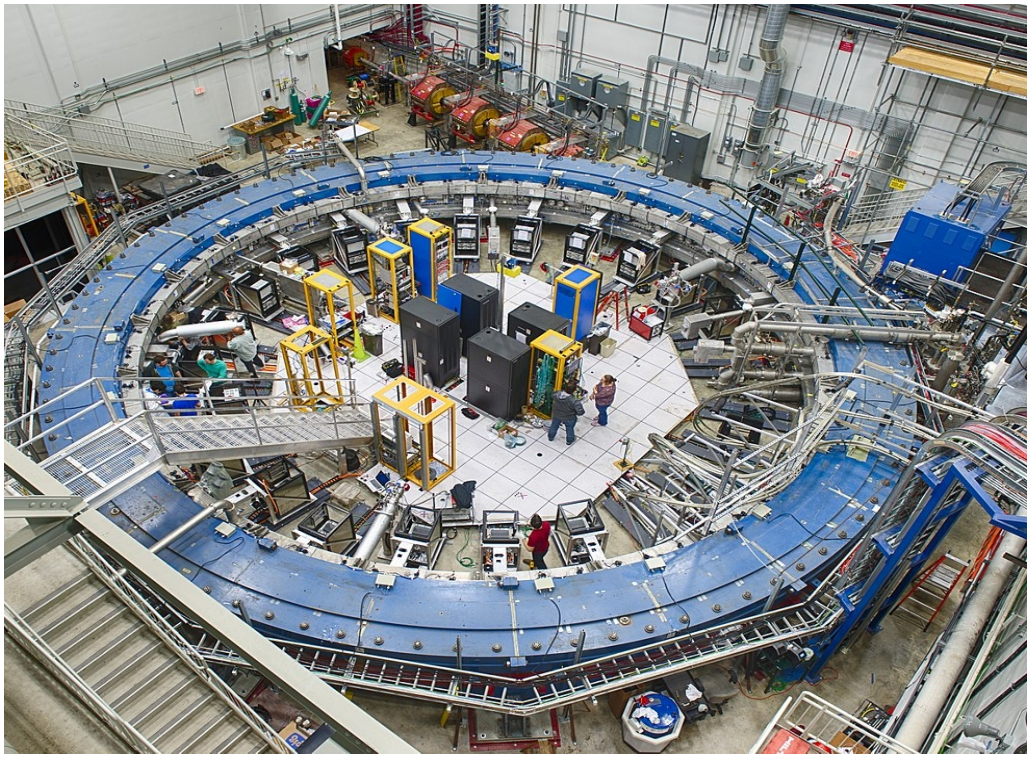

Latest results from the Muon g-2 Experiment at Fermilab

26th international symposium on spin physics
(SPIN2025)

26 Sep 2025

Paolo Girotti (INFN - LNF)
on behalf of the Muon g-2 collaboration

Overview

The Muon g-2

Experimental principles

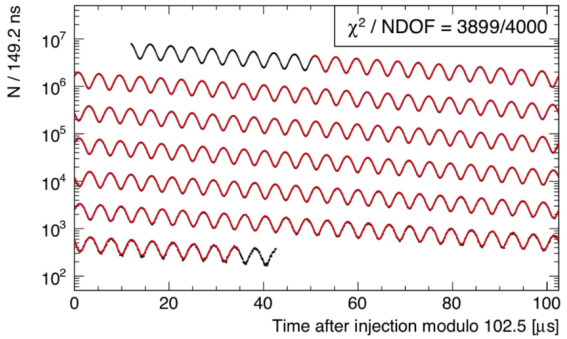

The Muon g-2 Experiment at Fermilab

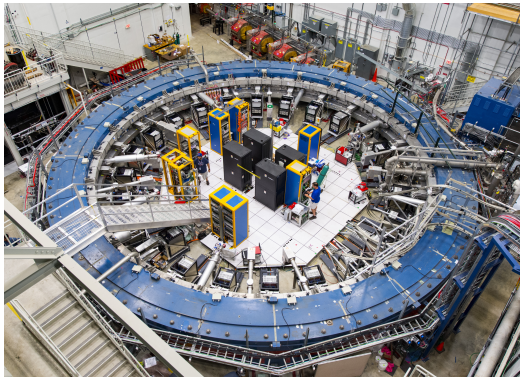

Latest results and overlook

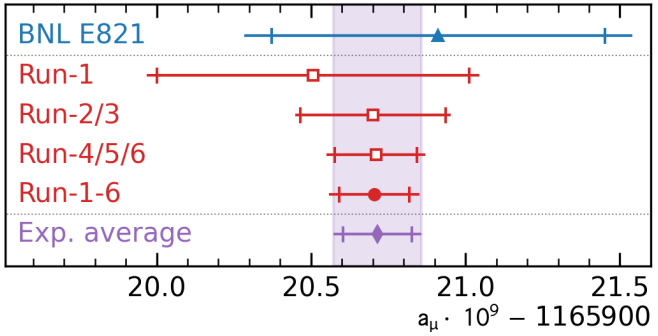

Overview

The Muon g-2

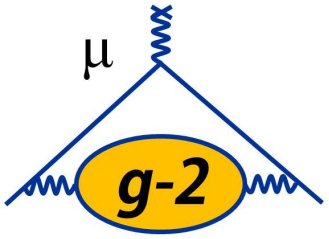

Experimental principles

The Muon g-2 Experiment at Fermilab

Latest results and overlook

The muon g-2

$$\vec{\mu} = g\frac{q}{2m}\vec{S}$$

- The magnetic moment of the muon is proportional to the g-factor
- **g** encodes all the possible virtual interactions between the muon and the magnetic field
  - With no virtual quantum interactions, **g=2**

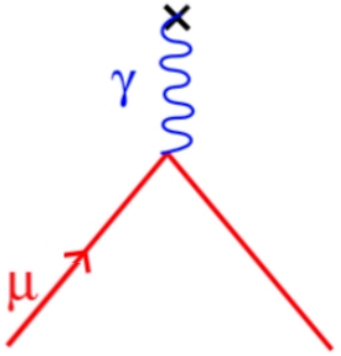

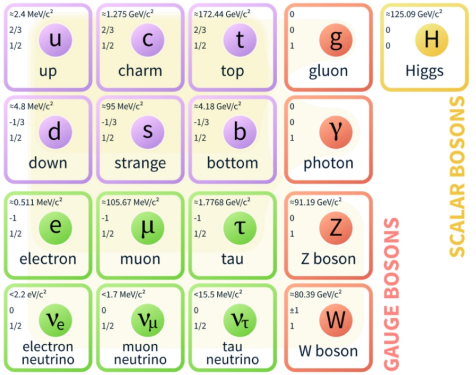

The muon g-2

$$\vec{\mu} = g\frac{q}{2m}\vec{S}$$

- The magnetic moment of the muon is proportional to the g-factor
- **g** encodes all the possible virtual interactions between the muon and the magnetic field
  - With no virtual quantum interactions, **g=2**
  - Considering the entire Standard Model, **g=2.002331...**

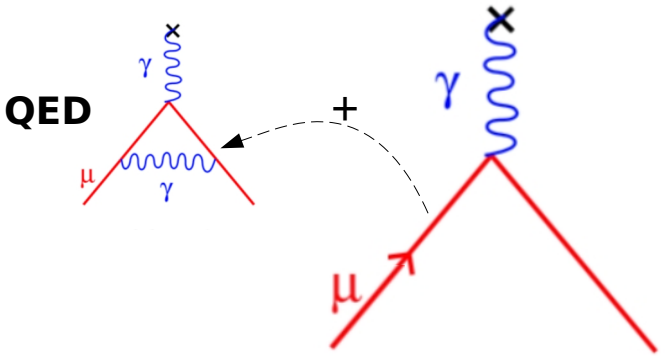

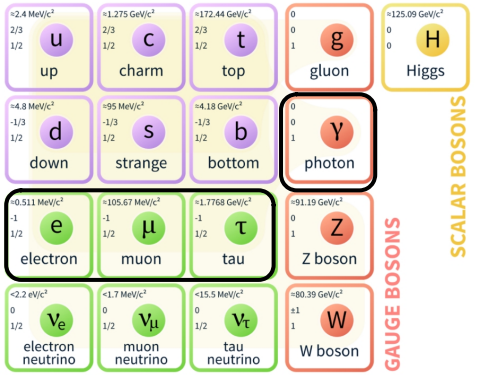

The muon g-2

$$\vec{\mu} = g\frac{q}{2m}\vec{S}$$

- The magnetic moment of the muon is proportional to the g-factor
- **g** encodes all the possible virtual interactions between the muon and the magnetic field
  - With no virtual quantum interactions, **g=2**
  - Considering the entire Standard Model, **g=2.00233183...**

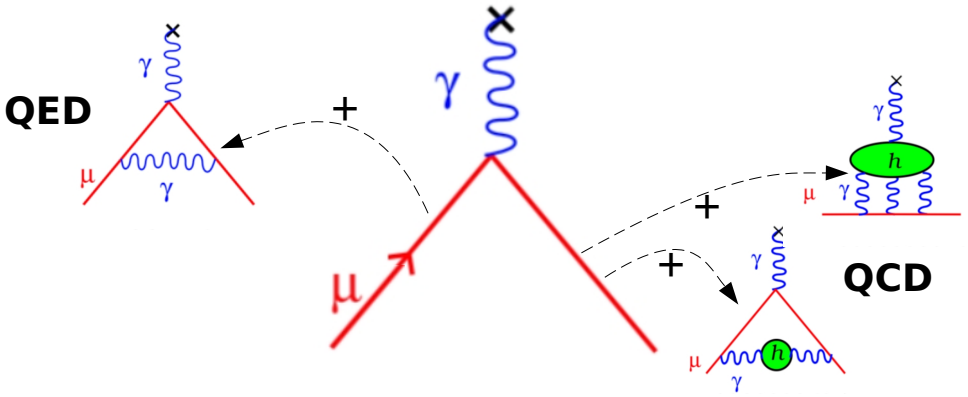

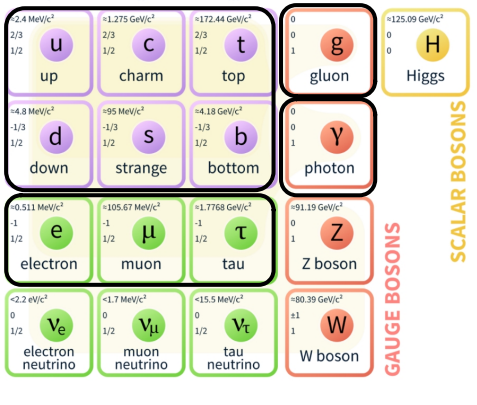

The muon g-2

$$\vec{\mu} = g\frac{q}{2m}\vec{S}$$

- The magnetic moment of the muon is proportional to the g-factor
- **g** encodes all the possible virtual interactions between the muon and the magnetic field
  - With no virtual quantum interactions, **g=2**
  - Considering the entire Standard Model, **g=2.00233183620(86)**

Aoyama et al. (2020)
https://doi.org/10.1016/j.physrep.2020.07.006

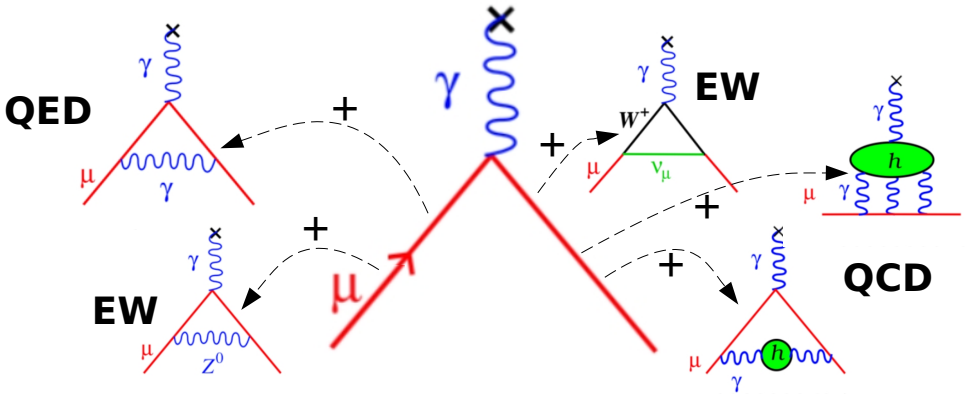

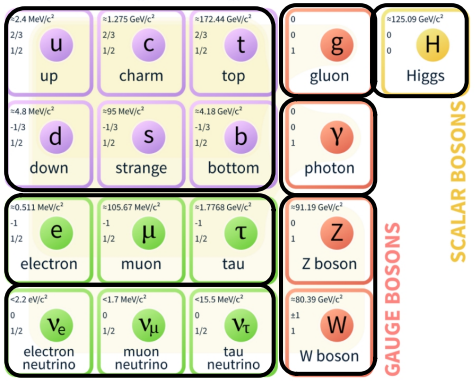

The muon g-2

$$\vec{\mu} = g\frac{q}{2m}\vec{S}$$

- The magnetic moment of the muon is proportional to the g-factor
- **g** encodes all the possible virtual interactions between the muon and the magnetic field
  - With no virtual quantum interactions, **g=2**
  - Considering the entire Standard Model, **g=2.00233183620(86)**
  - Is there something else?

Aoyama et al. (2020)
https://doi.org/10.1016/j.physrep.2020.07.006

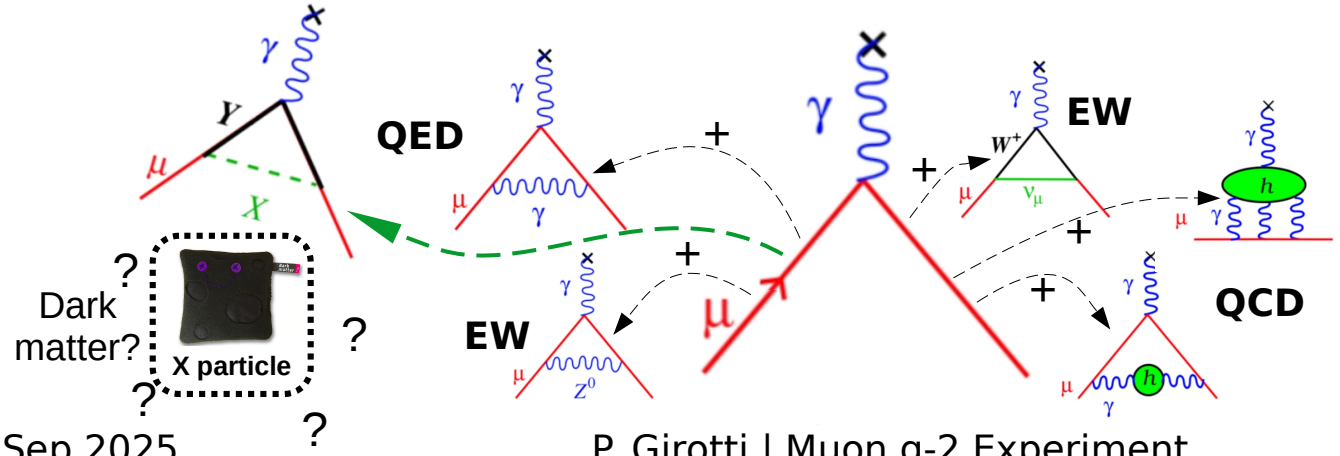

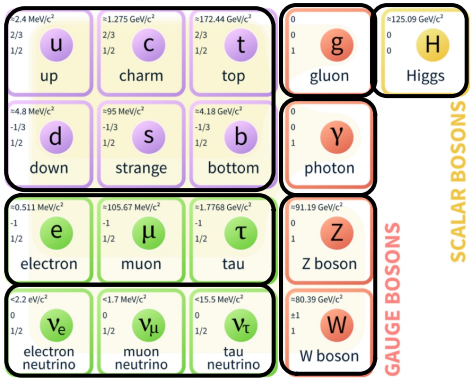

SM contributions

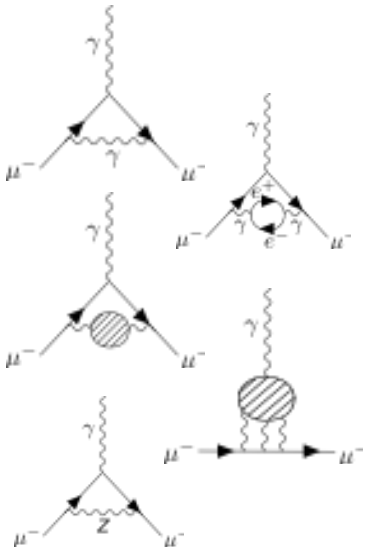

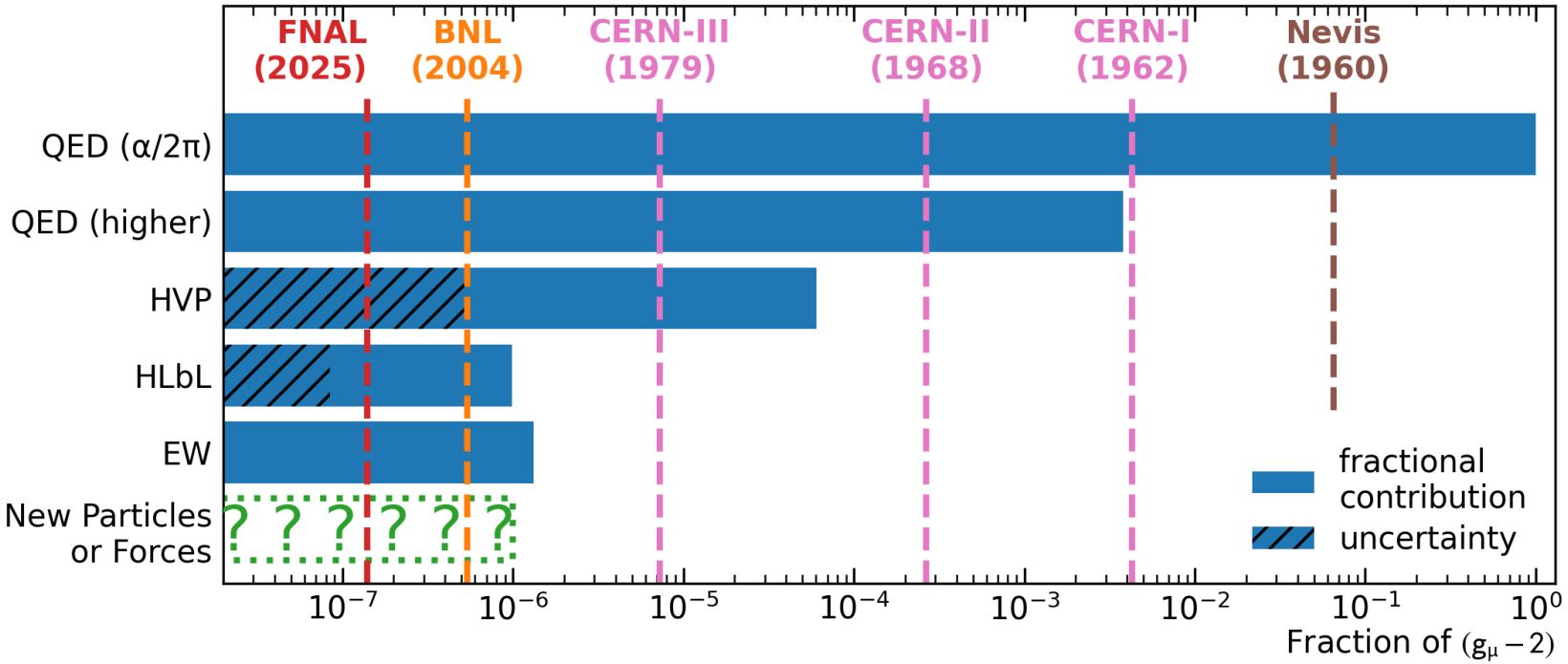

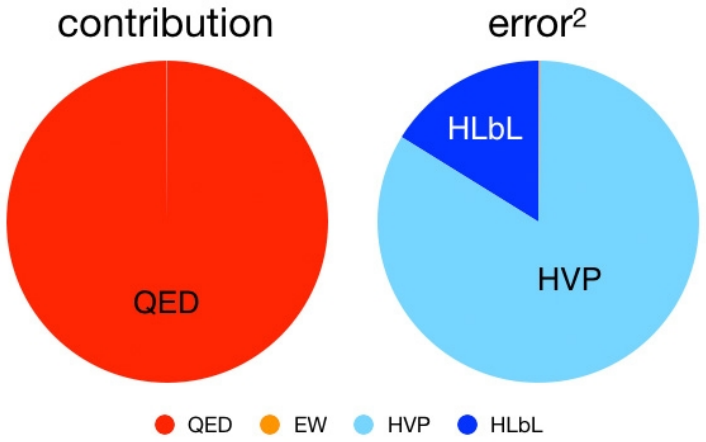

QCD loops account for:
- **0.006%** of the contribution
- **99.95%** of the uncertainty

Yes but why muons?

- Elementary fermion
  - Higher mass than electron → enhanced sensitivity to new heavy particles
- Series of “gifts” from nature facilitate experiments:
  - Pion decay produces highly polarized muons → **polarizer**
  - Decay $e^{+/-}$ encodes the muon’s spin information → **polarimeter**
  - Magic momentum of 3.1 GeV/c cancels effects from external electric fields
- Long enough lifetime to be stored and measured
- Many measurements and calculations since the ‘50s
  - Still a very active research topic

BNL measurement

- 2006 → Tantalizing hint of new physics at 3.7σ!
- 2009 → proposal to build new experiment at Fermilab by recycling BNL's magnet

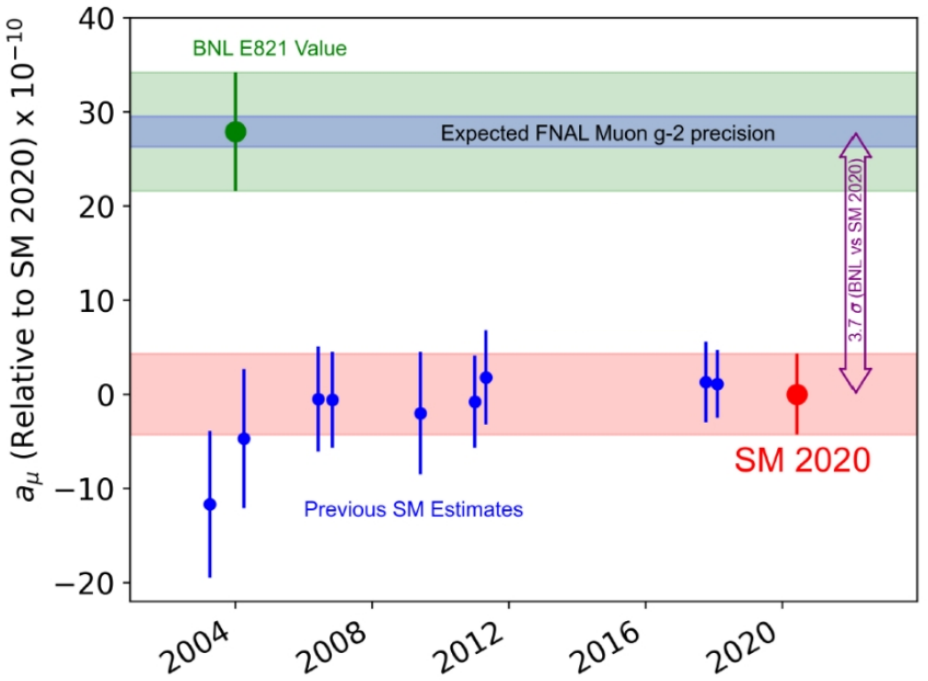

The big move

- 50 ton package shipped from Brookhaven (BNL) to Fermilab (FNAL) on the summer of 2013
- **35 days** and 5000+ km on water and land

FNAL (2013-2025)

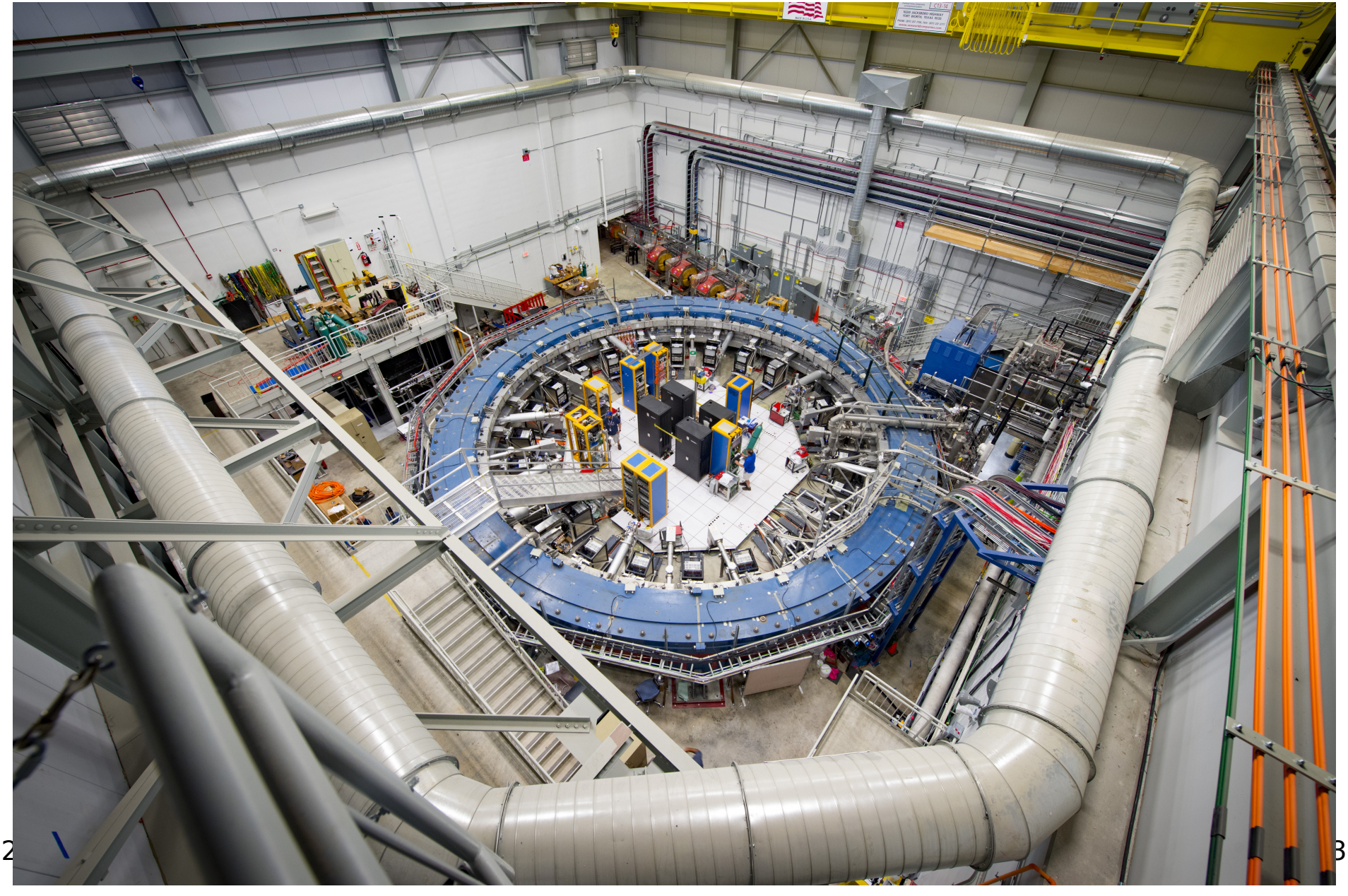

Six years of beam data

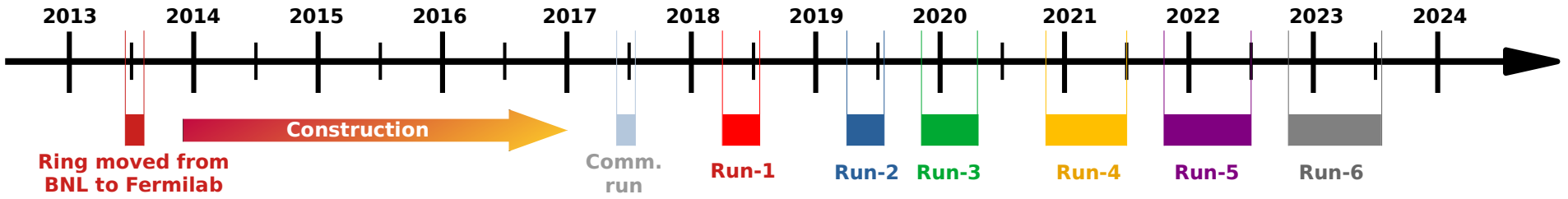

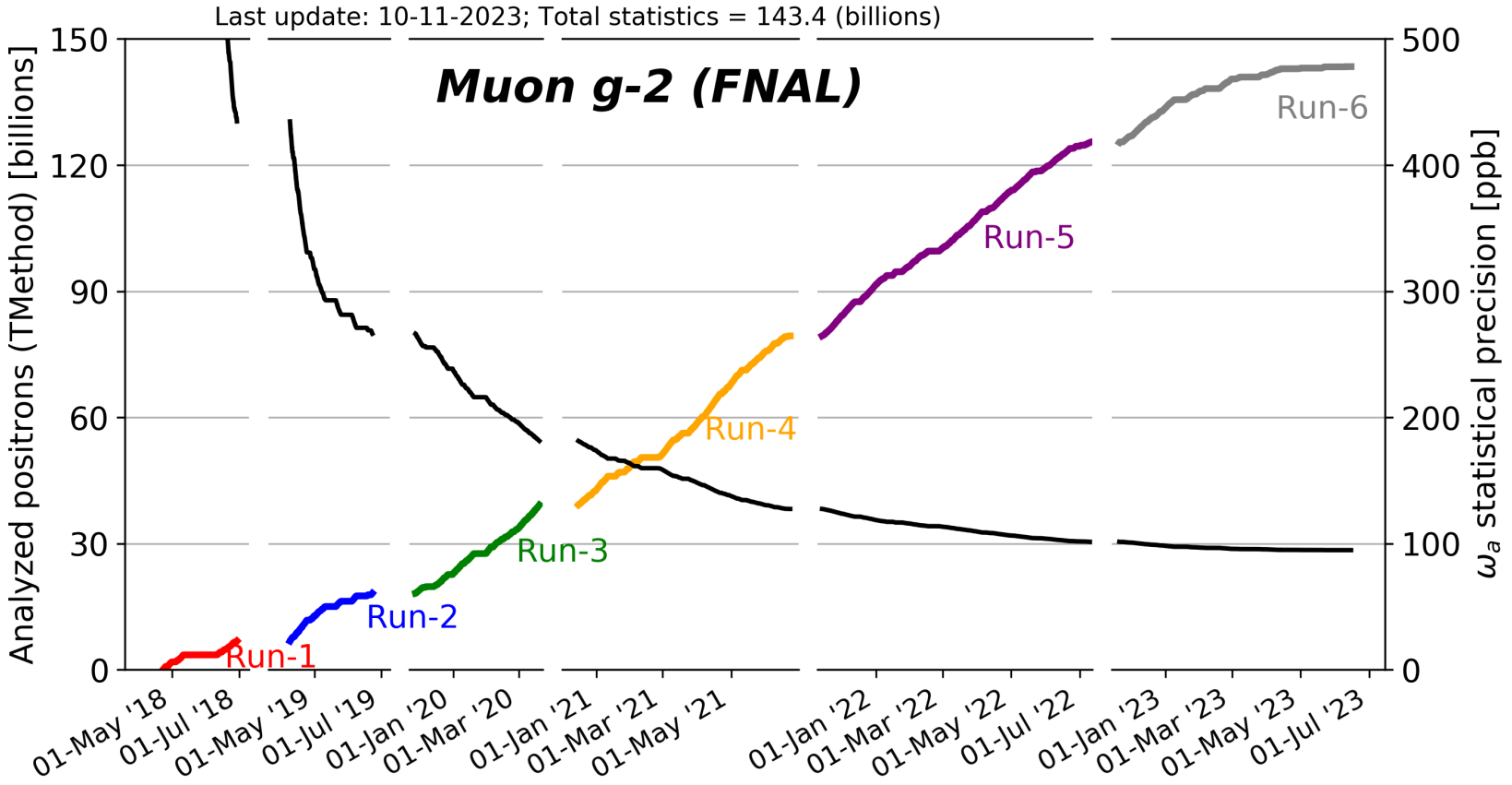

Overview

The Muon g-2

Experimental principles

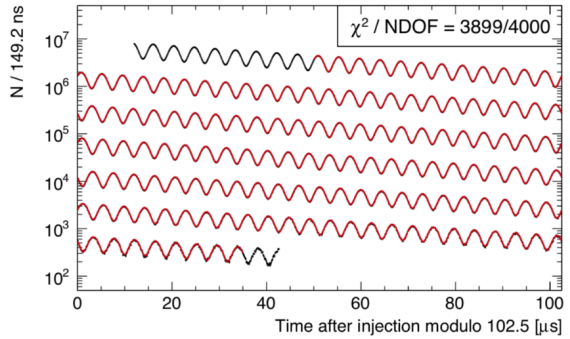

The Muon g-2 Experiment at Fermilab

Latest results and overlook

Experimental principle

$$\vec{\mu} = g\frac{q}{2m}\vec{S}$$

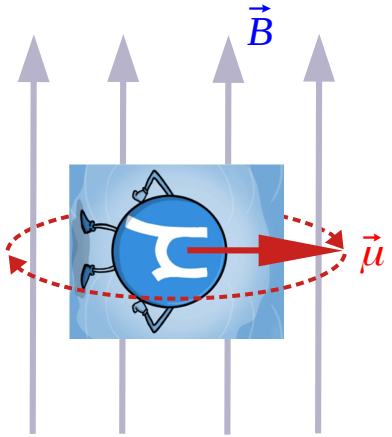

- In a magnetic storage ring, the muon spin precesses slightly faster than its cyclotron frequency

$$\vec{\omega}_s = -\frac{ge\vec{B}}{2m} - (1-\gamma)\frac{e\vec{B}}{m\gamma} \qquad \vec{\omega}_c = -\frac{e\vec{B}}{m\gamma}$$

- If we do the difference we get...

Experimental principle

$$\vec{\mu} = g\frac{q}{2m}\vec{S}$$

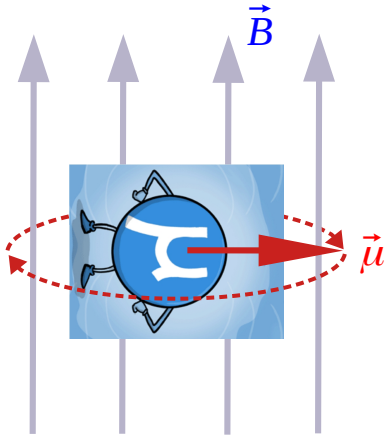

- In a magnetic storage ring, the muon spin precesses slightly faster than its cyclotron frequency

$$\vec{\omega}_s = -\frac{geB}{2m} - (1-\gamma)\frac{e\vec{B}}{m\gamma} \qquad \vec{\omega}_c = -\frac{e\vec{B}}{m\gamma}$$

- If we do the difference we get...

$$\vec{\omega}_a = \vec{\omega}_s - \vec{\omega}_c = -\left(\frac{g-2}{2}\right)\frac{e\vec{B}}{m} \equiv -a_\mu \frac{e\vec{B}}{m}$$

- This “anomalous” precession frequency is proportional to g-2 and to the magnetic field
- ω_a is entirely due to the virtual interactions between the muon and the field
- Measure $\boldsymbol{\omega_a}$ and **B** → obtain $\boldsymbol{a_\mu}$

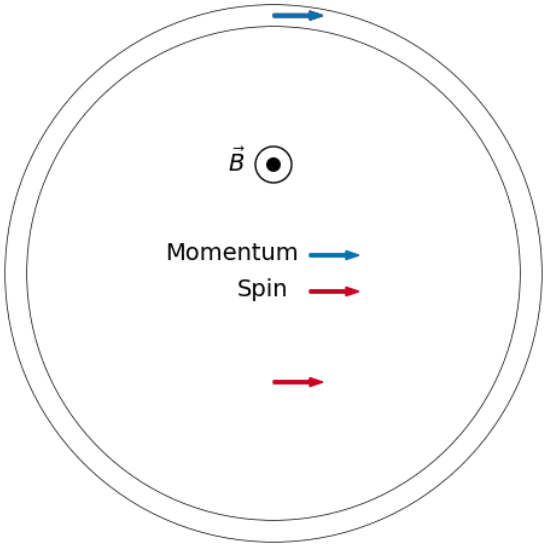

Experimental principle

$$\vec{\omega}_a = -a_\mu \frac{e\vec{B}}{m}$$

In a real experiment:

- Electric fields needed for vertical focusing
- Muon’s orbit can be slightly tilted

Experimental principle

$$\vec{\omega}_a = -a_\mu \frac{e\vec{B}}{m}$$

In a real experiment:

- Electric fields needed for vertical focusing
- Muon's orbit can be slightly tilted

$$\vec{\omega}_a = -\frac{e}{m}\left[a_\mu \vec{B} - \left(a_\mu - \frac{1}{\gamma^2 - 1}\right)\vec{\beta} \times \vec{E} - a_\mu \frac{\gamma}{\gamma + 1}(\vec{\beta} \cdot \vec{B})\vec{\beta}\right]$$

Experimental principle

$$\vec{\omega}_a = -a_\mu \frac{e\vec{B}}{m}$$

In a real experiment:

- Electric fields needed for vertical focusing
- Muon's orbit can be slightly tilted

$$\vec{\omega}_a = -\frac{e}{m}\left[a_\mu \vec{B} - \left(a_\mu - \frac{1}{\gamma^2 - 1}\right)\vec{\beta} \times \vec{E} - a_\mu \frac{\gamma}{\gamma + 1}(\vec{\beta} \cdot \vec{B})\vec{\beta}\right]$$

=0 for
p = 3.094 GeV/c

=0 for
planar orbits

- Any small deviation from perfect momentum and orbit can be measured and corrected at analysis stage

Parity violation

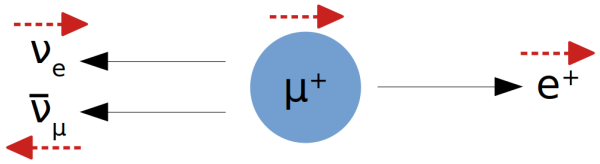

Muon decays in a positron and 2 neutrinos

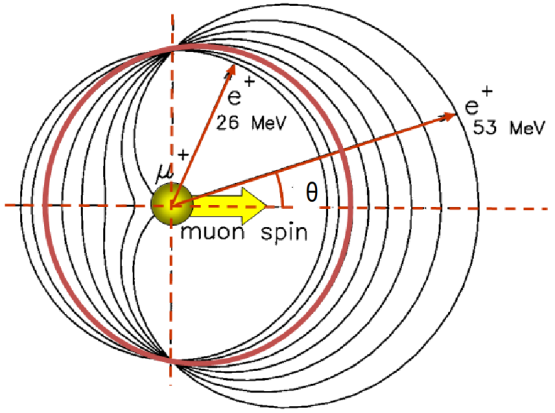

Parity violation → positrons in CM preferably in the direction of the muon spin

Parity violation

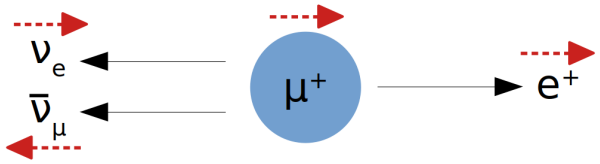

Muon decays in a positron and 2 neutrinos

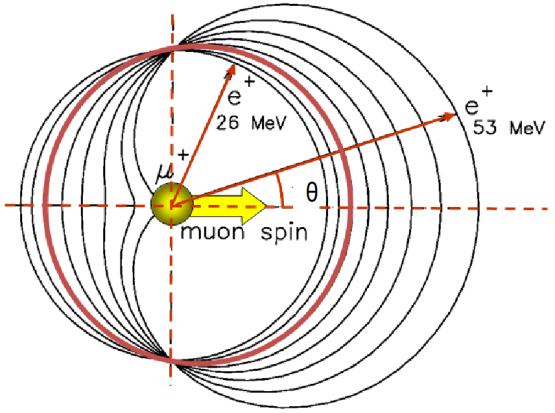

Parity violation → positrons in CM preferably in the direction of the muon spin

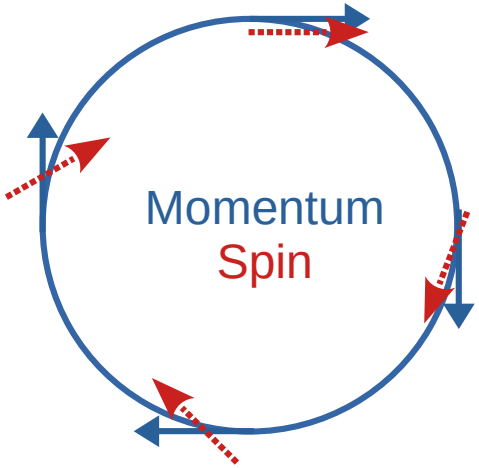

Spin precession → the energy spectrum in the lab frame **oscillates** through time

Parity violation

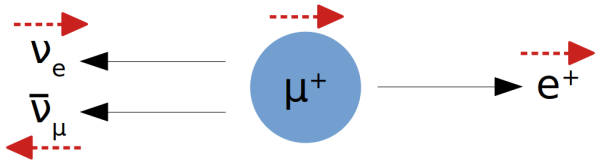

Muon decays in a positron and 2 neutrinos

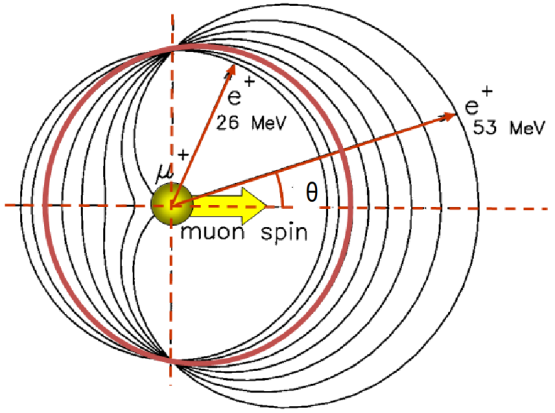

Parity violation → positrons in CM preferably in the direction of the muon spin

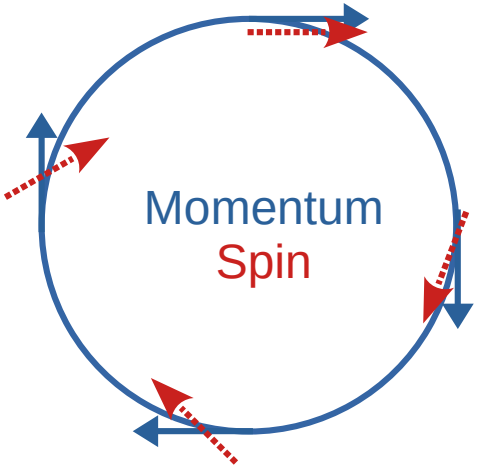

Spin precession → the energy spectrum in the lab frame **oscillates** through time

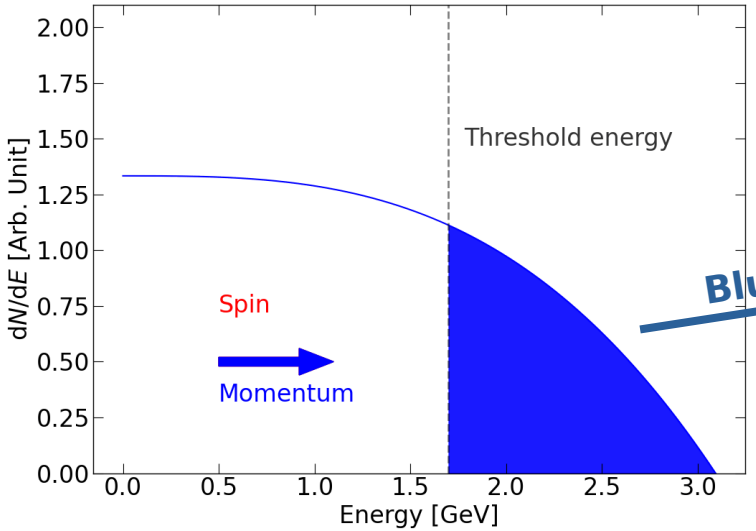

Blue integral

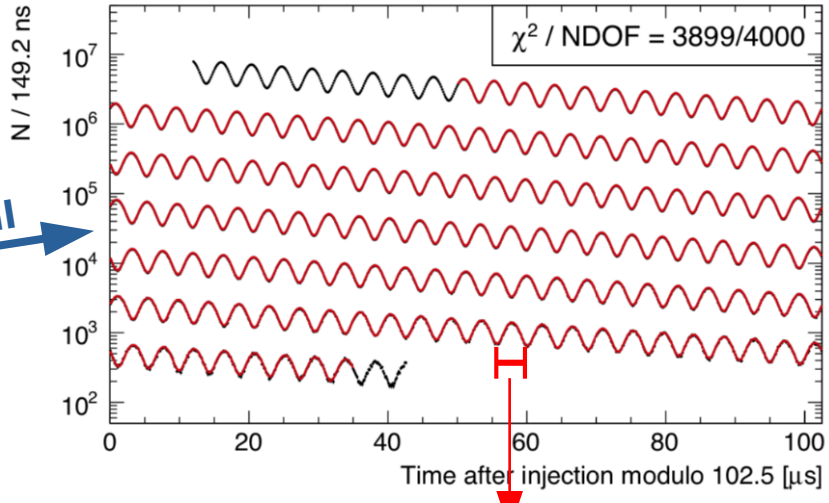

g-2 frequency!

Overview

The Muon g-2

Experimental principles

The Muon g-2 Experiment at Fermilab

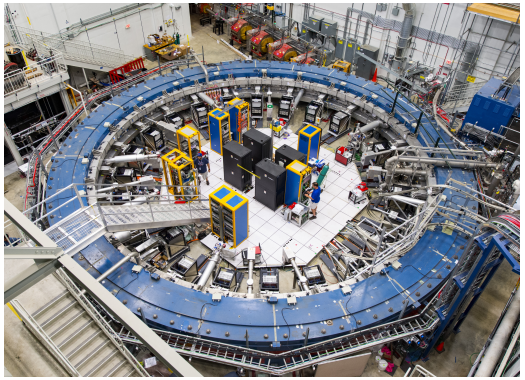

Latest results and overlook

Muon source

- 16 bunches of 10^{12} protons @8 GeV get boosted and delivered via the recycler ring every 1.4 seconds
- Each bunch hits a fixed Inconel® (NiCrFe) target
- Positive pions from shower extracted and decay in delivery ring
- Pure and polarized muon beam enters g-2 ring

$p \rightarrow \pi^+ \rightarrow \mu^+ \rightarrow e^+$

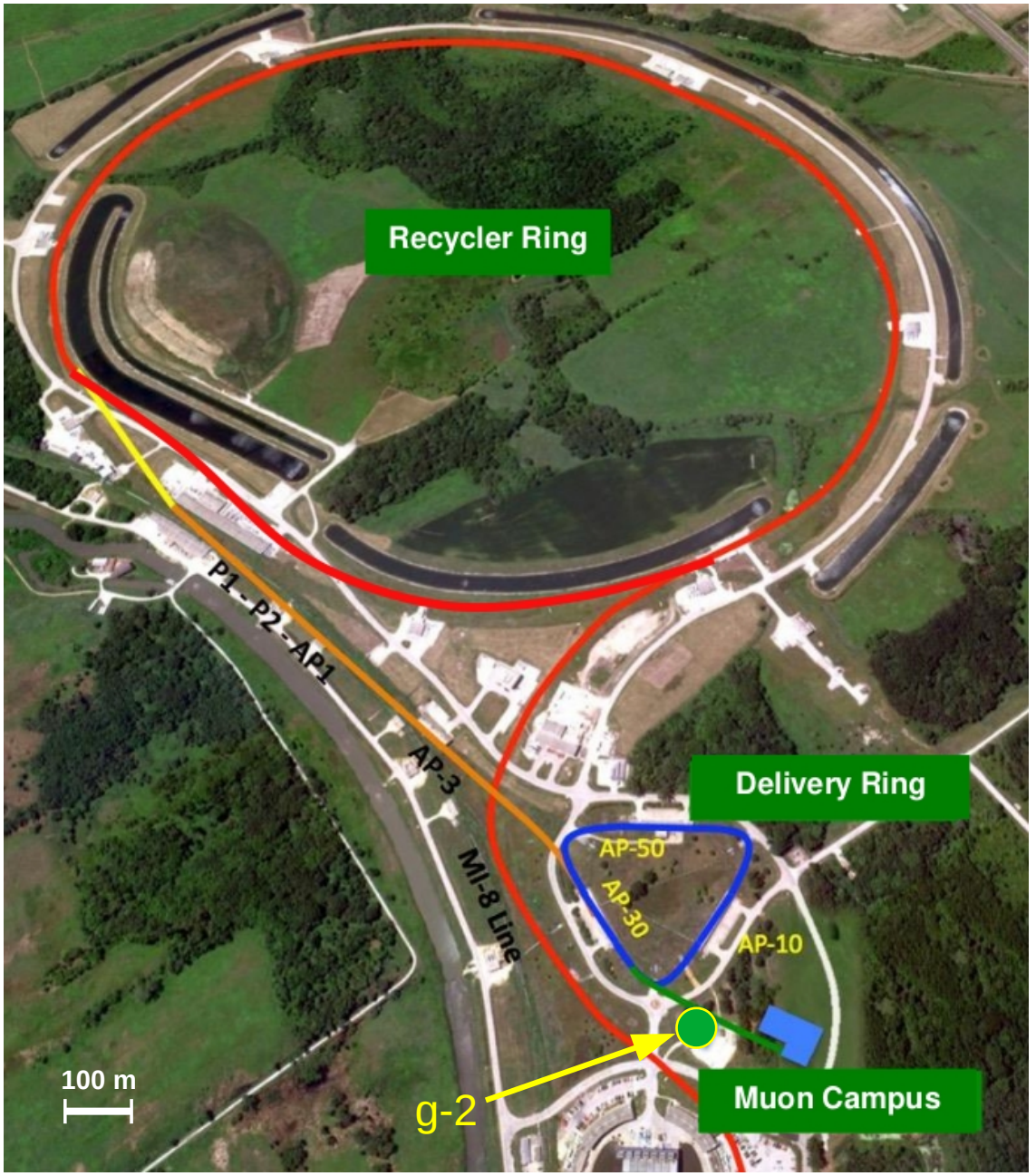

Muon g-2 Experiment

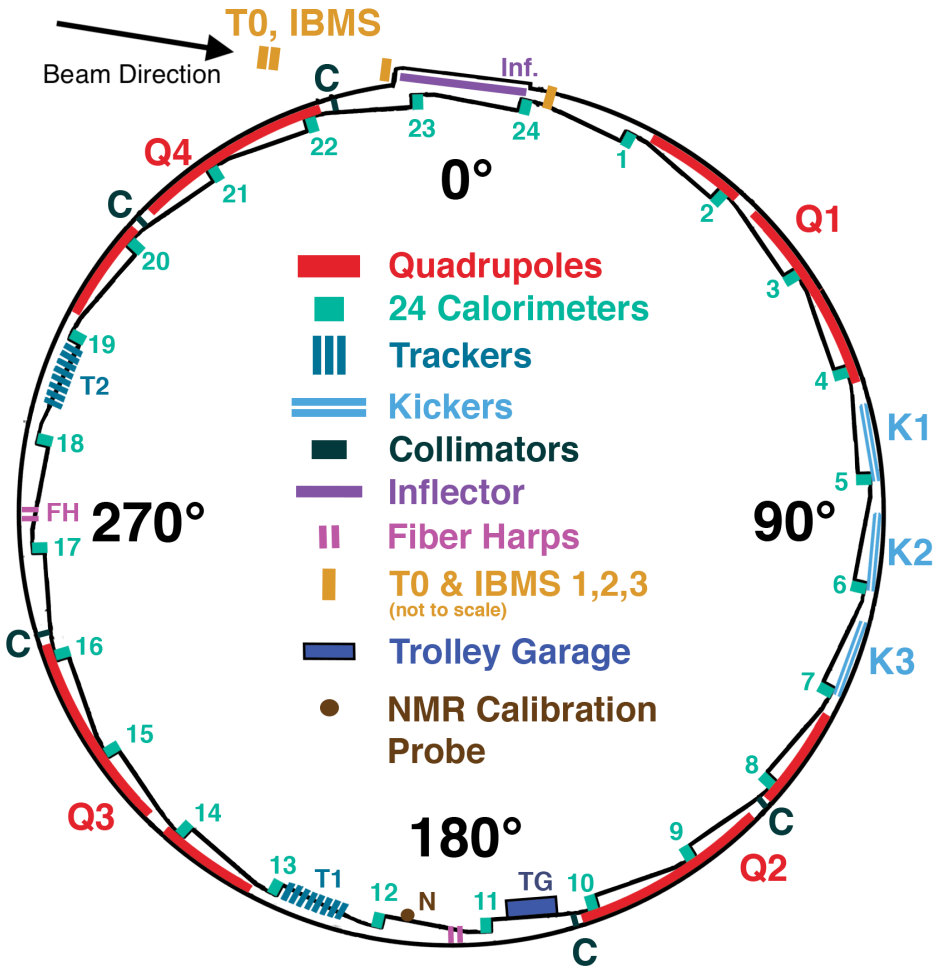

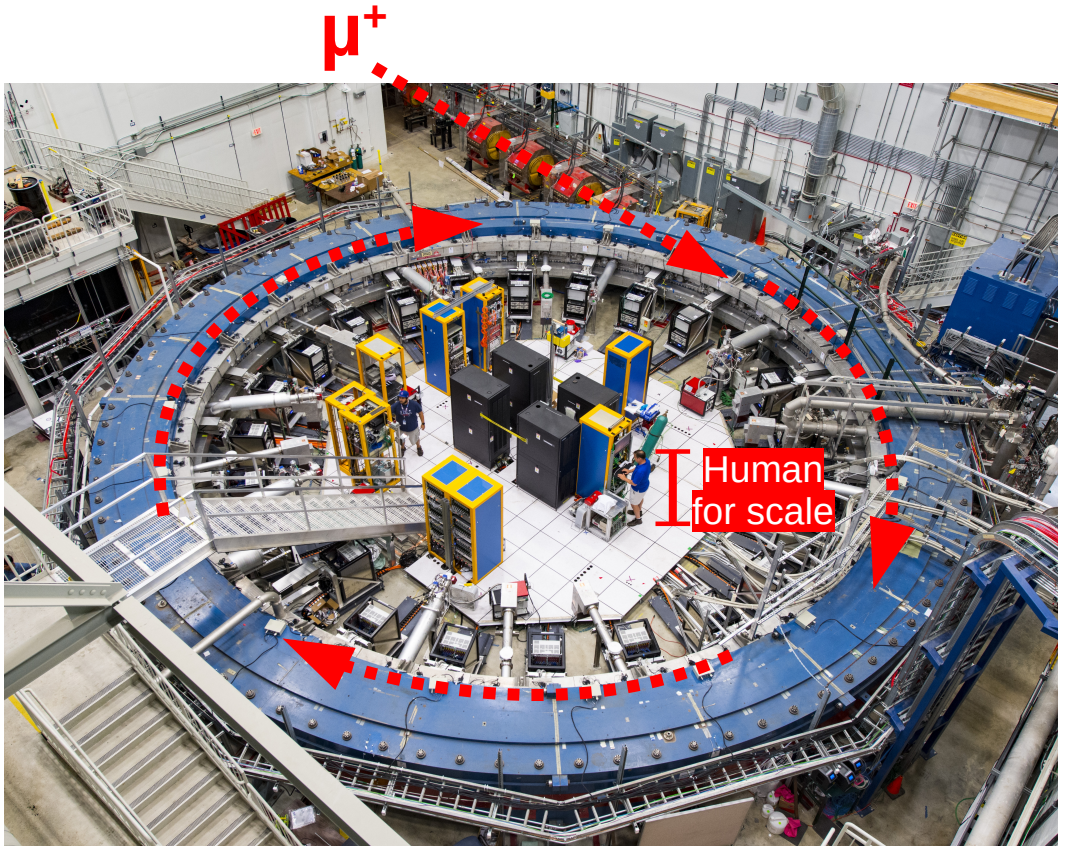

MC-1 building @Fermilab

Beam injection & kick

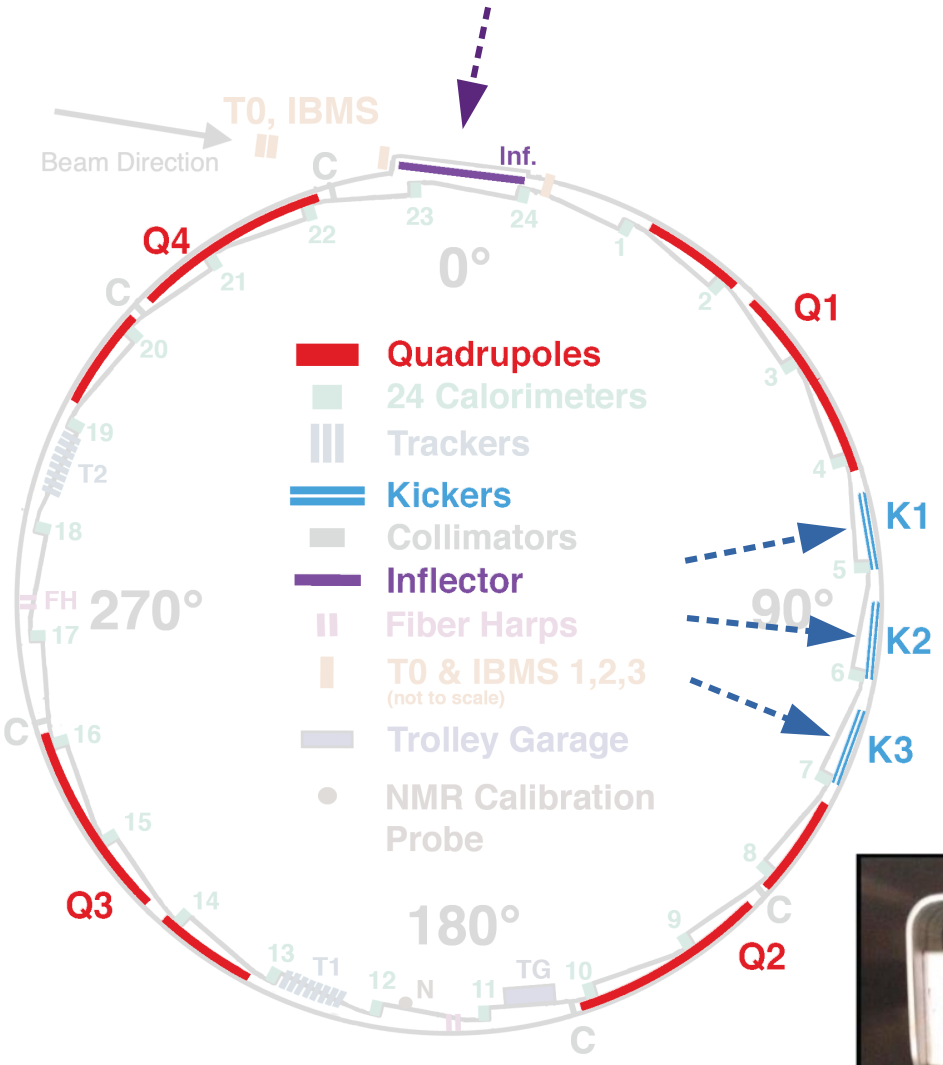

- Superconducting **inflector** ~8 cm offset from nominal orbit
- 3 fast magnetic **kickers** operated at ~4 kA current for ~200 ns

Inflector

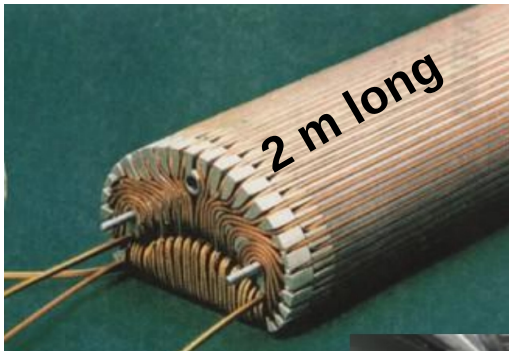

Kicker plates

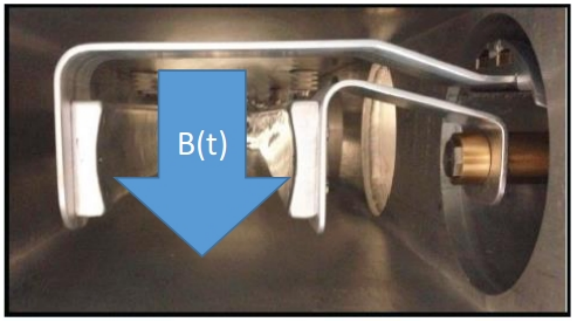

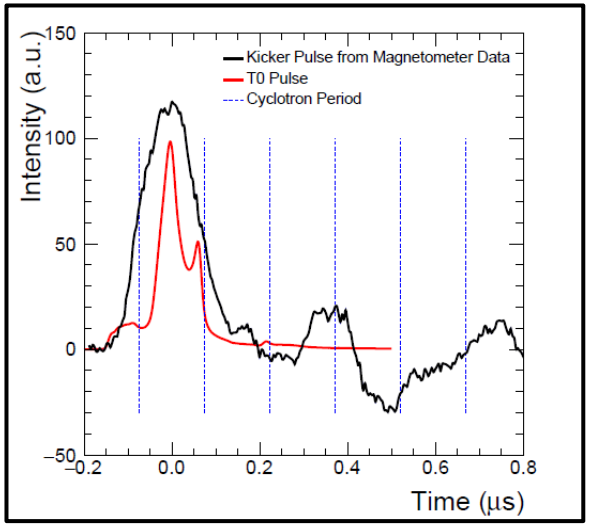

Electric quadrupoles

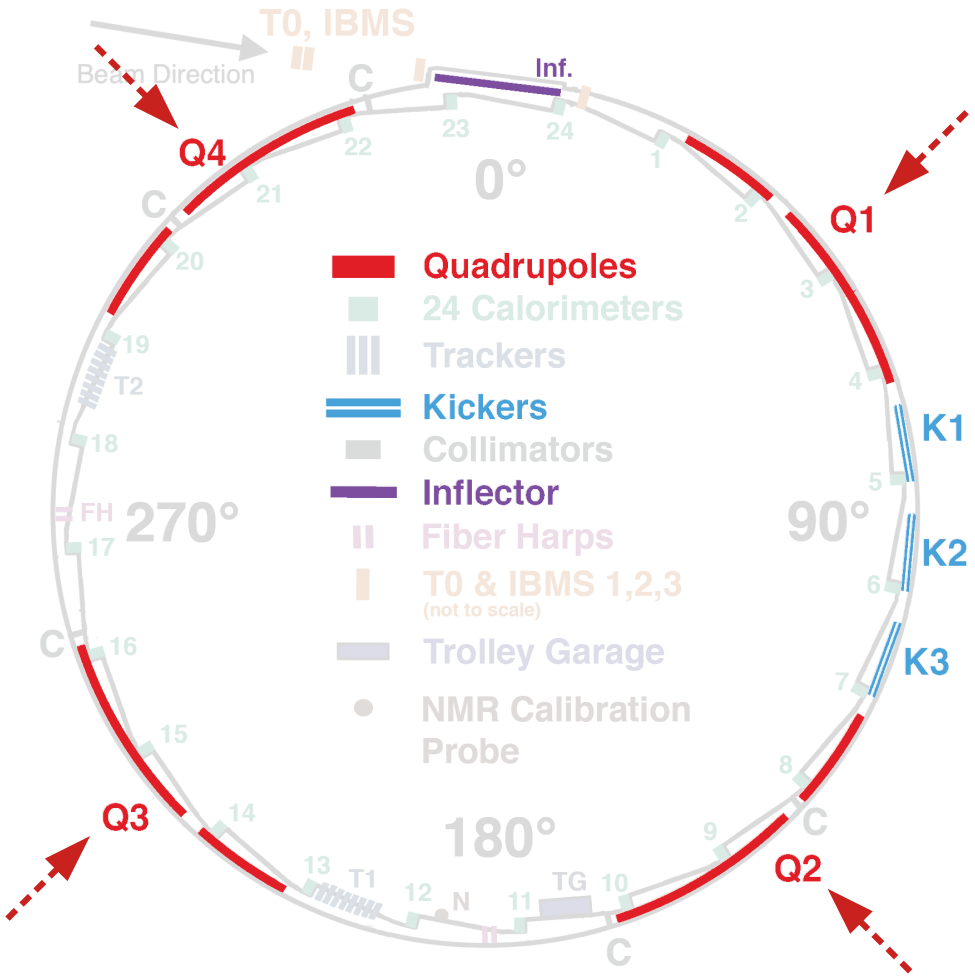

- 8 aluminum electrostatic **quadrupoles** at 13.8 kV to provide weak vertical focus

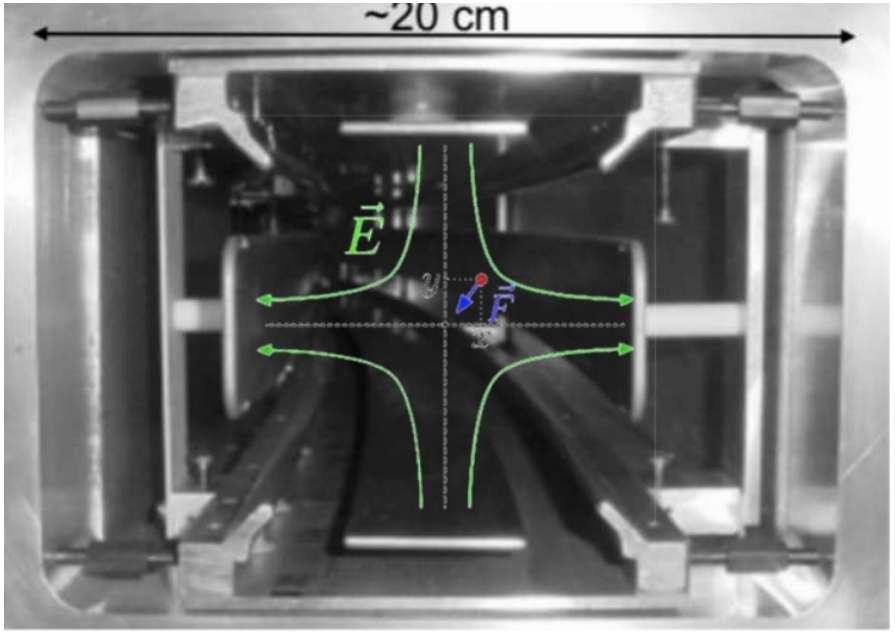

Magnet

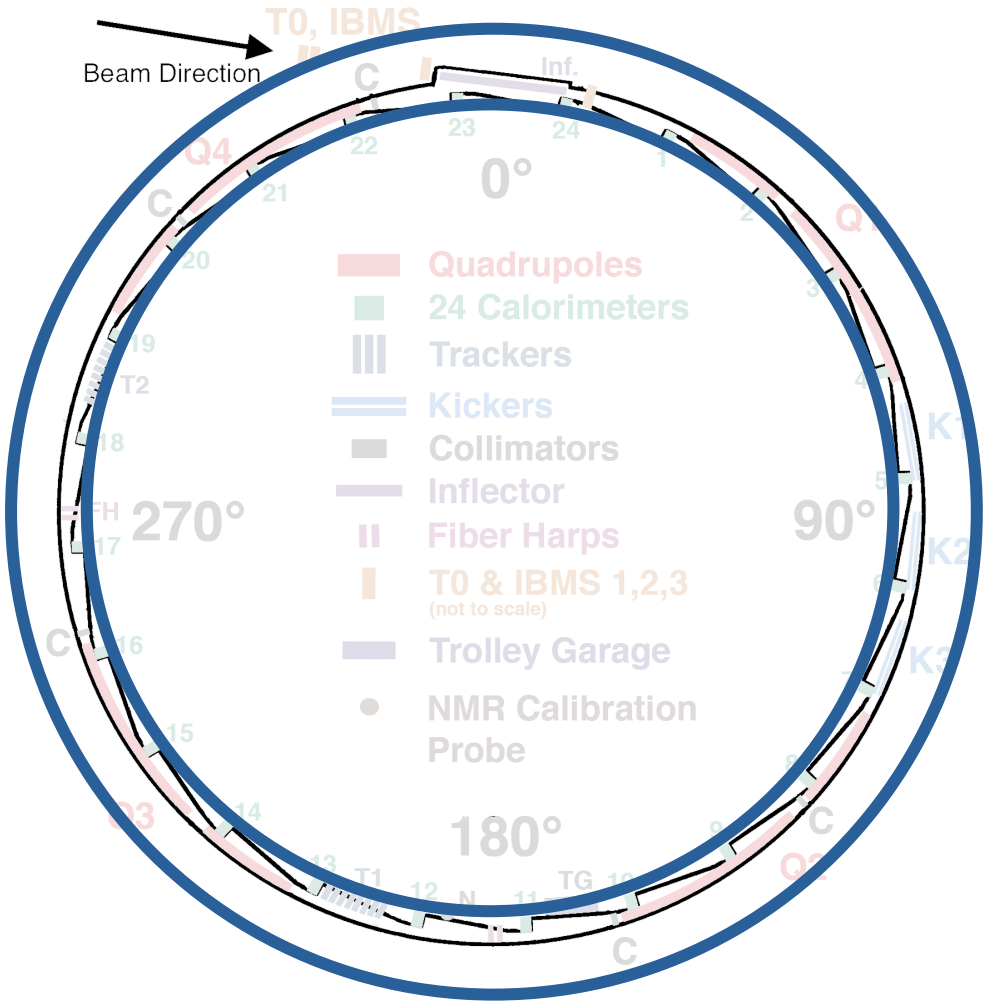

- Superconductive **magnet** cooled at ~5 K with LHe
- 7.112 m radius, highly **uniform 1.45 T** vertical magnetic field
- Shimmed passively and actively stabilized. Better than 14 ppm RMS field homogeneity across the full azimuth

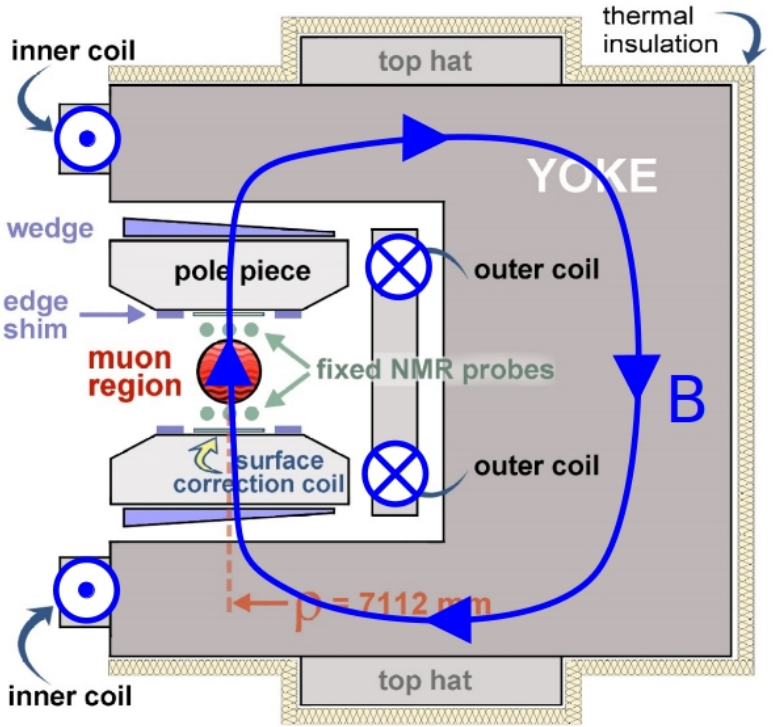

Detectors

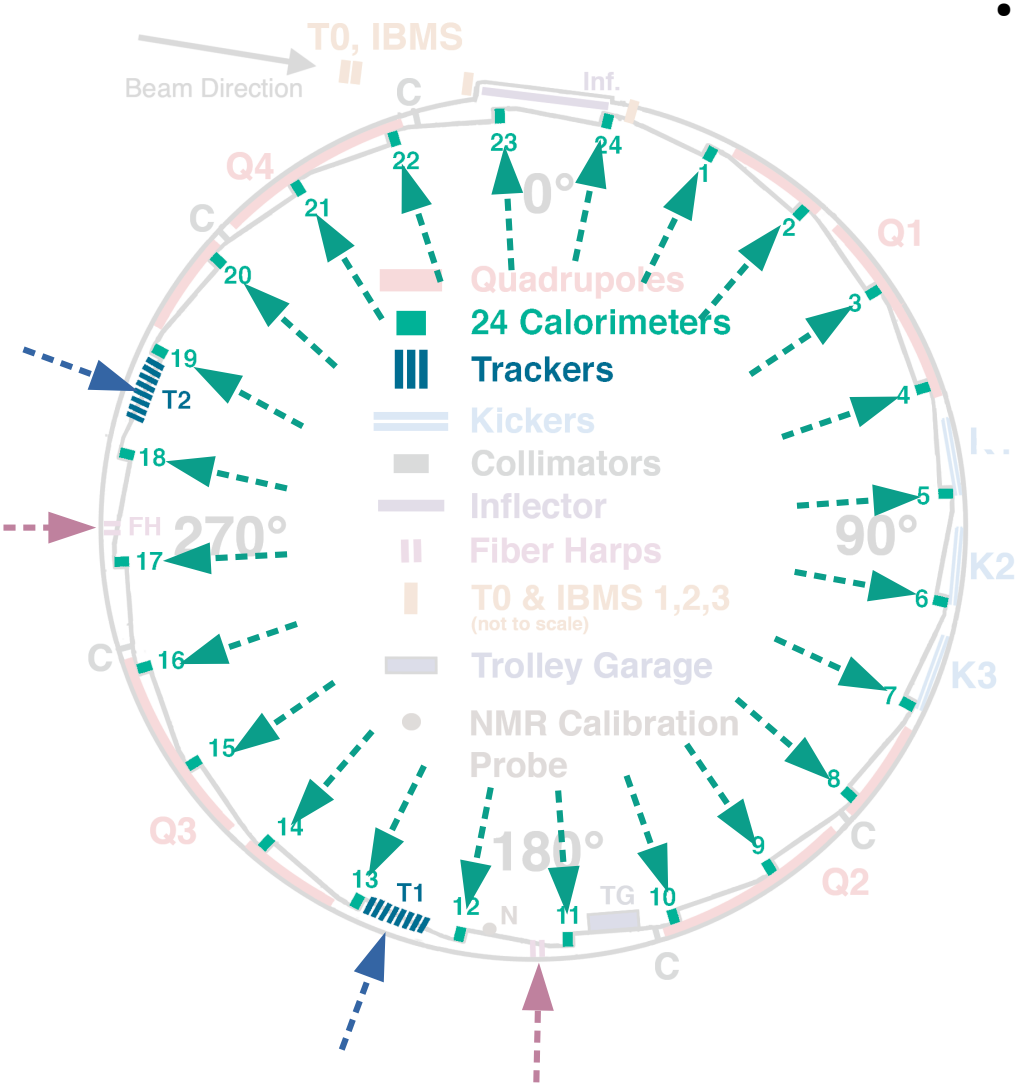

- 24 electromagnetic **calorimeters** for positron energy and time measurement
- 2 **tracker** stations to extrapolate decay vertex location and measure beam distribution

Calorimeter

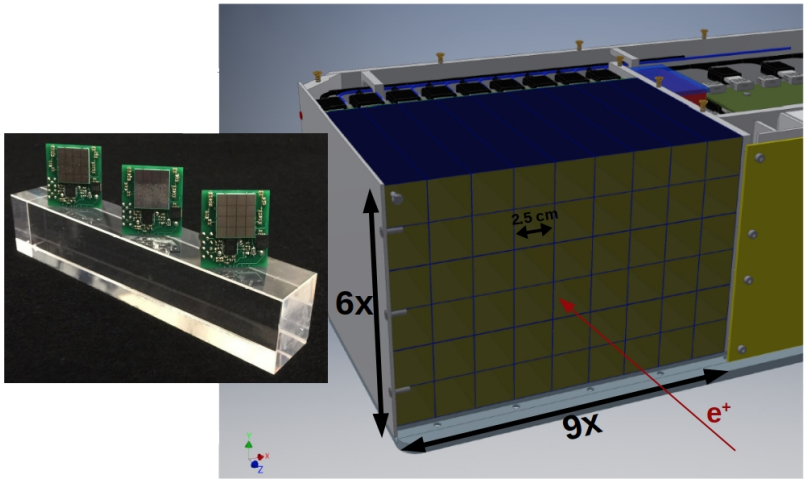

Tracker module

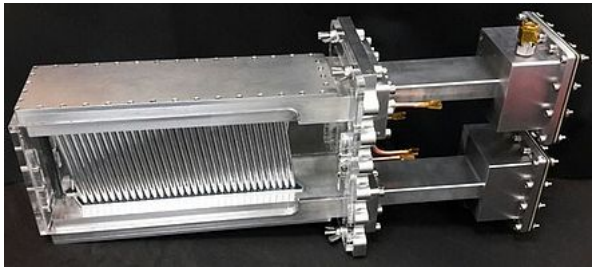

Laser Calibration System

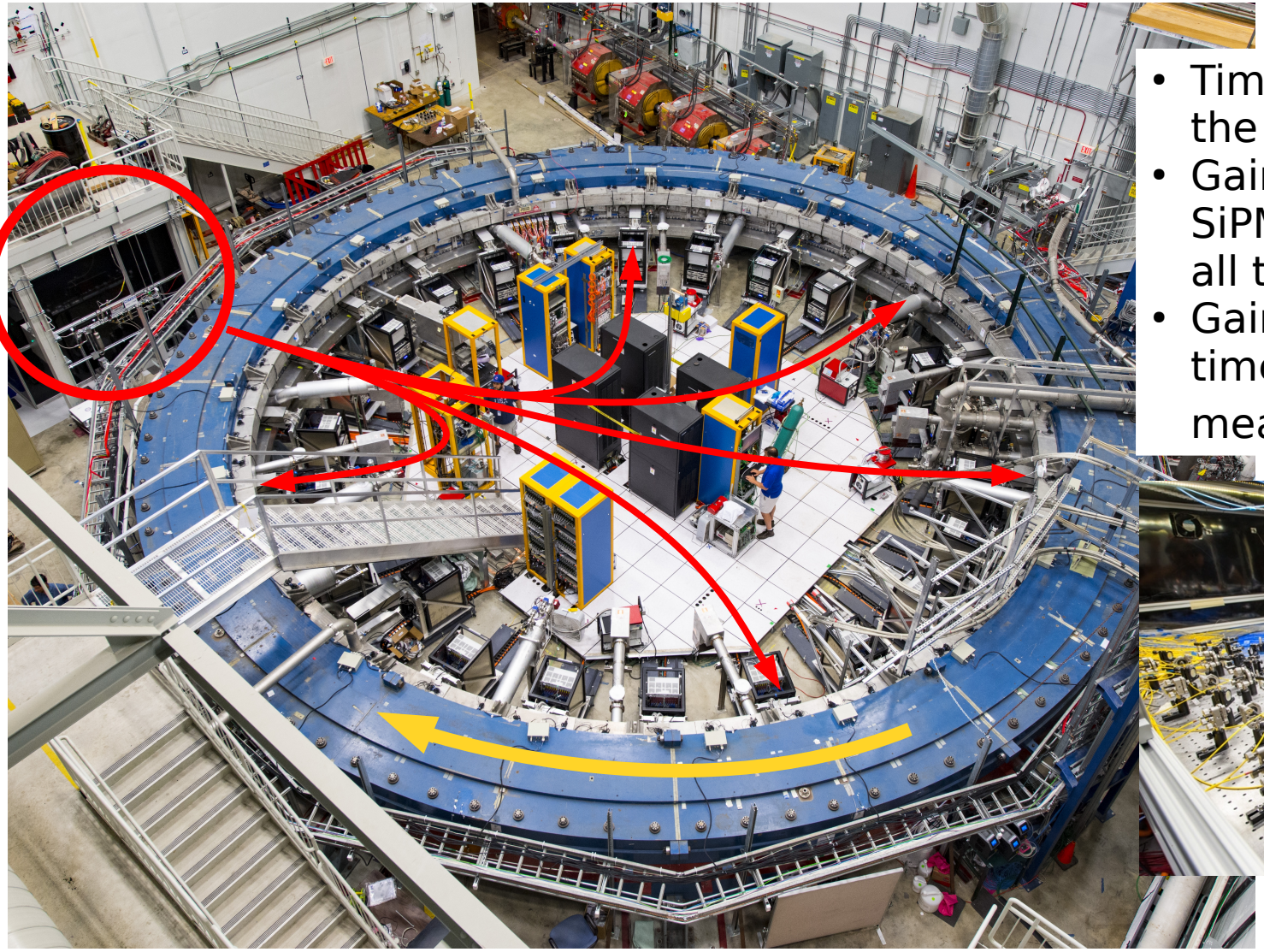

- Time synchronization at the ~50 ps level
- Gain calibration of the SiPMs at the 10^{-4} level at all timescales
- Gain stability through time is crucial for ω_a measurement

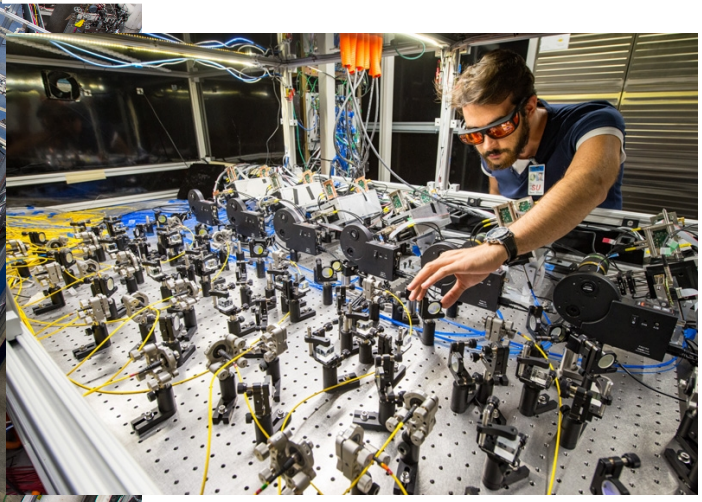

Master formula

$$\vec{\omega}_a = a_\mu \frac{e\vec{B}}{m} \longrightarrow a_\mu = \frac{\omega_a}{\tilde{\omega}'_p(T_r)} \boxed{\frac{\mu'_p(T_r)}{\mu_e} \frac{m_\mu}{m_e} \frac{g_e}{2}}$$

Constants known from other experiments with high precision (25 ppb)

Master formula

$$\vec{\omega}_a = a_\mu \frac{e\vec{B}}{m} \longrightarrow a_\mu = \frac{\omega_a}{\tilde{\omega}'_p(T_r)} \frac{\mu'_p(T_r)}{\mu_e} \frac{m_\mu}{m_e} \frac{g_e}{2}$$

Constants known from other experiments with high precision (25 ppb)

$$a_\mu \propto \frac{f_{clock}\, \omega_a^m \,(1 + C_e + C_p + C_{ml} + C_{pa})}{f_{calib} \left\langle \omega'_p(x, y, \phi) \times M(x, y, \phi) \right\rangle (1 + B_k + B_q)}$$

Three key measurements:

- ω_a: Muon anomalous precession frequency
- ω_p: Larmor precession frequency of protons (B field)
- ρ_r: Muon distribution

ω_a

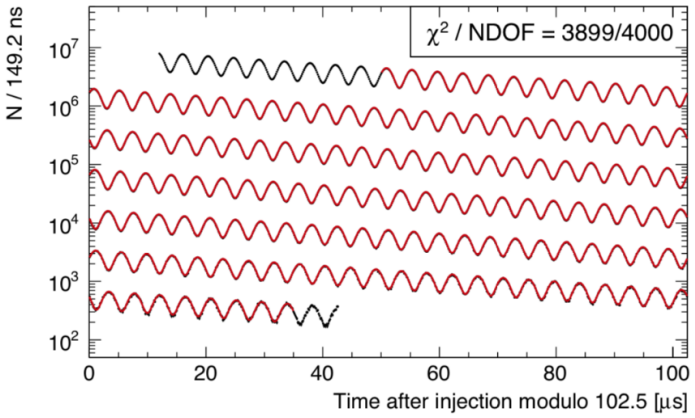

ω_p

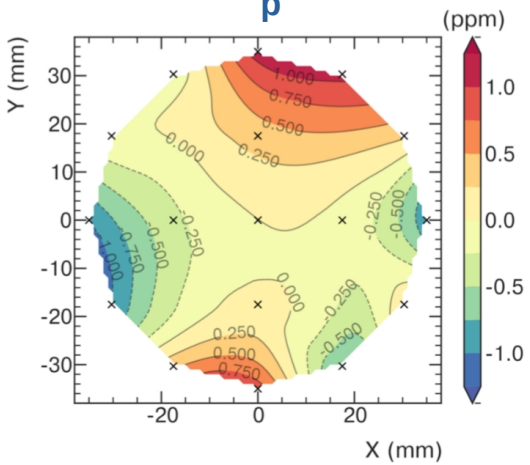

$\rho(r)$

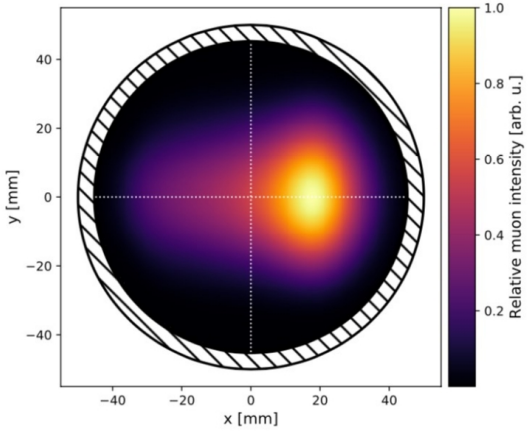

Measuring ω_a

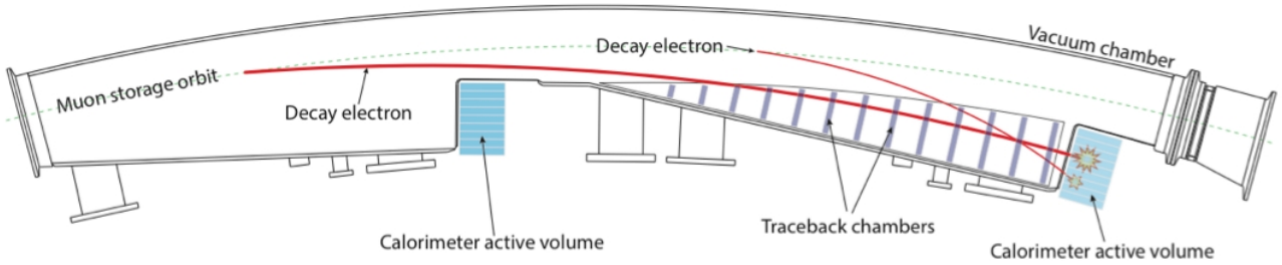

- Positrons above 1 GeV are counted vs time (weighted by their asymmetry)
- "Wiggle" plot fitted for exponential decay and ω_a oscillation

Positron count

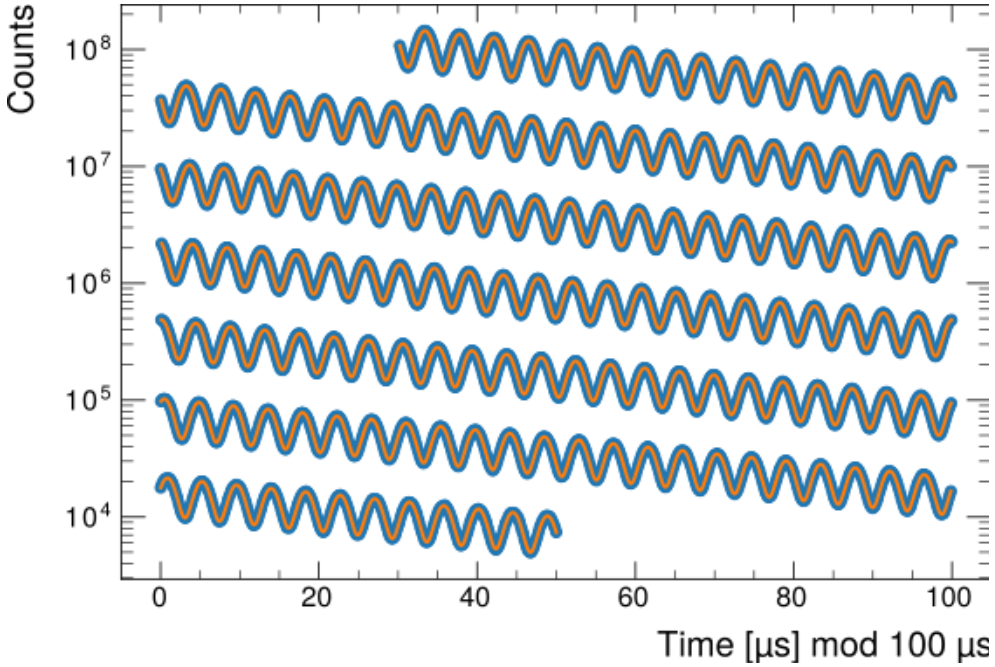

FFT of fit residual

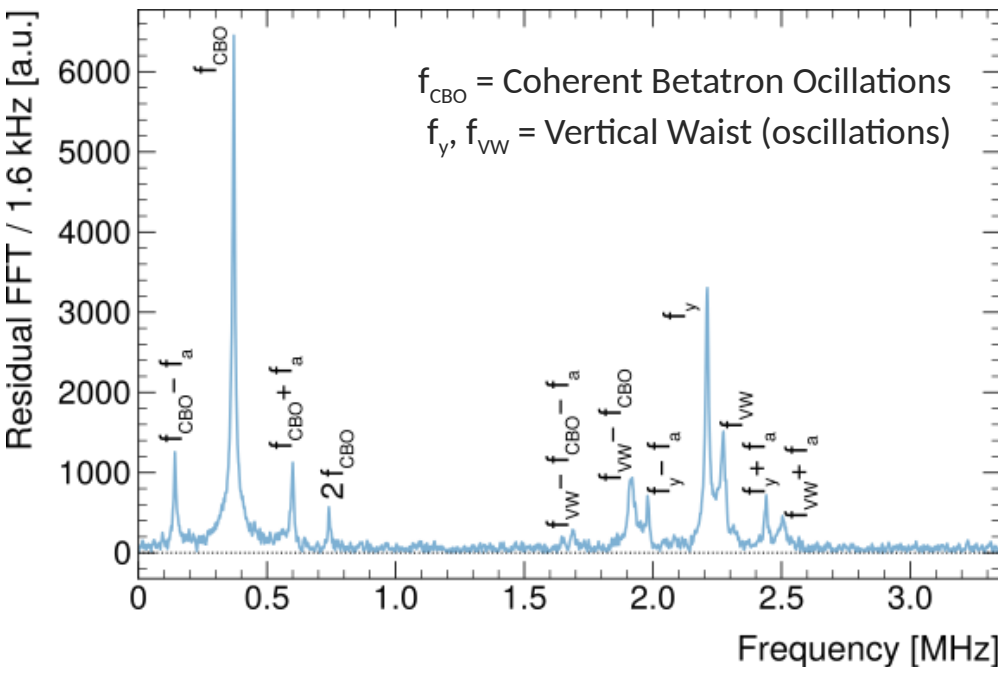

Measuring ω_a

- Must account for beam oscillations, muons losses, detector effects
- Complete fit has 27 or more free parameters
- 5 analysis groups, 8 hist/fit methods, 3 energy reconstructions

$$
\begin{aligned}
N(t) = {} & N e^{-t/\tau_\mu} \left[1 + A \cdot \cos(\omega_a t - \phi + \phi_{BO}(t))\right] \cdot \\
& \cdot \left(1 + A_{CBO} \cos(\omega_{CBO} t - \phi_{CBO}) e^{-\frac{t}{\tau_{CBO}}}\right) \cdot \\
& \cdot \left(1 + A_{VW} \cos(\omega_{VW} t - \phi_{VW}) e^{-\frac{t}{\tau_{VW}}}\right) \cdot \\
& \cdot \left(1 + A_{2CBO} \cos(\omega_{2CBO} t - \phi_{2CBO}) e^{-\frac{t}{\tau_{2CBO}}}\right) \cdot \\
& \cdot \left(1 + A_y \cos(\omega_y t - \phi_y) e^{-\frac{t}{\tau_y}}\right) \cdot \\
& \cdot \left(1 - k_{LM} \int_0^t L(t') e^{t'/\tau_\mu} dt'\right) \cdot \\
& \cdot \left(1 + \left[A_+ \cos(\omega_+(t) t - \phi_+) + A_- \cos(\omega_-(t) t - \phi_-)\right] e^{-\frac{t}{\tau_{CBOVW}}}\right)
\end{aligned}
$$

Measuring ω_a

- Must account for beam oscillations, muons losses, detector effects
- Complete fit has 27 or more free parameters
- 5 analysis groups, 8 hist/fit methods, 3 energy reconstructions

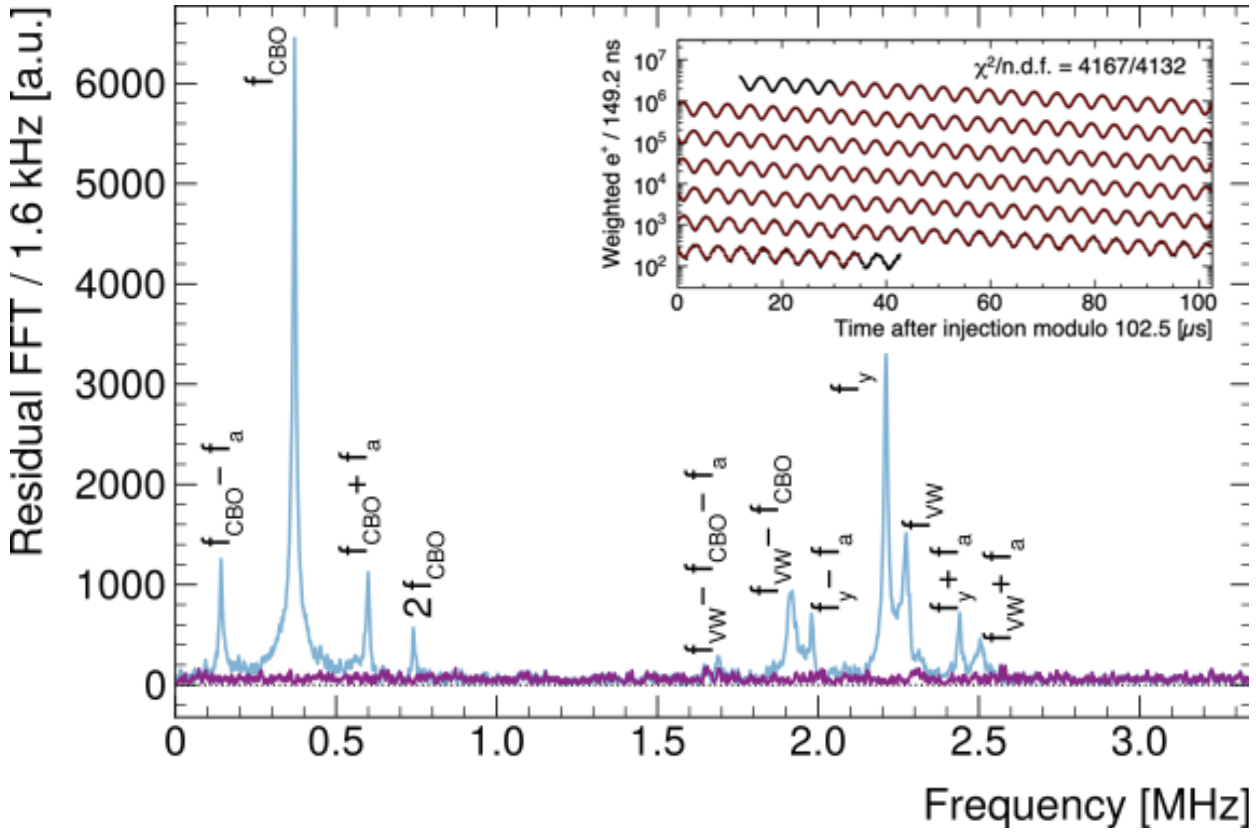

Measuring the beam

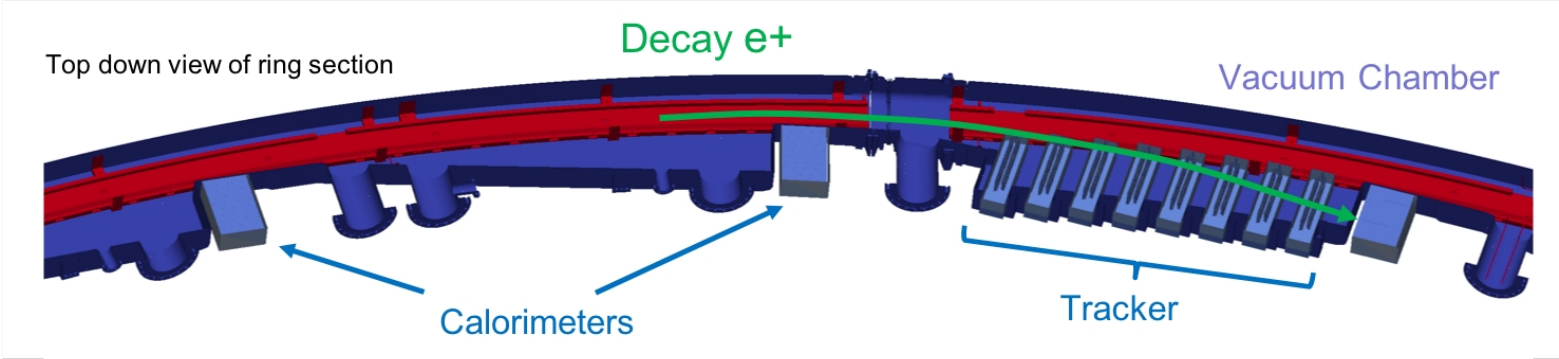

- Trackers at 180° and 270° reconstruct the positron trajectory to extrapolate the decay vertex in the storage region
- Muon distribution maps extrapolated to the entire ring azimuth with Geant4 simulation (gm2ringsim)
- Calorimeter hit energy matching to perform particle identification

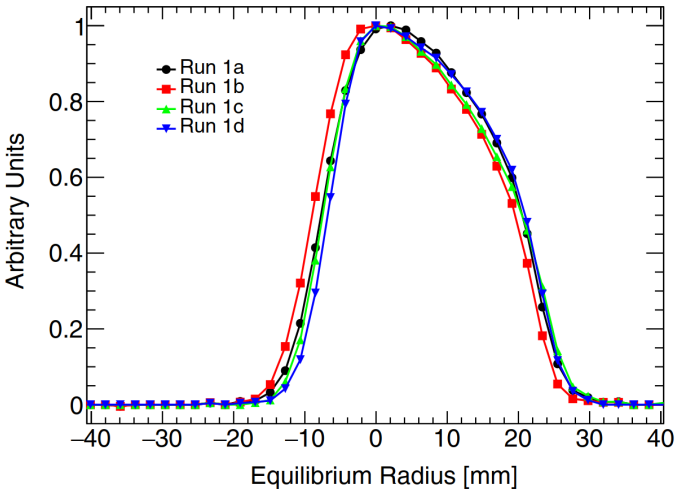

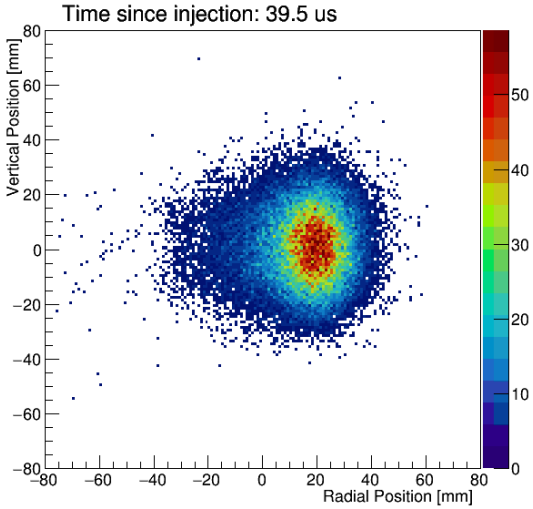

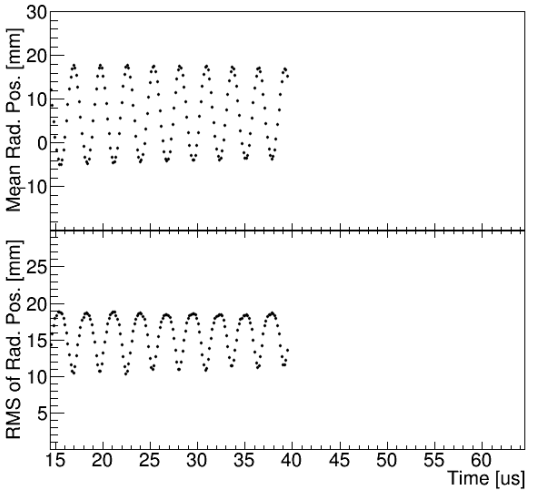

Measuring the field

- Field intensity measured with Nuclear Magnetic Resonance (NMR) probes in terms of proton precession frequency ω_p
- Continuously monitored around the storage region and periodically measured inside the storage region

378 fixed probes
continuous monitoring

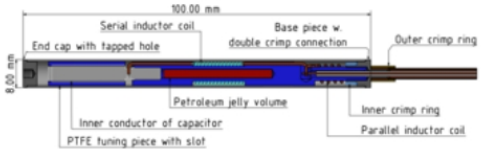

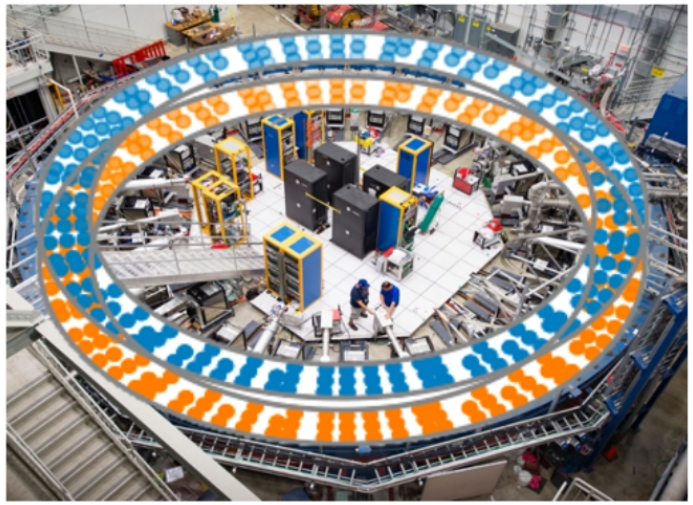

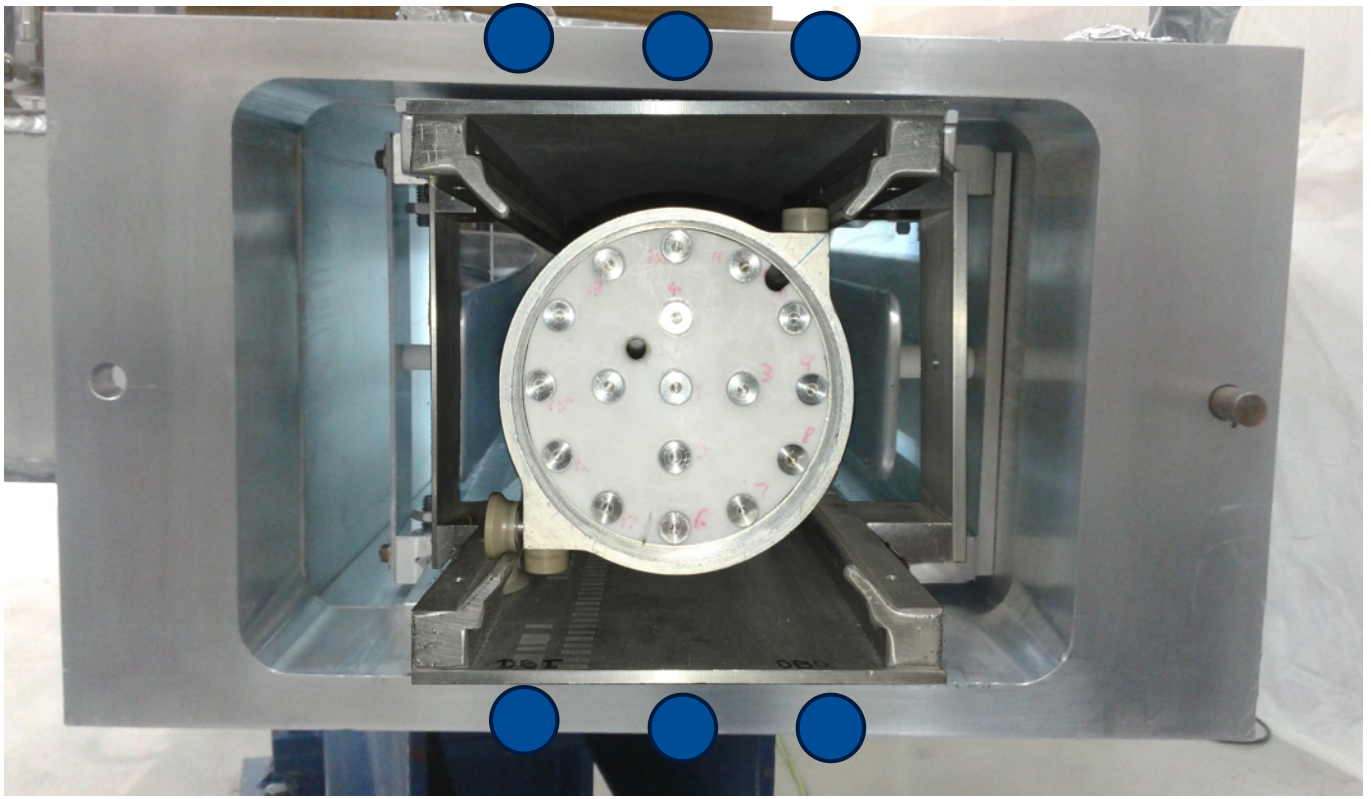

Measuring the field

- Every ~3 days, a trolley equipped with 17 probes runs through the storage region
- 9000 2D slices for complete magnetic field map

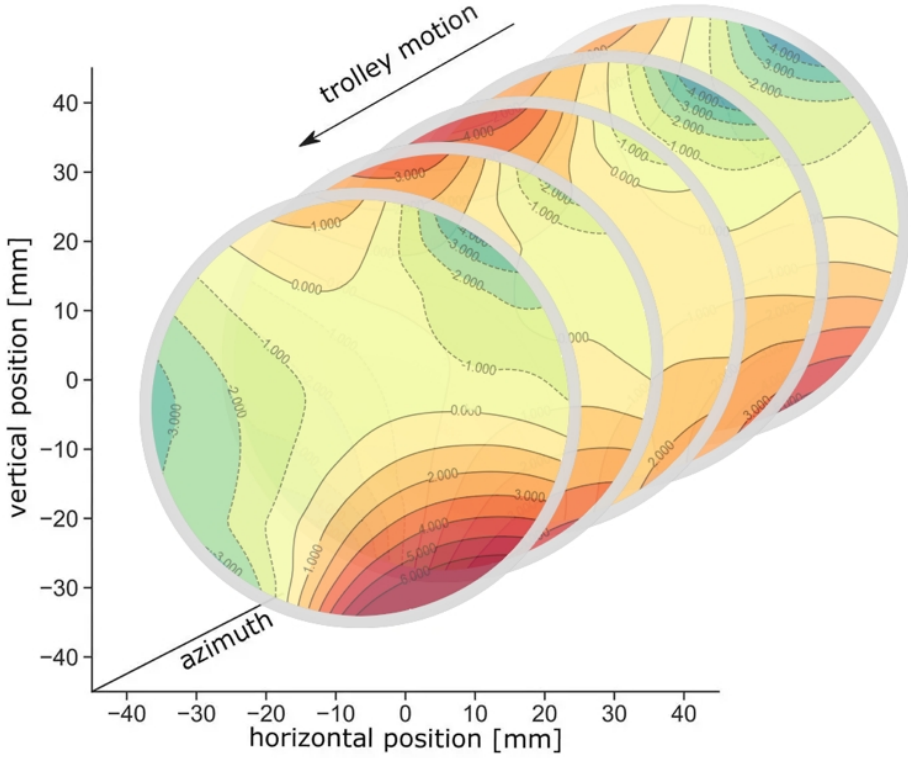

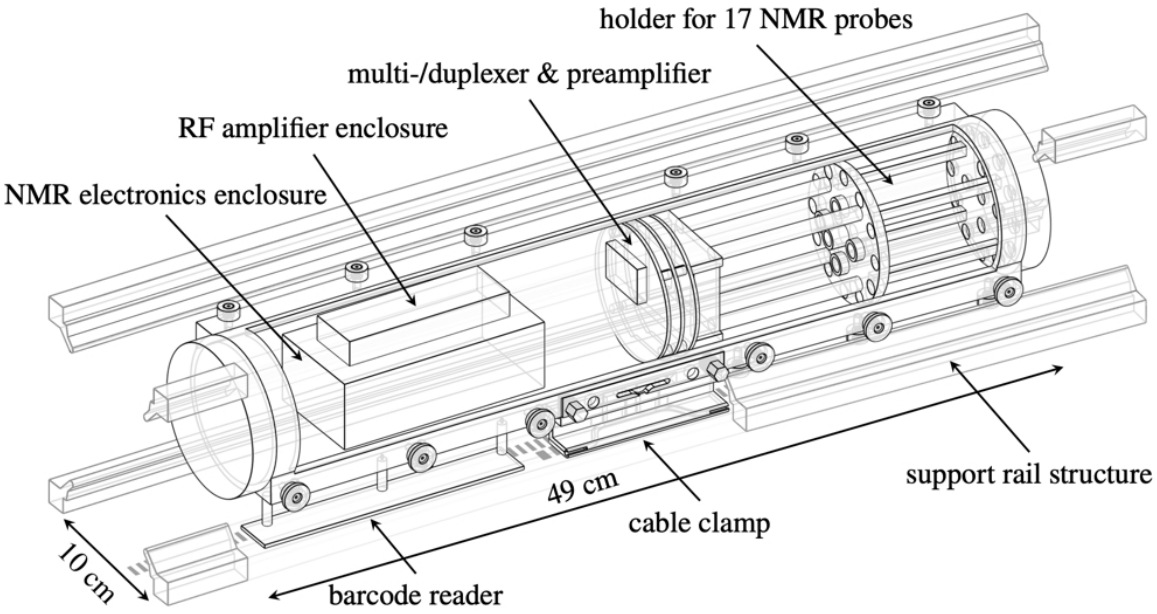

Measuring the field

- Field measurements are calibrated in-situ with a water-based cylindrical Fixed Calibration Probe and externally with shielded protons in sperical sample

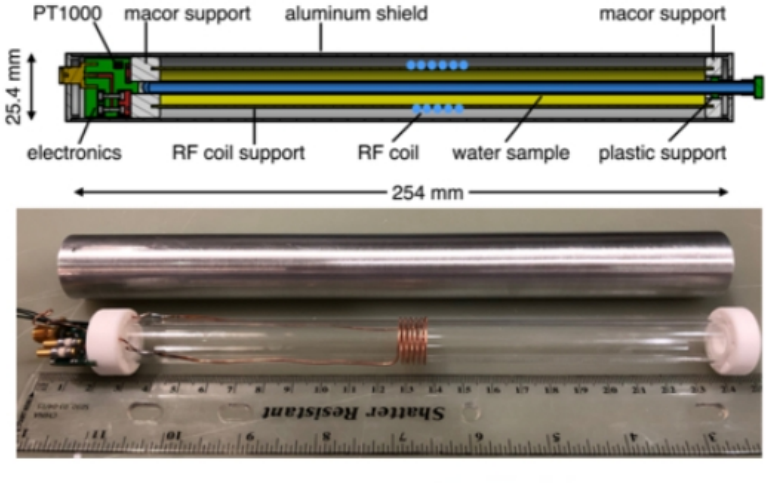

Cross-calibrations:

- 3He magnetometer
- J-PARC Muon g-2/EDM continuous-wave based NMR calibration probe

Measuring the field

- Field measurements are calibrated in-situ with a water-based cylindrical Fixed Calibration Probe and externally with shielded protons in sperical sample
- Finally, magnetic field is weighted by the measured beam distribution

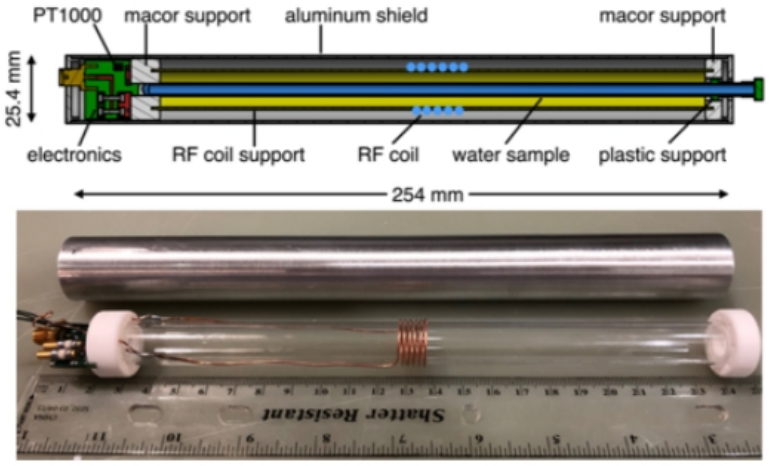

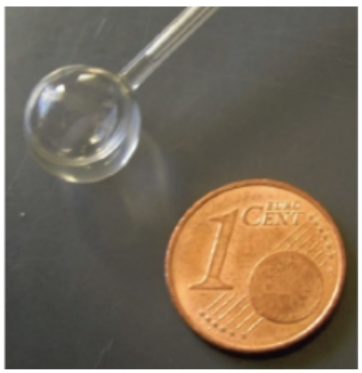

Cross-calibrations:
- 3He magnetometer
- J-PARC Muon g-2/EDM continuous-wave based NMR calibration probe

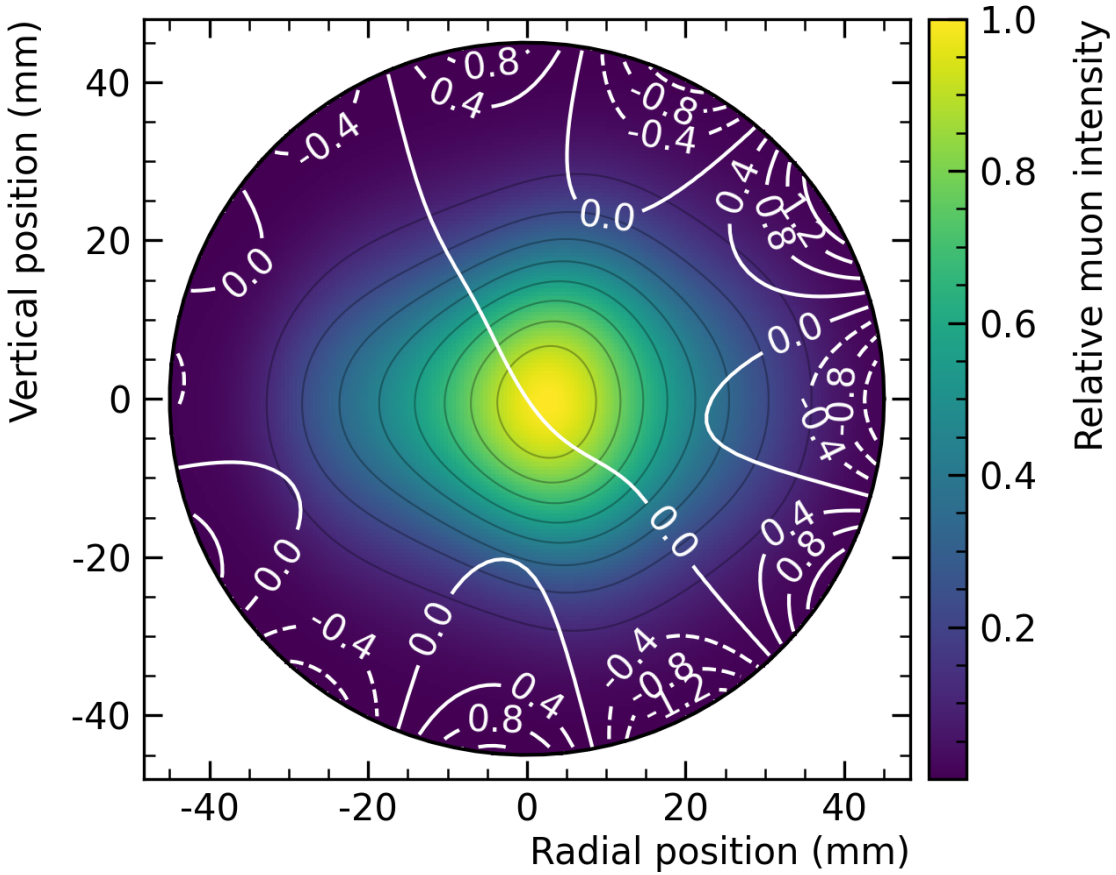

Master formula

$$\frac{\omega_a}{\omega_p} = \frac{\omega_a^m}{\omega_p^m}\frac{1 + C_e + C_p + C_{pa} + C_{dd} + C_{ml}}{1 + B_k + B_q}$$

$C_e \approx 2n(1-n)\beta_0 \frac{\langle x_e^2 \rangle}{R_0^2}$

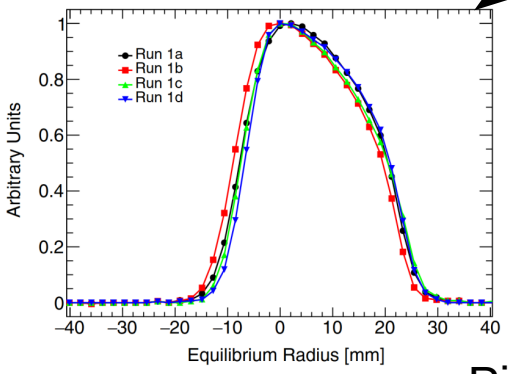

Electric field correction

Phase-acceptance correction

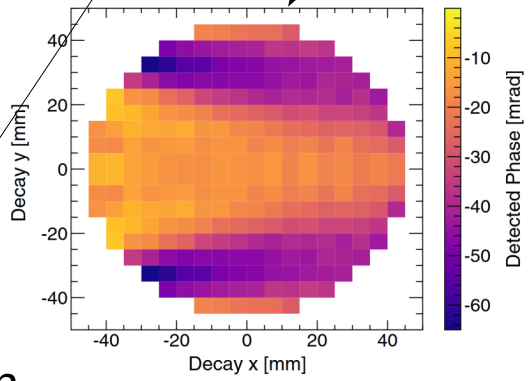

Pitch correction

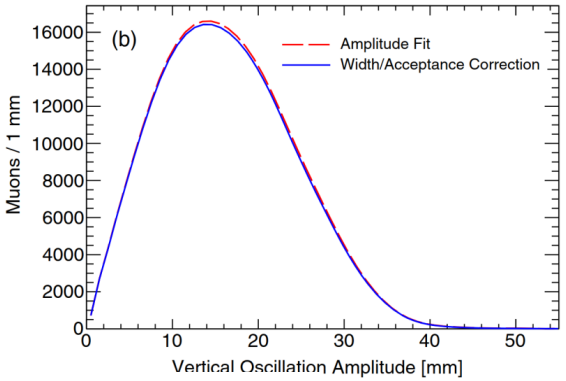

Differential decay correction

$C_{dd} = -\frac{\Delta\omega_a}{\omega_a} = \frac{1}{\omega_a}\frac{d\phi_0}{dt} = \frac{1}{\omega_a}\frac{d\phi_0}{dp}\left(\frac{dp}{dt}\right)_{dd}$

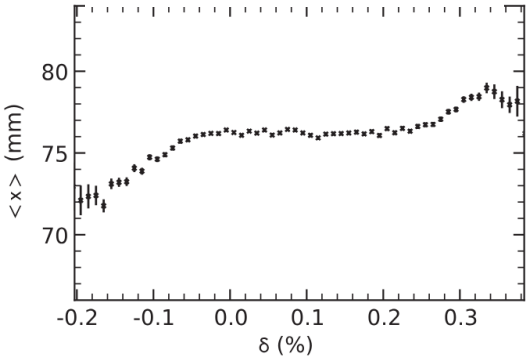

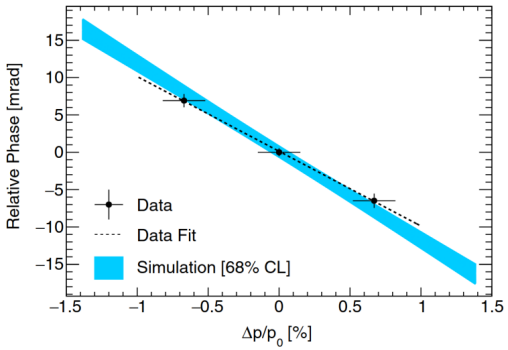

Lost muons momentum correlation

$C_p \approx \frac{n}{4}\frac{\langle A_y^2 \rangle}{R_0^2}$

Master formula

$$\frac{\omega_a}{\omega_p} = \frac{\omega_a^m}{\omega_p^m} \frac{1 + C_e + C_p + C_{pa} + C_{dd} + C_{ml}}{1 + B_k + B_q}$$

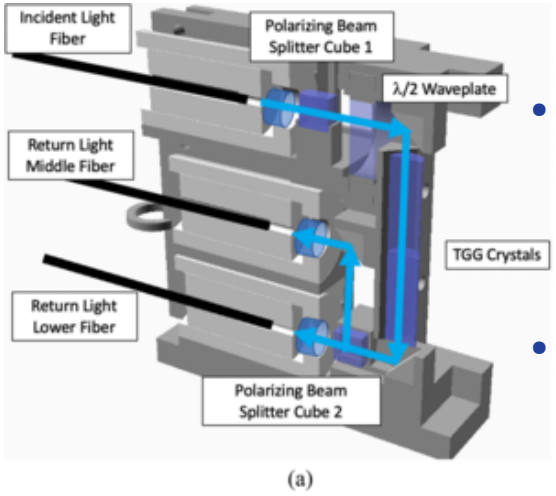

(a)

- Millisecond-long eddy currents induced by the kicker pulse
- Measured with dedicated Faraday magnetometers

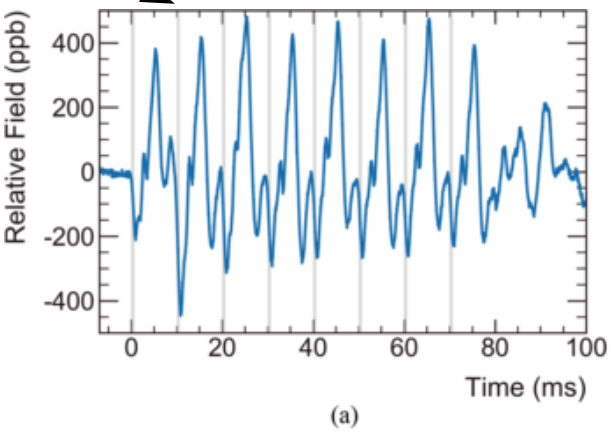

(a)

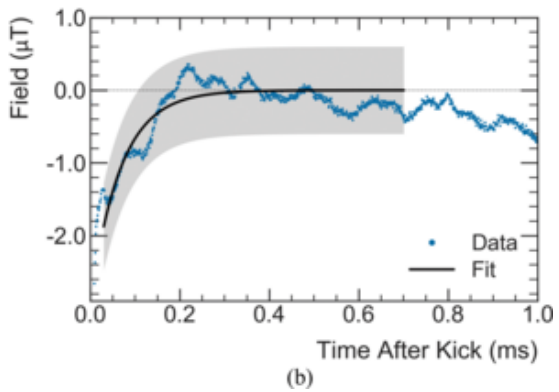

(b)

- Low-frequency oscillations of the electrostatic quadrupole plates
- Measured with dedicated probes

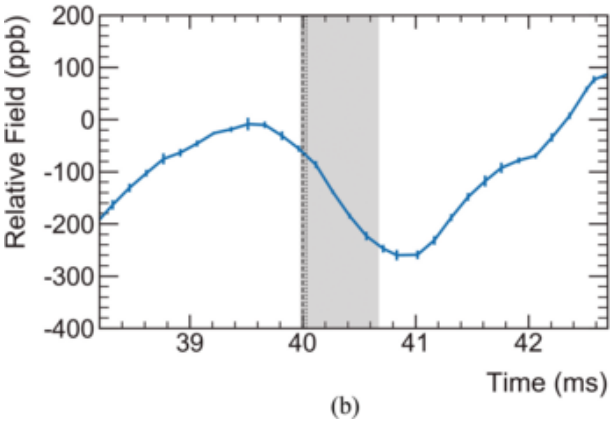

(b)

Overview

The Muon g-2

Experimental principles

The Muon g-2
Experiment at Fermilab

Latest results
and overlook

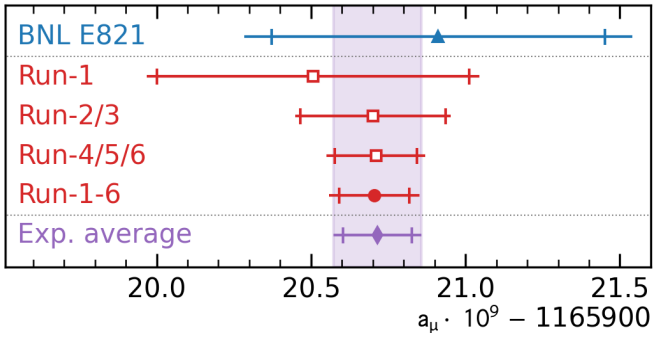

Run-456 results

- Final three datasets taken from 2020 to 2023
- They account for ~70% of total statistics
- Statistical design goal achieved in February 2023 and surpassed thereafter
- I will go through some of the most important improvements with respect to previous runs

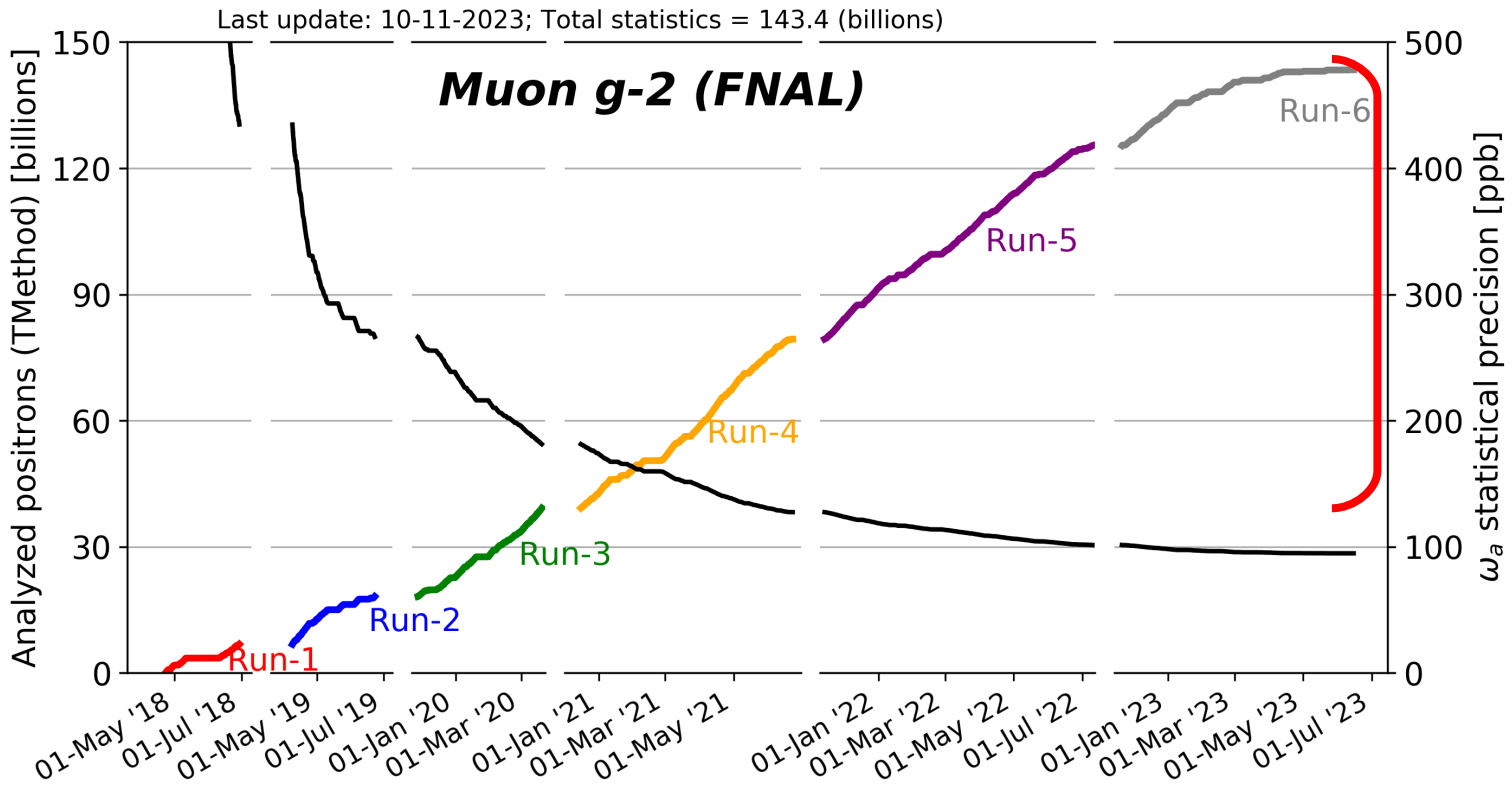

Kicker performance

- Toward the end of Run-3, upgraded kicker cables and improved impedance matching: kick now at design specs
- Result: better centering of muon distribution

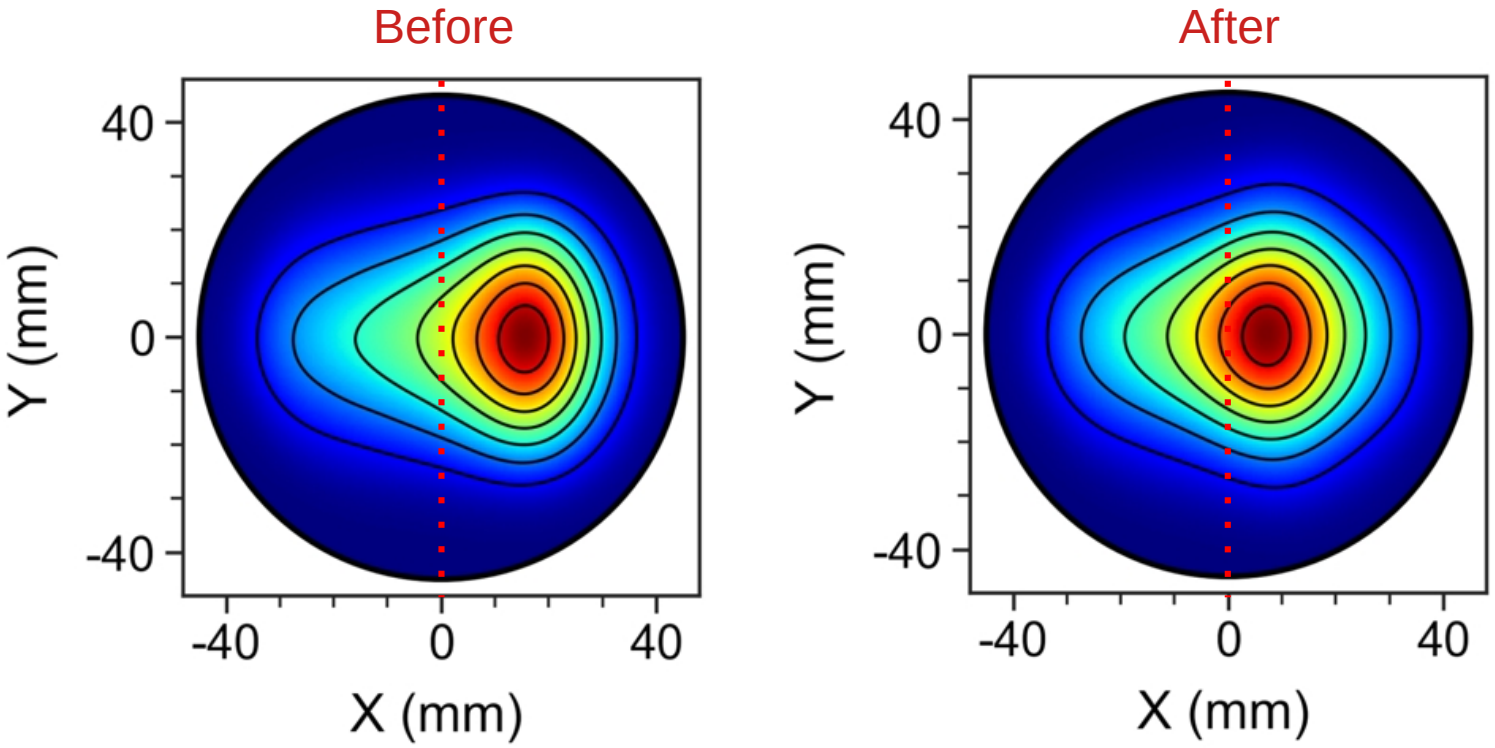

Quadrupole RF

- A quadrupole radio-frequency dampening system has been installed at the end of Run-4
- The RF pulsing scheme generates a resonant kick within 10 μs after the beam injection. This reduces the radial and vertical oscillations of the beam
- Turned on starting from Run-5

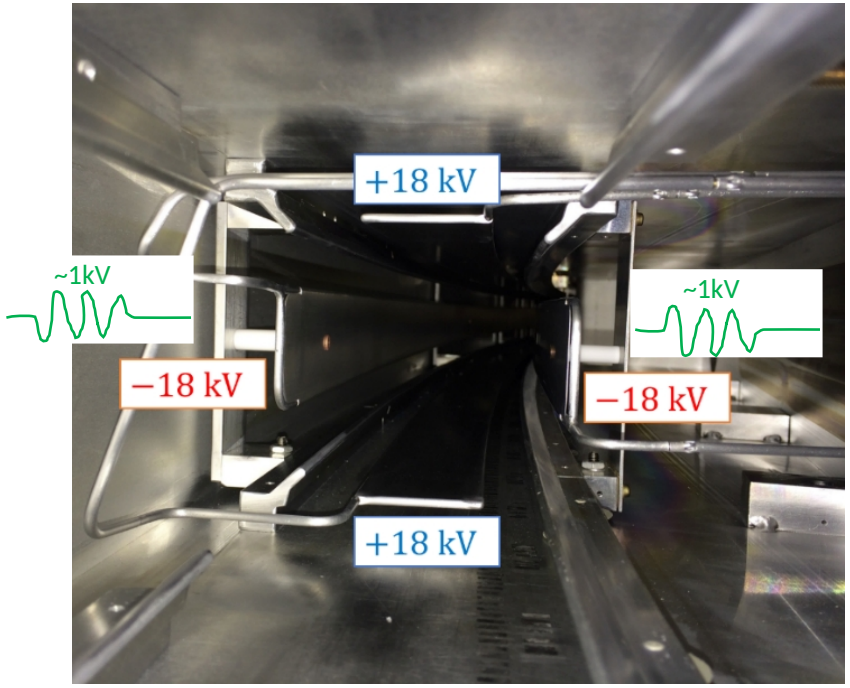

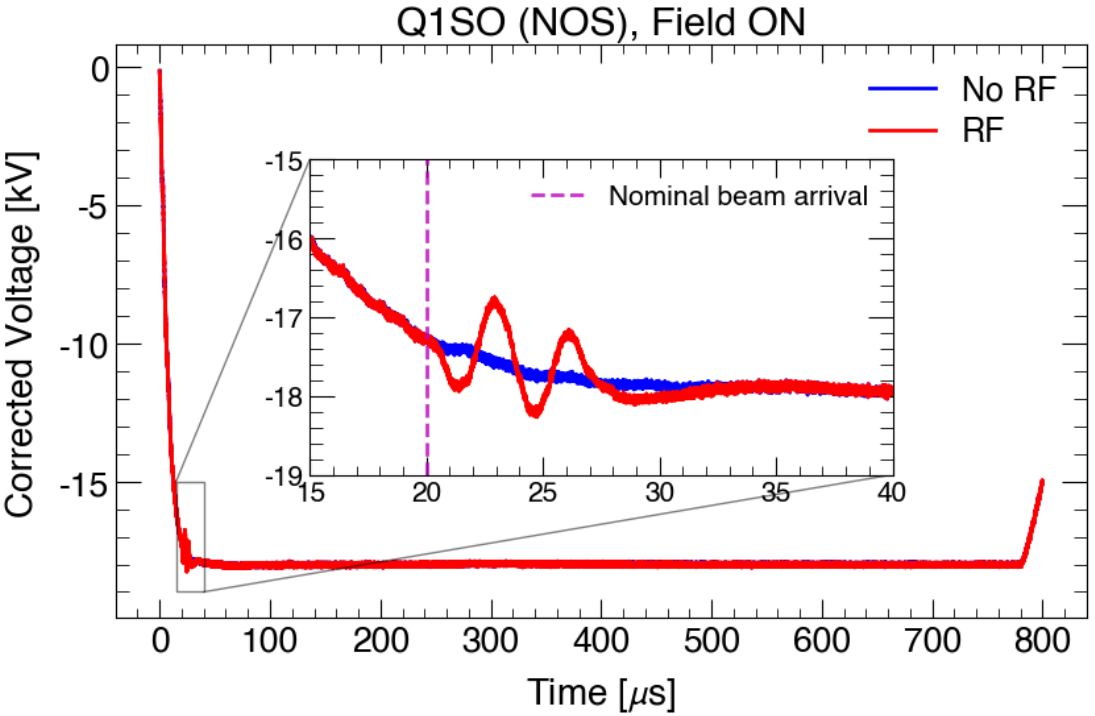

Quadrupole RF

- Coherent Betatron Oscillation (CBO) amplitude decreased by factor ~9
- Decreasing CBO systematic uncertainties, among the largest ones in Run-23

No RF

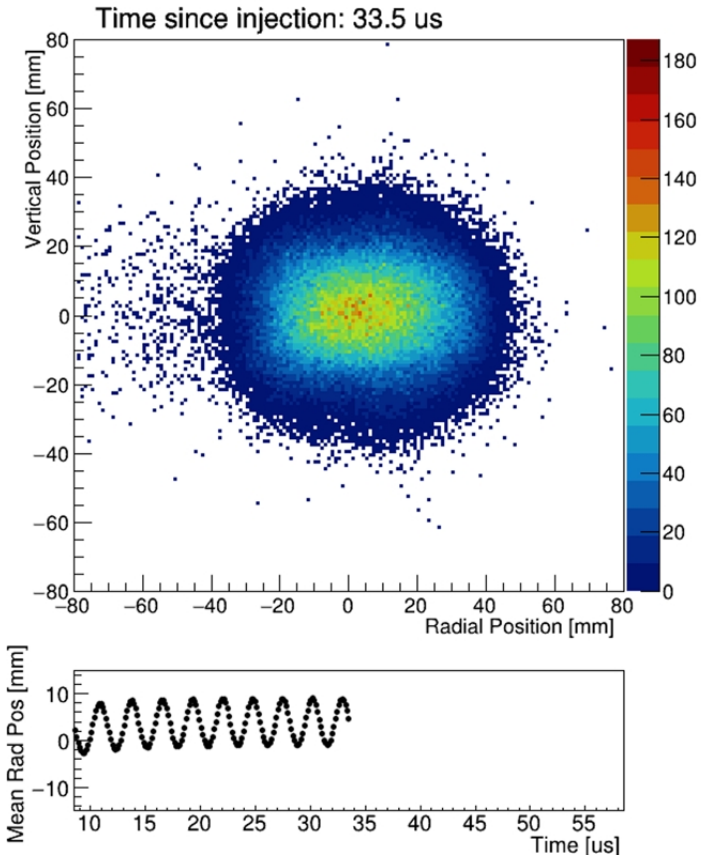

With RF

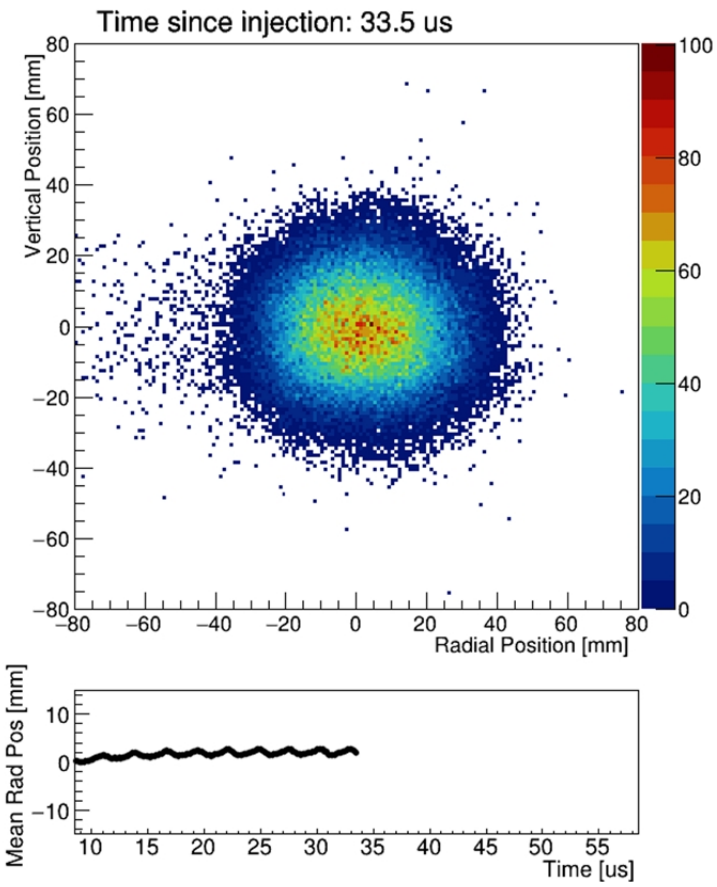

E-field correction

$$\left(a_\mu - \frac{1}{\gamma^2 - 1}\right) \vec{\beta} \times \vec{E}$$

=0 for
p = 3.094 GeV/c

$$\frac{\omega_a}{\omega_p} = \frac{\omega_a^m}{\omega_p^m} \frac{1 + C_e + C_p + C_{pa} + C_{dd} + C_{ml}}{1 + B_k + B_q}$$

- Not all muons have perfect magic momentum of 3.094 GeV/c
  - Higher momentum → larger orbit radius → longer period
  - Lower momentum → smaller orbit radius → shorter period
- Dephasing and radial position are used to extract the stored momentum spectrum

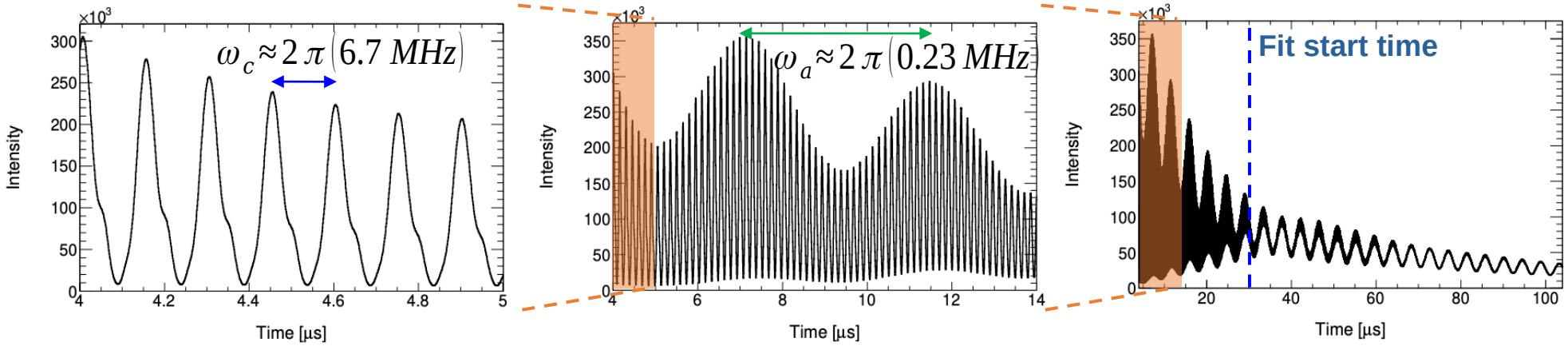

Momentum distribution

- **Trackers**
  - Parasitic: measure muon dispersion from decay positrons and use beam dynamics
- **Calorimeters**
  - Parasitic: measure muon dephasing (how muons spread into the beam) to infer radial distribution
  - Improved robustness of method
- Two new **Mini**mally intrusive **Sci**ntillating **Fi**ber (Mini-SciFi) detectors installed before Run-6
  - Vertical and Horizontal versions
  - Destructive: Cross-checks and uncertainty determination (tracker)

Momentum distribution

- **Trackers**
  - Parasitic: measure muon dispersion from decay positrons and use beam dynamics
- **Calorimeters**
  - Parasitic: measure muon dephasing (how muons spread into the beam) to infer radial distribution
  - Improved robustness of method
- Two new **Mini**mally intrusive **Sci**ntillating **Fi**ber (Mini-SciFi) detectors installed before Run-6
  - Vertical and Horizontal versions
  - Destructive: Cross-checks and uncertainty determination (tracker)

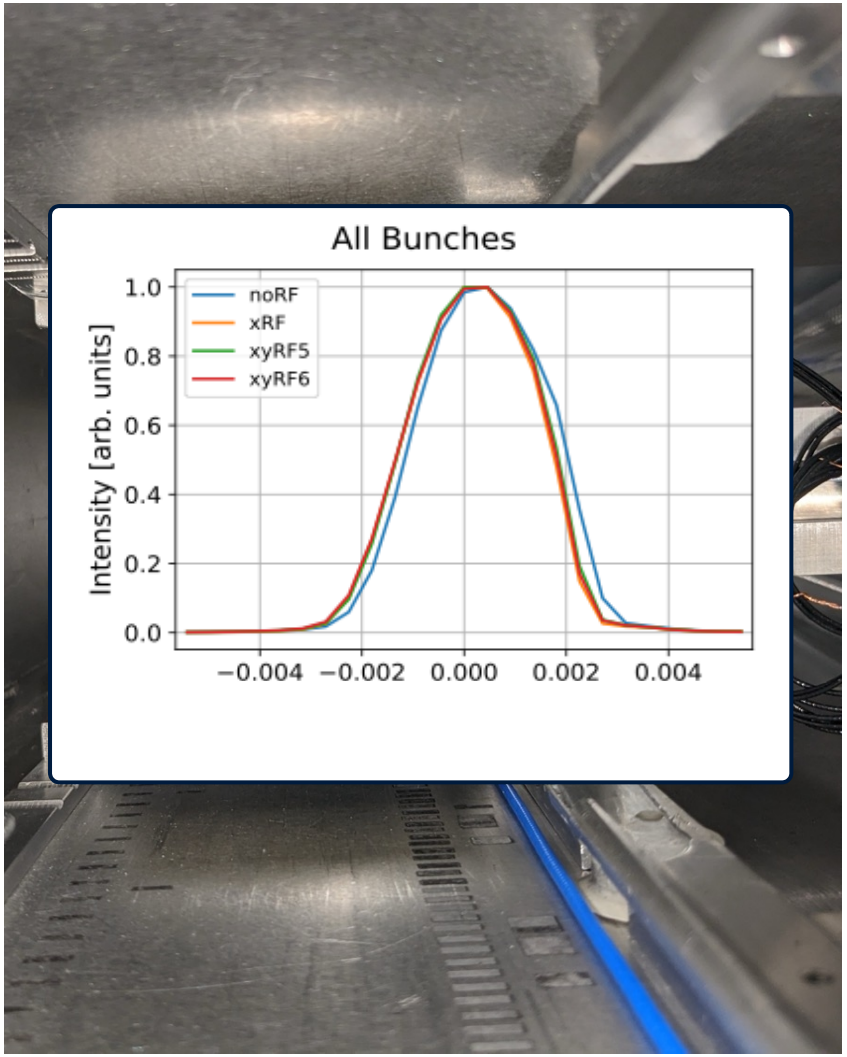

E-field correction

- The largest correction: 347 ppb
- The three different approaches increased confidence and resulted in small reduction of uncertainties to total of only 27 ppb

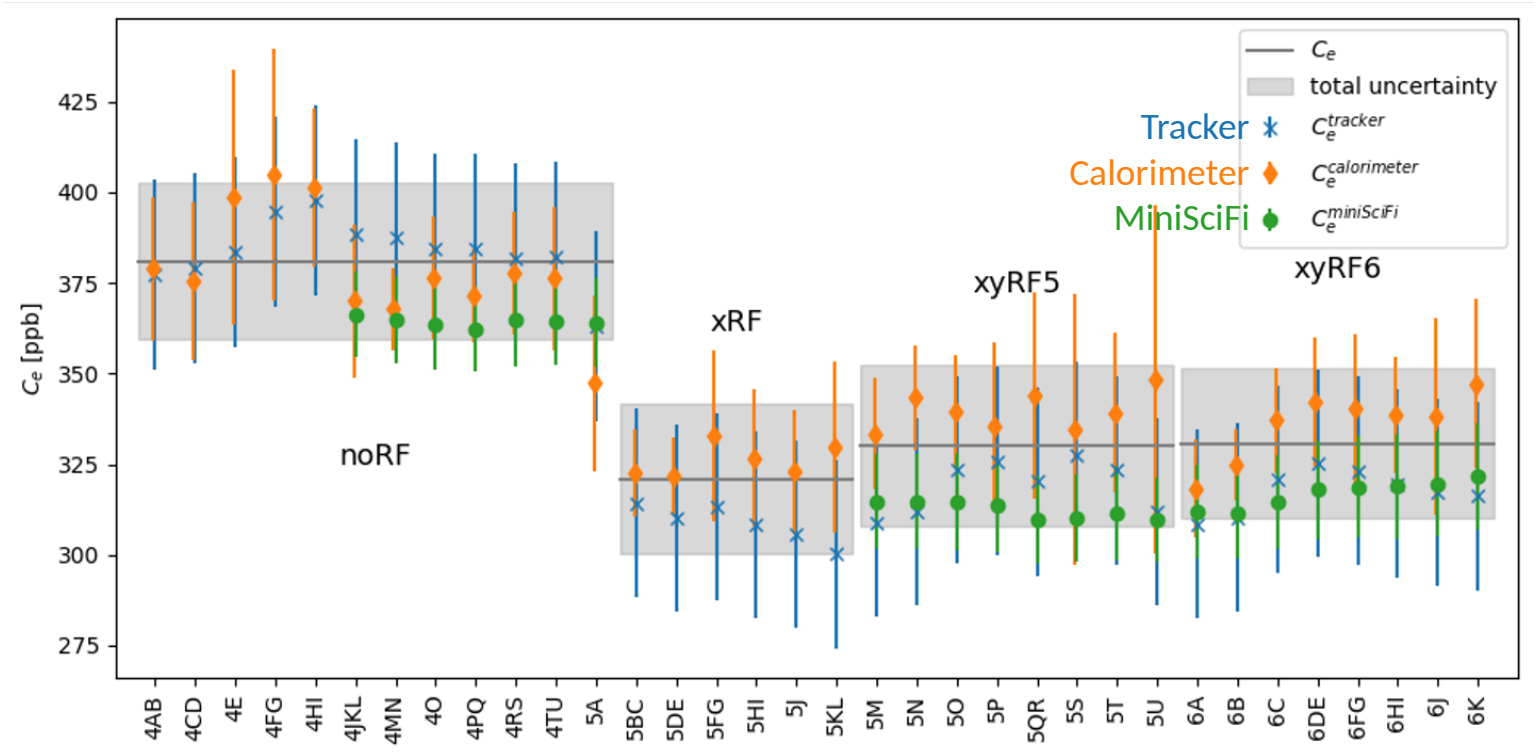

Field calibrations

- Excellent performance of field determinations in Run-23, already exceeding TDR goals
- Some improvements and cross checks in Run-456 analysis to increase trust in methods
- New tests on absolute calibration with ^{3}He probe
- Cross calibration measurements with Japan collaboration
- Improved trolley position algorithms

$$\frac{\omega_a}{\omega_p} = \frac{\omega_a^m}{\omega_p^m} \frac{1 + C_e + C_p + C_{pa} + C_{dd} + C_{ml}}{1 + B_k + B_q}$$

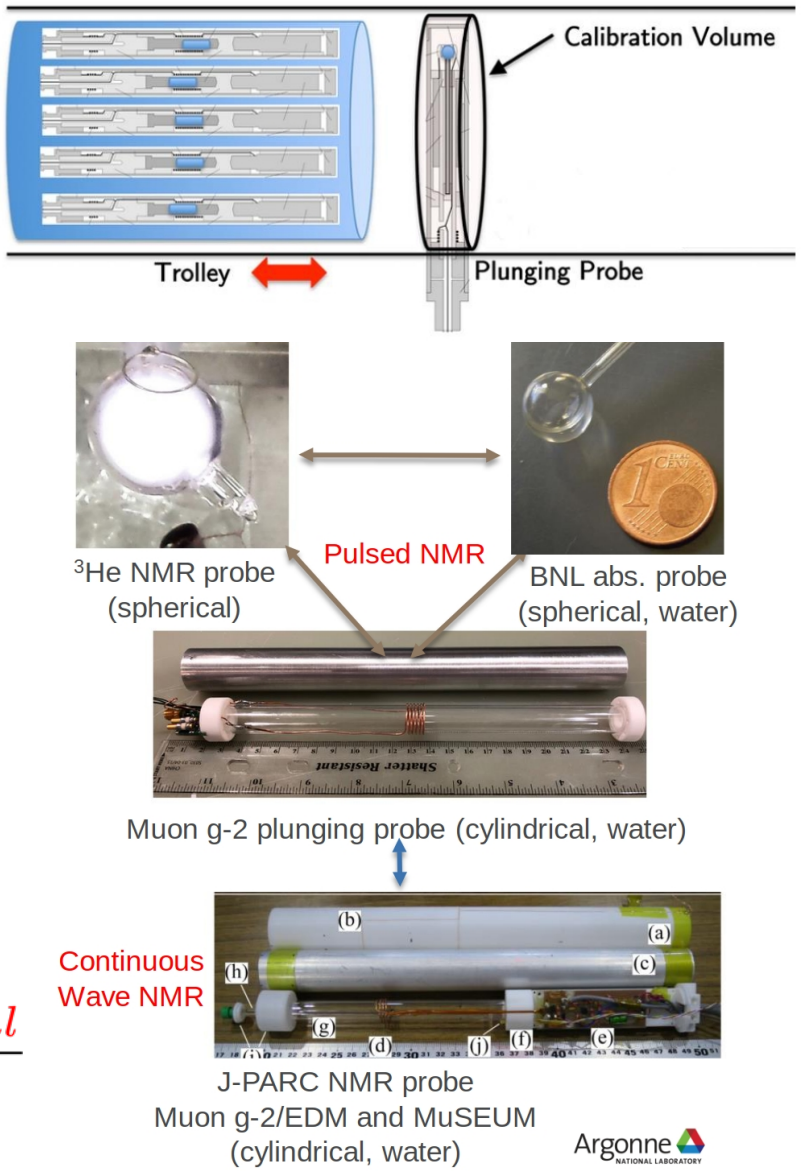

Kicker transient

- Kickers induce slowly decaying eddy currents in the surrounding aluminum
- Two Faraday magnetometers to measure the effect: one with optic fibers and a new one with free-space laser since the end of Run-5
- Improved suppression of mechanical vibrations and multiple radial position measurements

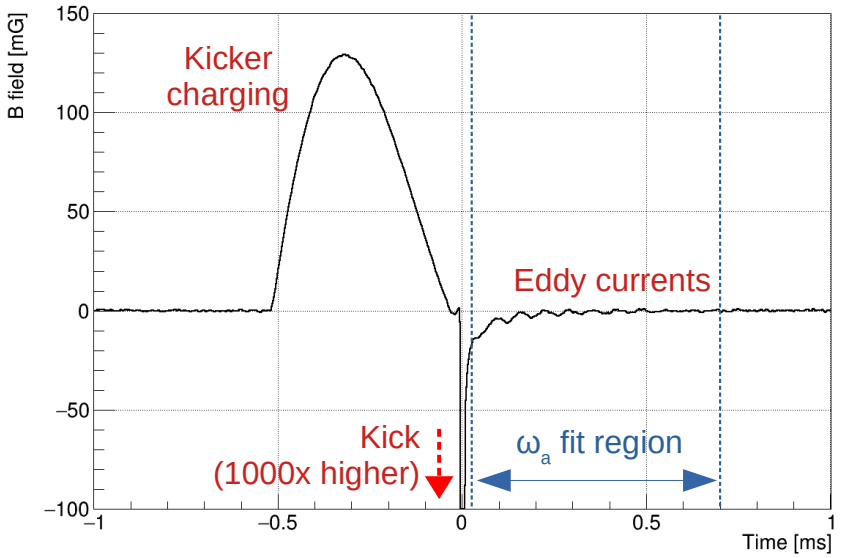

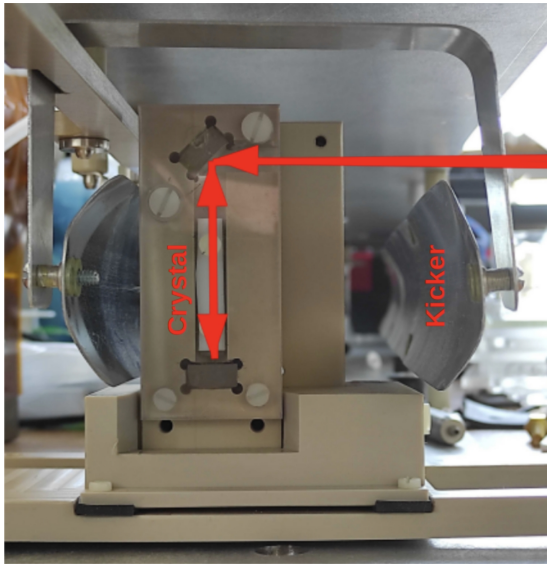

Laser

$$\frac{\omega_a}{\omega_p} = \frac{\omega_a^m}{\omega_p^m} \frac{1 + C_e + C_p + C_{pa} + C_{dd} + C_{ml}}{1 + B_k + B_q}$$

Kicker transient

- We the new measurements we found that the effect from eddy currents has a radial position dependency
- Confirmed with independent laboratory mock-up measurements

Measured data and prediction

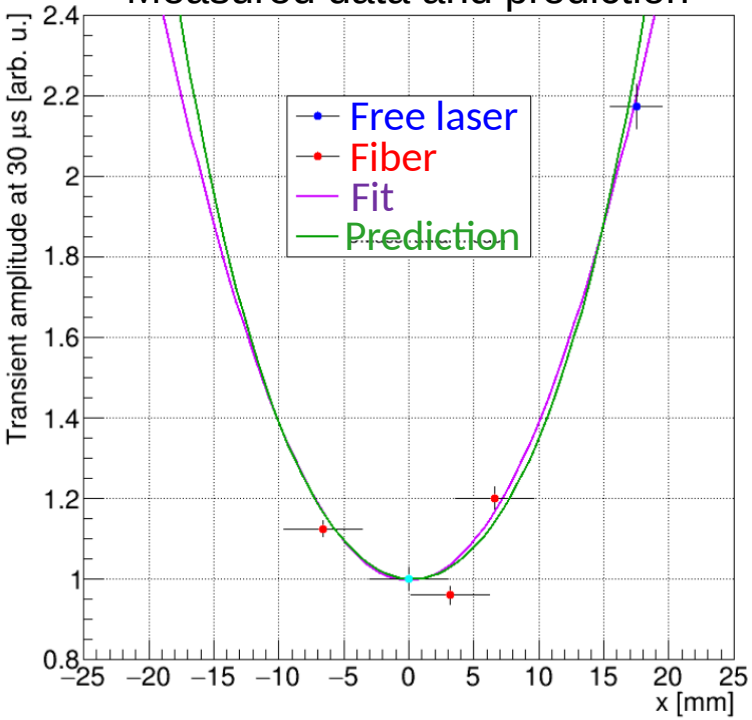

Measurement-based spatial model

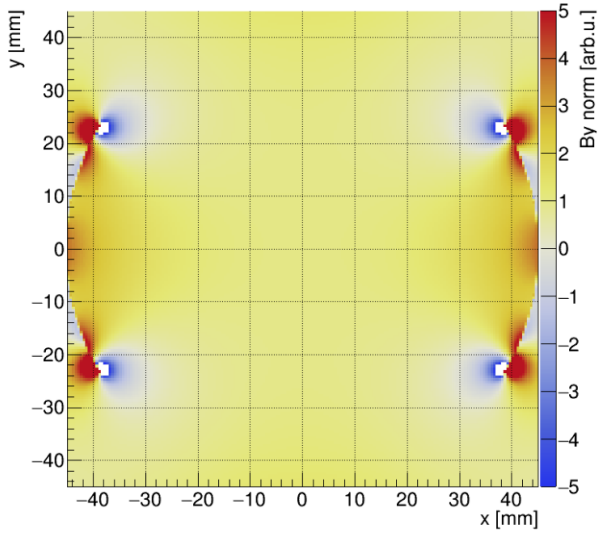

Mock-up with pickup coils

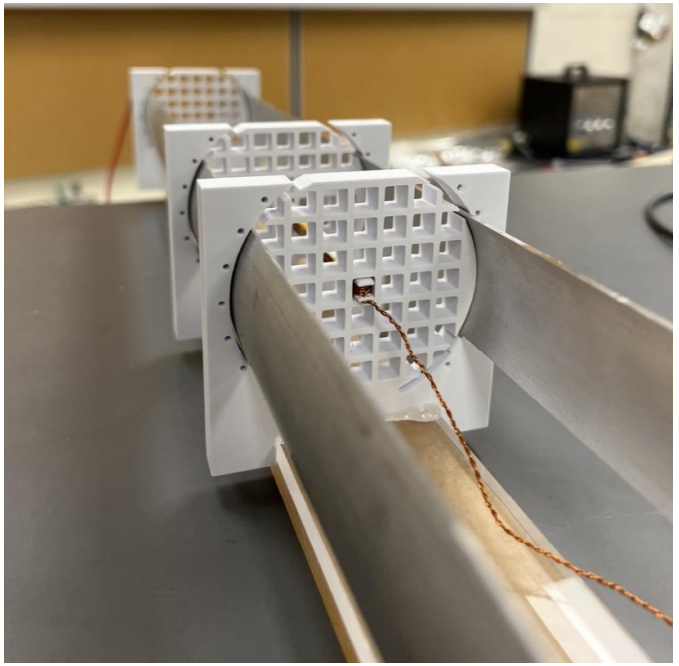

Positron reconstruction

- Three calorimeter positron reconstructions techniques, with a new one since Run-4
- All have been upgraded to further improve pulse fitting and positron cluster separation
- Pileup has been reduced by 2x or more, and is no longer a dominant systematic in ω_a measurement
- Improved energy reconstruction accuracy

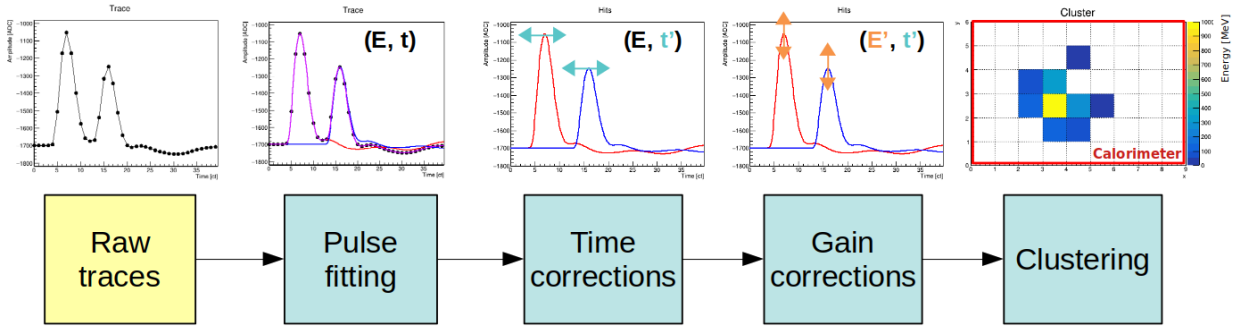

$$\frac{\omega_a}{\omega_p} = \frac{\omega_a^m}{\omega_p^m} \frac{1 + C_e + C_p + C_{pa} + C_{dd} + C_{ml}}{1 + B_k + B_q}$$

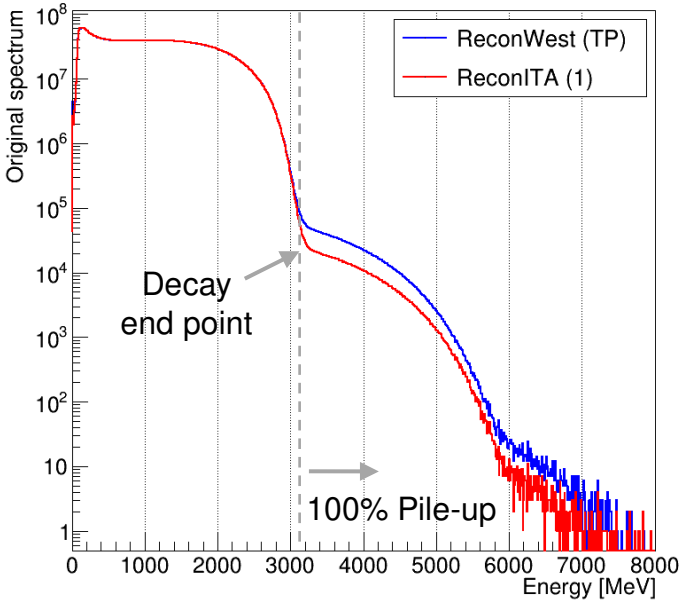

Uncertainties

	Statistical (ppb)	Systematic (ppb)	Total (ppb)
Run-1	434	159	462
Run-2/3	201	78	216
Run-4/5/6	114	76	137
Run-1-6	98	78	125

TDR goal:
100 ppb ✓

TDR goal:
100 ppb ✓

TDR goal:
140 ppb ✓

Systematic unc.

Run-4/5/6

Quantity		Correction (ppb)	Uncertainty (ppb)
ω_a^m	(statistical)	···	114
ω_a^m	(systematic)	···	30
C_e	Electric Field	347	27
C_p	Pitch	175	9
C_{pa}	Phase Acceptance	-33	15
C_{dd}	Differential Decay	26	27
C_{ml}	Muon Loss	0	2
$\langle \omega_p' \times M \rangle$	(mapping, tracking)	···	34
$\langle \omega_p' \times M \rangle$	(calibration)	···	34
B_k	Transient Kicker	-37	22
B_q	Transient ESQ	-21	20
μ_p'/μ_B		···	4
m_μ/m_e		···	22
Total systematic for $\mathcal{R}_\mu'$		···	76
Total for a_μ		572	139

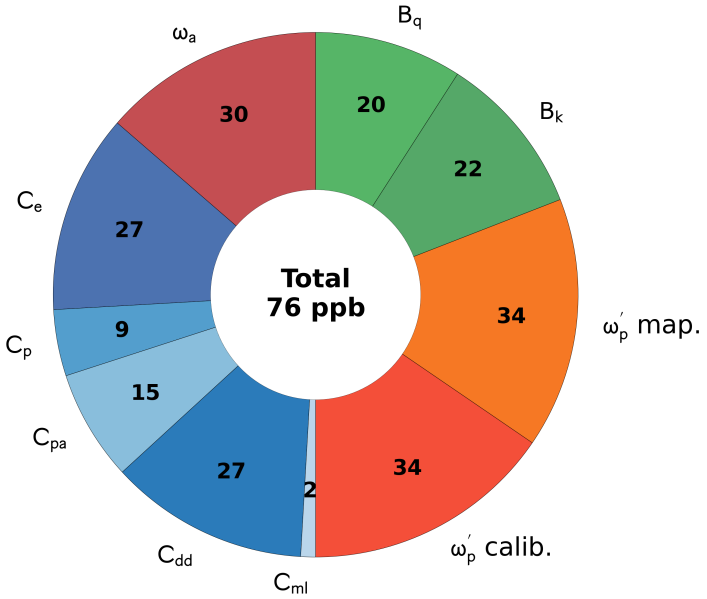

- TDR goal: 100 ppb ✓
- "evenly" distributed
  - No dominant source
  - Further improving would require to reduce in many categories

Unblinding process

- Calorimeter digitization clocks are artificially de-tuned by a secret <40 ppm amount by two individuals external to the Muon g-2 collaboration
- Many review stages for all analyses. After the final global review, we unblind by revealing the secret offset
- The Run-4/5/6 unblinding took place on May 20th, 2025

Final results

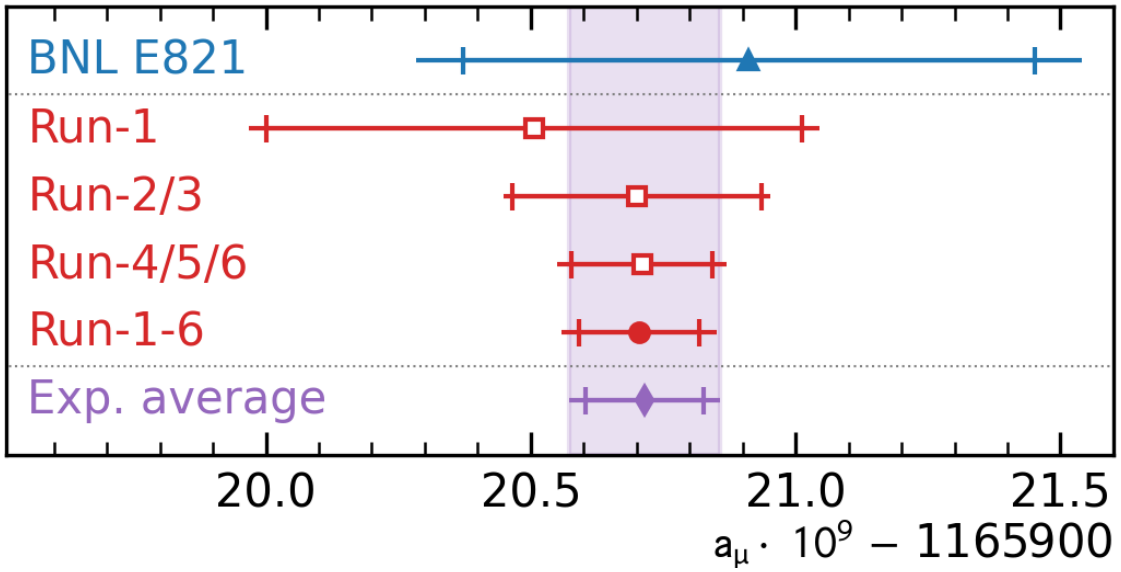

- Fantastic agreement with previous runs and with BNL experiment
- World most precise measurement of the muon anomaly
- This measurement will remain a benchmark for many years to come

Consistency check

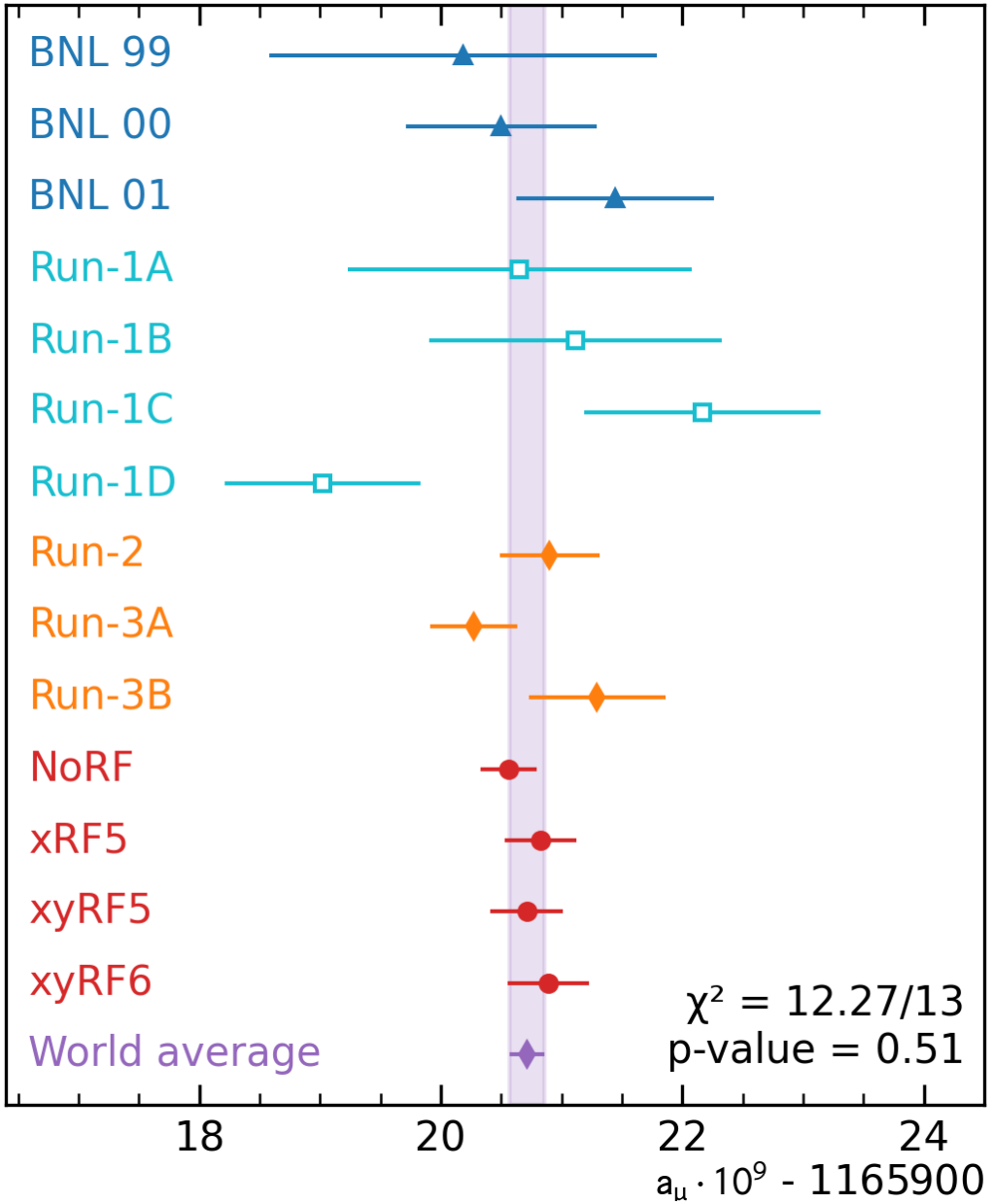

History

Before the Fermilab Muon g-2 Experiment

- 100+ theorist compile the theoretical input and provide recommendations
- muon-gm2-theory.illinois.edu

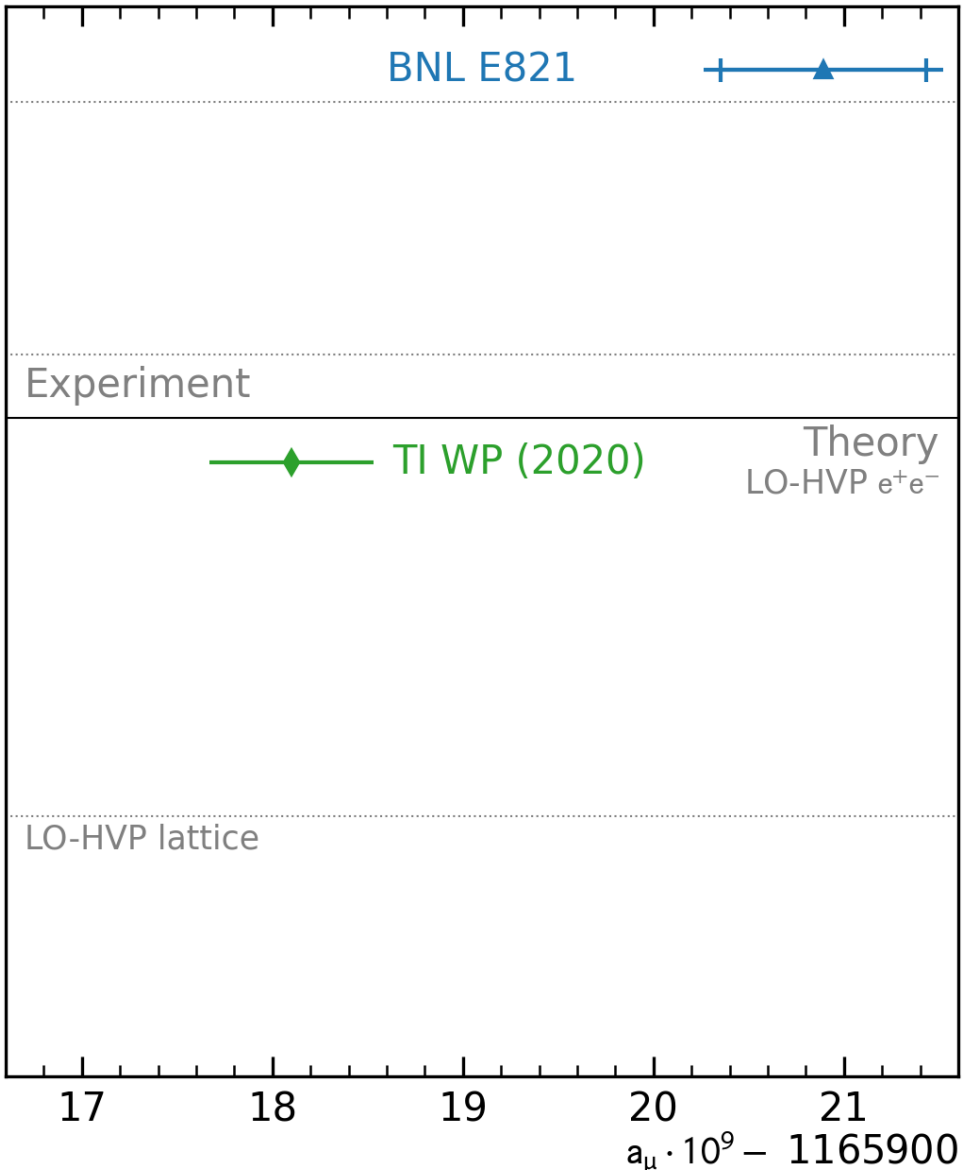

- TI White Paper 2020
  Physics Reports 887 (2020) 1-166

History

TI White Paper 2020

- Hadronic Vacuum Polarization (HVP)

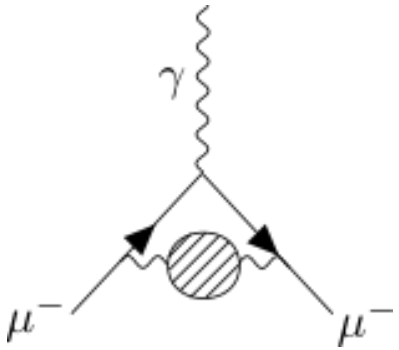

- data-driven dispersive approach from data from different experiments over 20+ years

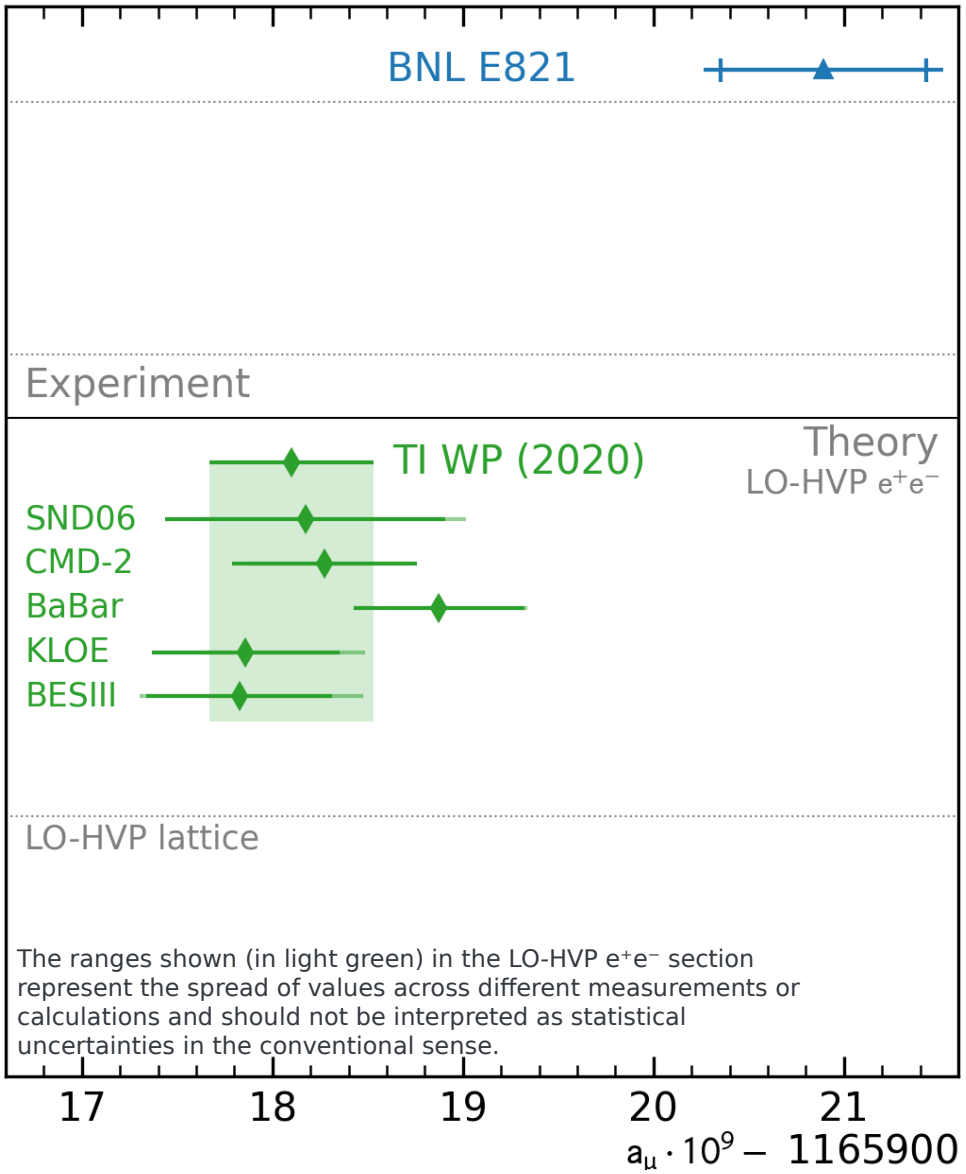

History

April 2021: Fermilab Run-1

- 5% of our full dataset
- In good agreement with previous results

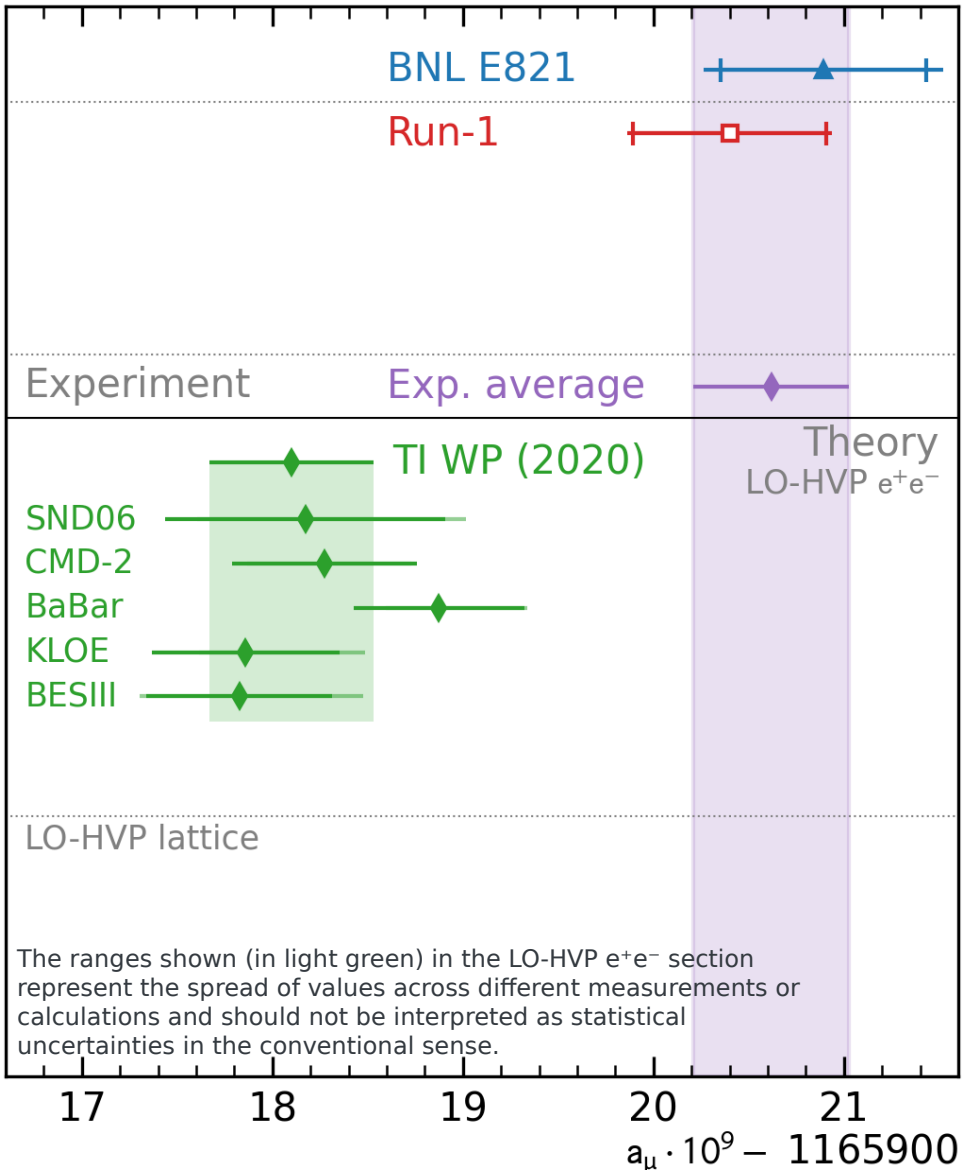

History

HVP lattice calculation

- First high-precision calculations of LO-HVP on lattice-QCD

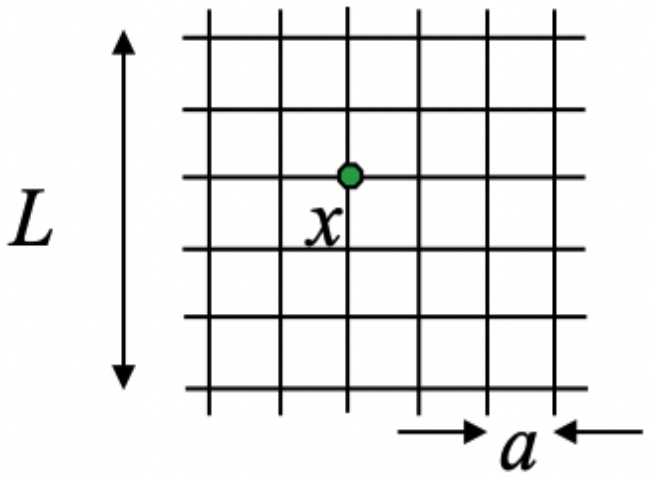

- in tension with the data-driven approach

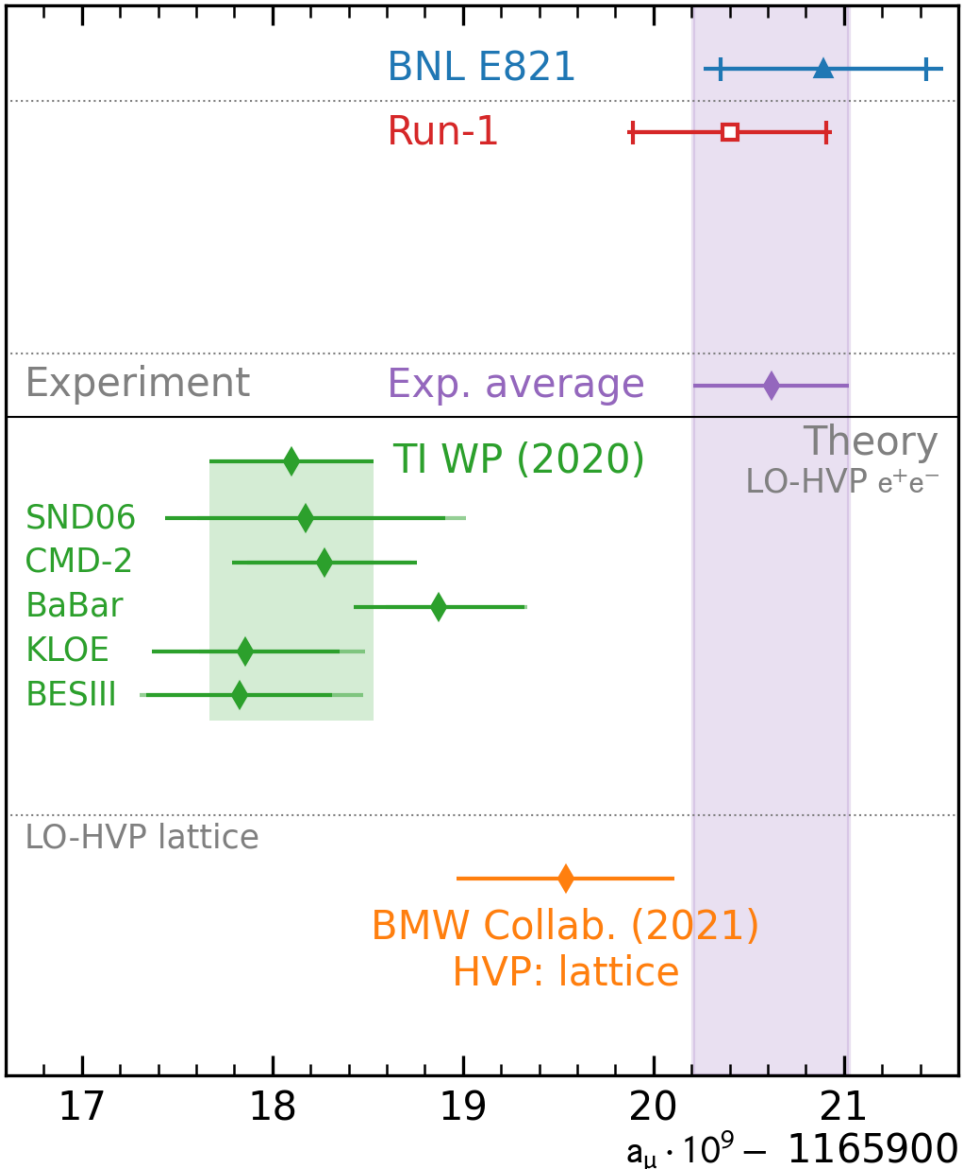

History

New Input Data

- New results from the CMD-3 experiment are in tension with WP (2020) input

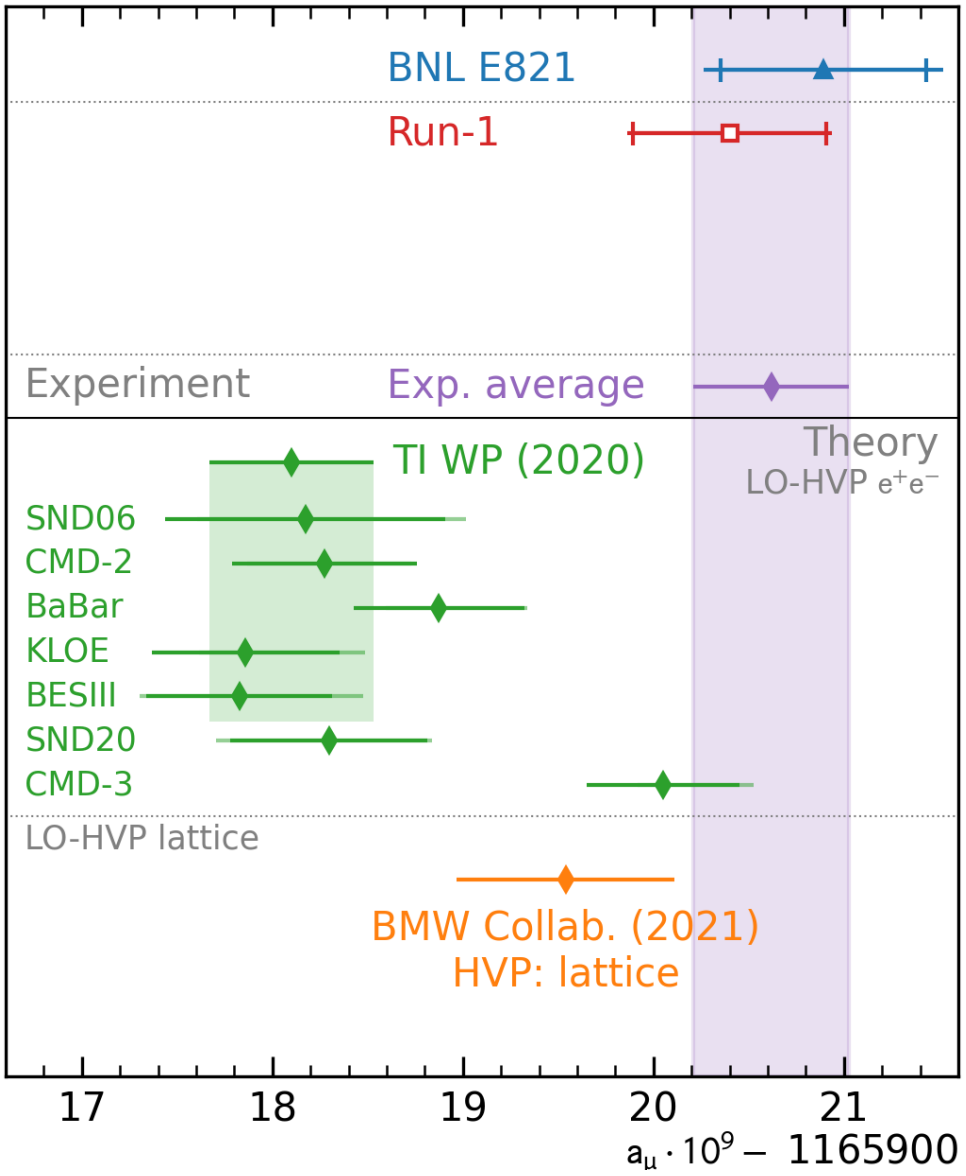

History

August 2023: Fermilab Run-2/3

- 4.6 times more data
- More than a two-fold increase in precision

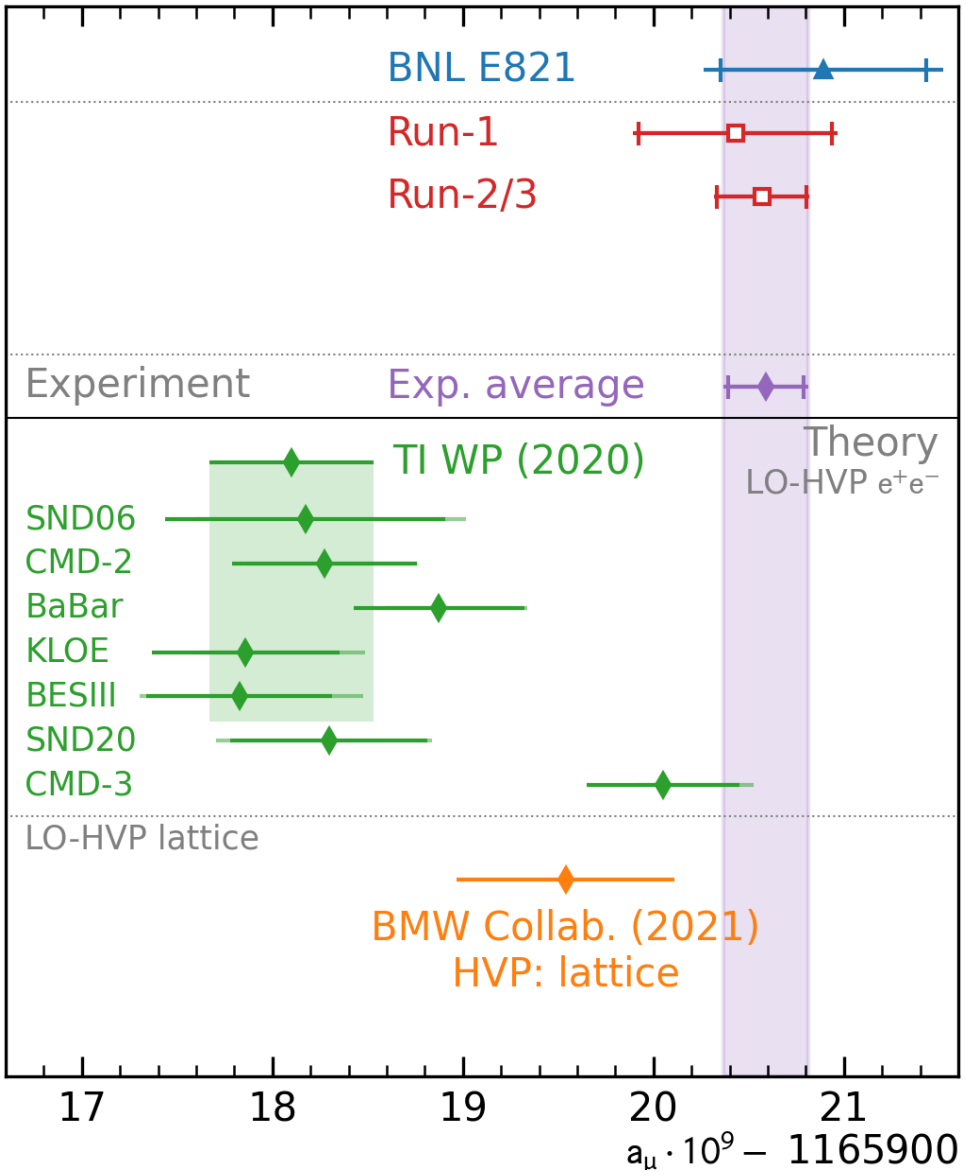

History

TI White Paper 2025

- New TI White Paper (2025) using only lattice-QCD based LO-HVP determination
- Uses input from several published lattice-QCD calculations to compile the WP (2025) value
- *small changes in the points from other (not HVP-LO) contribution
- **TI White Paper 2025** arXiv:2505.21476

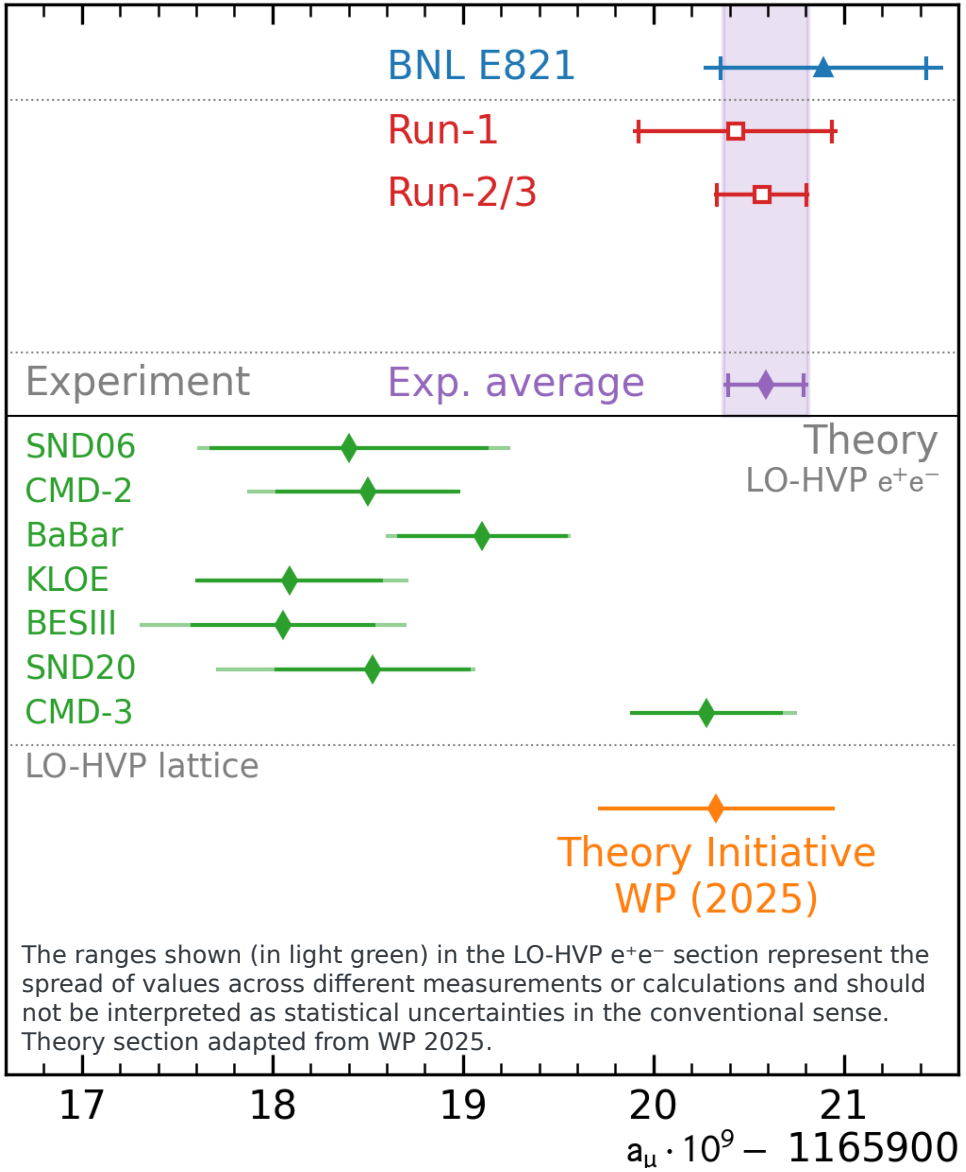

History

June 2025: Run-4/5/6

- 2.6 times more data
- Final precision of 127 ppb, more than a 4-fold improvement over the BNL result

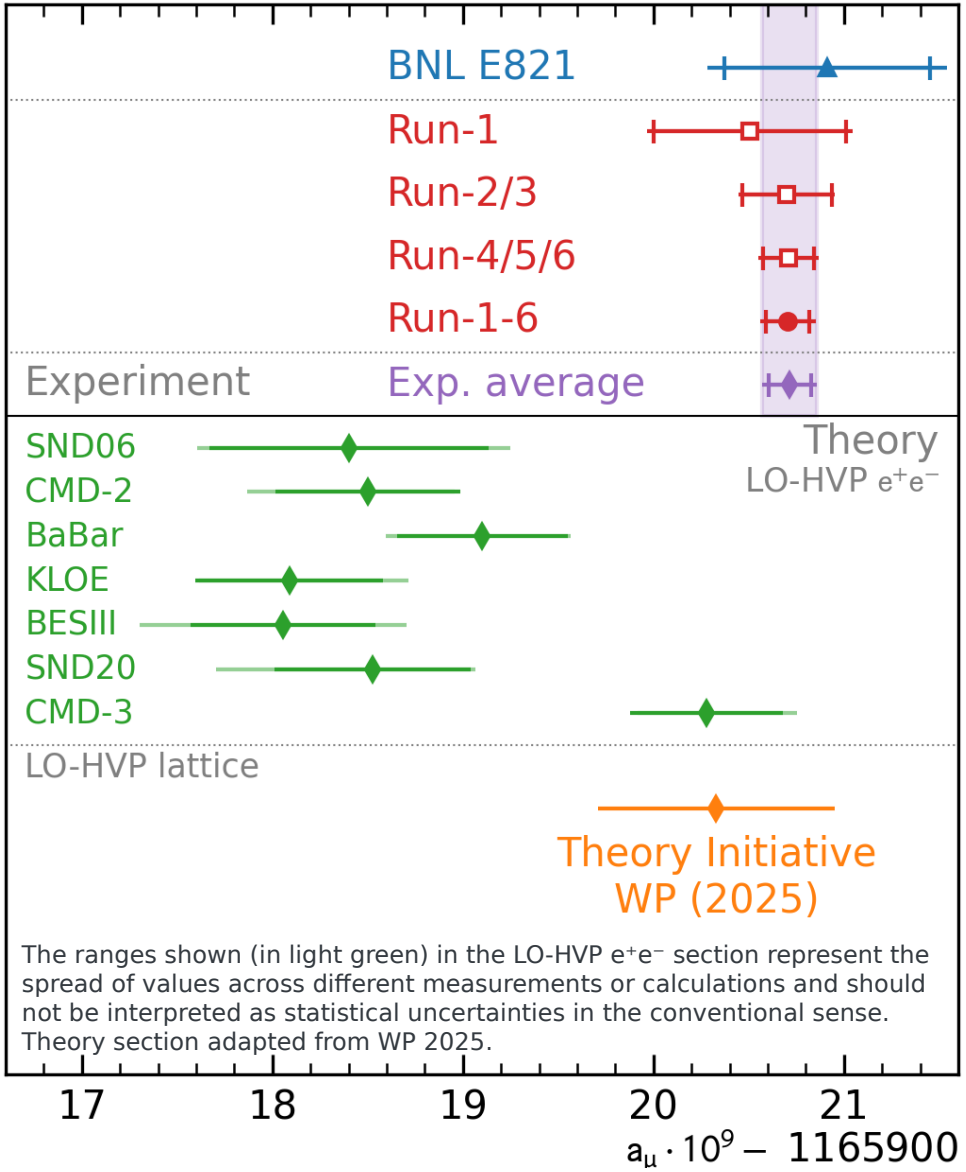

Not only a_μ

- **Electric Dipole Moment (EDM)**
  - If the muon has EDM, the spin precession plane will be tilted
  - Run-1/2/3 results are expected soon
  - Current limit (BNL): 1.8×10^{-19} e*cm
  - Projected limit: $< 3 \times 10^{-20}$ e*cm
- **CPT and Lorentz Invariance violation**
  - Sidereal modulation of ω_a frequency
  - Run-2/3 in review
  - Current limit (BNL): 1.4×10^{-24} GeV
  - Projected limit: $O(10^{-25})$ GeV
- **Ultralight Muonic Dark Matter (scalar)**
  - ω_a modulated at the DM compton frequency
  - Run-2/3 in progress

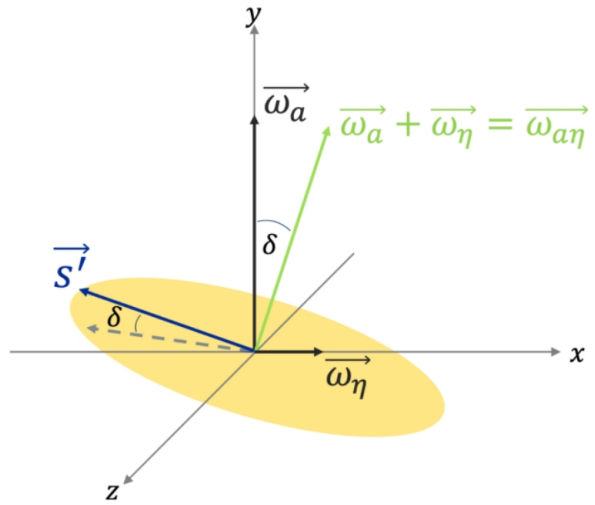

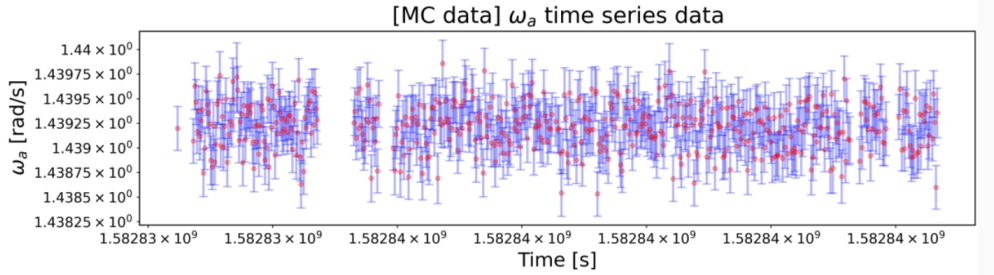

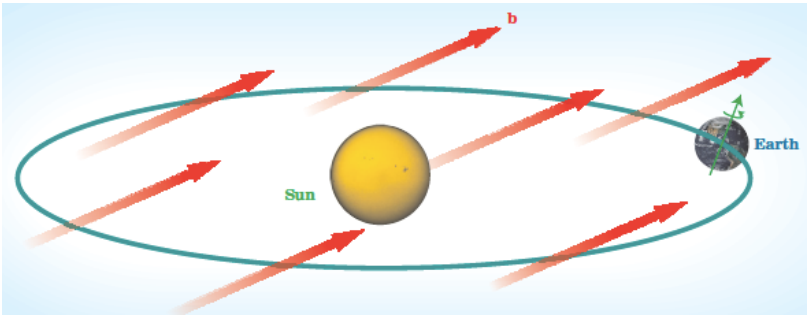

Future experiments

- **Muon g-2/EDM** Experiment **@J-PARC**
  - Innovative novel techniques (muon acceleration, spiral injection, etc.)

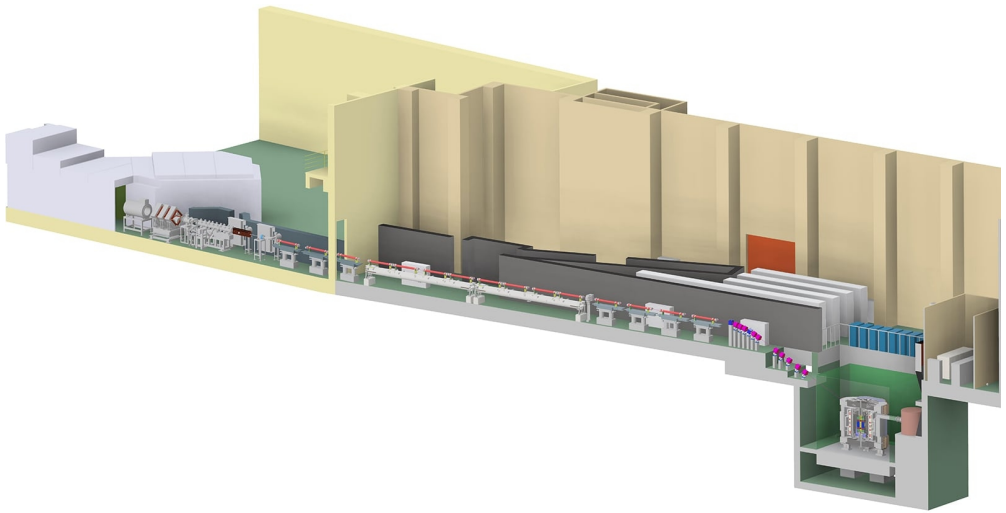

- Proposed **MUonE @CERN**

$$a_\mu^{HLO} = \frac{\alpha}{\pi}\int_0^1 dx(1-x)\Delta\alpha_{had}[t(x)]$$

- hadronic contribution to the running of $\Delta\alpha_{had}$ in the space-like region
- can be extracted from the shape of differential cross section

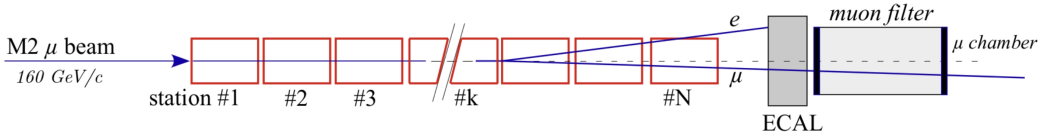

Future theory improvements

- Ongoing work in experimental inputs on $\sigma(e^+e^- \rightarrow \text{hadrons})$
- Initial State Radiation technique:
  - BaBar: new analysis of large $\pi\pi$ data set with better detector
  - KLOE: new analysis of 7x larger $\pi\pi$ set
  - BESIII: new results for $\pi\pi$ channel and $\pi\pi\pi$
  - Belle II: larger statistics than BaBar or KLOE and similar or better systematics for low-energy cross sections
- Energy scan (VEPP-2000 machine in Novosibirsk)
  - SND: new results for $\pi\pi$ channel
  - CMD-3: more channels to be analyzed
- The RadioMonteCarLow2 initiative is committed to improving the Monte Carlo event generators

Summary

PHYSICAL REVIEW LETTERS **135,** 101802 (2025)

Editors' Suggestion | Featured in Physics

Measurement of the Positive Muon Anomalous Magnetic Moment to 127 ppb

D. P. Aguillard,[33] T. Albahri,[30] D. Allspach,[7] J. Annala,[7] K. Badgley,[7] S. Baeßler,[35] I. Bailey,[16,a] L. Bailey,[27] E. Barlas-Yucel,[28,b] T. Barrett,[6] E. Barzi,[7] F. Bedeschi,[10] M. Berz,[17] M. Bhattacharya,[7] H. P. Binney,[36] P. Bloom,[18] J. Bono,[7] E. Bottalico,[30] T. Bowcock,[30] S. Braun,[36] M. Bressler,[32] G. Cantatore,[12,c] R. M. Carey,[2] B. C. K. Casey,[7] D. Cauz,[26,d] R. Chakraborty,[29] A. Chapelain,[6] S. Chappa,[7] S. Charity,[30] C. Chen,[22,21,e] M. Cheng,[28] R. Chislett,[27] Z. Chu,[21,e] T. E. Chupp,[33] C. Claessens,[36] F. Confortini,[9,f] M. E. Convery,[7] S. Corrodi,[1] L. Cotrozzi,[30] J. D. Crnkovic,[7] S. Dabagov,[8,g] P. T. Debevec,[28] S. Di Falco,[10] G. Di Sciascio,[11] S. Donati,[10,h] B. Drendel,[7] A. Driutti,[10,29] M. Eads,[19] A. Edmonds,[2,37] J. Esquivel,[7] M. Farooq,[33] R. Fatemi,[29] K. Ferraby,[30] C. Ferrari,[10,i] M. Fertl,[14] A. T. Fienberg,[36] A. Fioretti,[10,i] D. Flay,[32] S. B. Foster,[29,2] H. Friedsam,[7] N. S. Froemming,[19] C. Gabbanini,[10,i] I. Gaines,[7] S. Ganguly,[7] J. George,[32,j] L. K. Gibbons,[6] A. Gioiosa,[25,k] K. L. Giovanetti,[13] P. Girotti,[10,l] W. Gohn,[29] L. Goodenough,[7] T. Gorringe,[29] J. Grange,[33] S. Grant,[1,27] F. Gray,[20] S. Haciomeroglu,[5,m] T. Halewood-Leagas,[30] D. Hampai,[8] F. Han,[29] J. Hempstead,[36] D. W. Hertzog,[36] G. Hesketh,[27] E. Hess,[10] A. Hibbert,[30] Z. Hodge,[36] S. Y. Hoh,[22,21,e] K. W. Hong,[35] R. Hong,[1,29] T. Hu,[22,21,e] Y. Hu,[21,e] M. Iacovacci,[9,f] M. Incagli,[10] S. Israel,[2,32] P. Kammel,[36] M. Kargiantoulakis,[7] M. Karuza,[12,n] J. Kaspar,[36] D. Kawall,[32] L. Kelton,[29,23] A. Keshavarzi,[31] D. S. Kessler,[32] K. S. Khaw,[22,21,e] Z. Khechadoorian,[6] B. Kiburg,[7] M. Kiburg,[7,18] O. Kim,[34] N. Kinnaird,[2] E. Kraegeloh,[33] K. R. Labe,[6] J. LaBounty,[36] M. Lancaster,[31] S. Lee,[5] B. Li,[21,o] D. Li,[21,p] L. Li,[21,e] I. Logashenko,[4,q] A. Lorente Campos,[29] Z. Lu,[21,e] A. Lucà,[7] G. Lukicov,[27] A. Lusiani,[10,r] A. L. Lyon,[7] B. MacCoy,[36] R. Madrak,[7] K. Makino,[17] S. Mastroianni,[9] R. McCarthy,[2,s] J. P. Miller,[2] S. Miozzi,[11] B. Mitra,[34] J. P. Morgan,[7] W. M. Morse,[3] J. Mott,[7] A. Nath,[9,f] J. K. Ng,[22,21,e] H. Nguyen,[7] Y. Oksuzian,[1] Z. Omarov,[15,5] W. Osar,[6] R. Osofsky,[36] S. Park,[5] G. Pauletta,[26,*,d] J. Peck,[29] G. M. Piacentino,[25,k] R. N. Pilato,[30] K. T. Pitts,[28,b] B. Plaster,[29] D. Počanić,[35] N. Pohlman,[19] C. C. Polly,[7] J. Price,[30] B. Quinn,[34] M. U. H. Qureshi,[14] G. Rakness,[7] S. Ramachandran,[1,j] E. Ramberg,[7] R. Reimann,[14] B. L. Roberts,[2] D. L. Rubin,[6] M. Sakurai,[27] L. Santi,[26,*,d] C. Schlesier,[28,t] A. Schreckenberger,[7] Y. K. Semertzidis,[5,15] A. K. Soha,[7] M. Sorbara,[11,u] J. Stapleton,[7] D. Still,[7] D. Stöckinger,[24] C. Stoughton,[7] D. Stratakis,[7] H. E. Swanson,[36] G. Sweetmore,[31] D. A. Sweigart,[6] M. J. Syphers,[19] Y. Takeuchi,[22,21,e] D. A. Tarazona,[6] T. Teubner,[30] A. E. Tewsley-Booth,[29,33] V. Tishchenko,[3] N. H. Tran,[2,v] W. Turner,[30] E. Valetov,[17] D. Vasilkova,[30] G. Venanzoni,[30,w] T. Walton,[7] A. Weisskopf,[17] L. Welty-Rieger,[7] P. Winter,[1] Y. Wu,[1] B. Yu,[34] M. Yucel,[7] E. Zaid,[30] Y. Zeng,[22,21,e] and C. Zhang[30]

(Muon $g-2$ Collaboration)

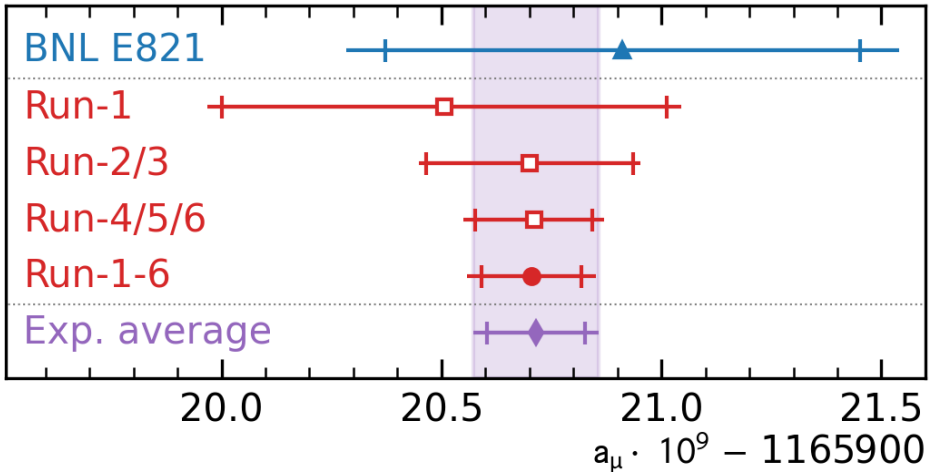

- Phys. Rev. Lett. **135**, 101802 https://doi.org/10.1103/7clf-sm2v
- Release talk (June 3rd) and 8-minute explainer video at https://www.youtube.com/@fermilab
- Visit https://muon-g-2.fnal.gov

谢谢 for listening!

Acknowledgements

- Department of Energy (USA)
- National Science Foundation (USA)
- Istituto Nazionale di Fisica Nucleare (Italy)
- Science and Technology Facilities Council (UK)
- Royal Society (UK)
- Leverhulme Trust (UK)
- European Union's Horizon 2020
- Strong 2020 (EU)
- German Research Foundation (DFG)
- National Natural Science Foundation of China
- MSIP, NRF and IBS-R017-D1 (Republic of Korea)

Backup

WP25 – dispersive

- Calculated from data for σ(e⁺e⁻→ hadrons)

Analyticity & Unitarity

$$a_\mu^{\mathrm{HVP,LO}} = \frac{\alpha^2}{3\pi^2}\int_{s_{th}}^{\infty}\frac{K(s)}{s}R(s)ds$$

Hadronic R-ratio (Data Driven)

- Uses **data** from different experiments from **20+ years**
- 1/s weights low energy strongly: 73% from **π⁺π⁻ channel**

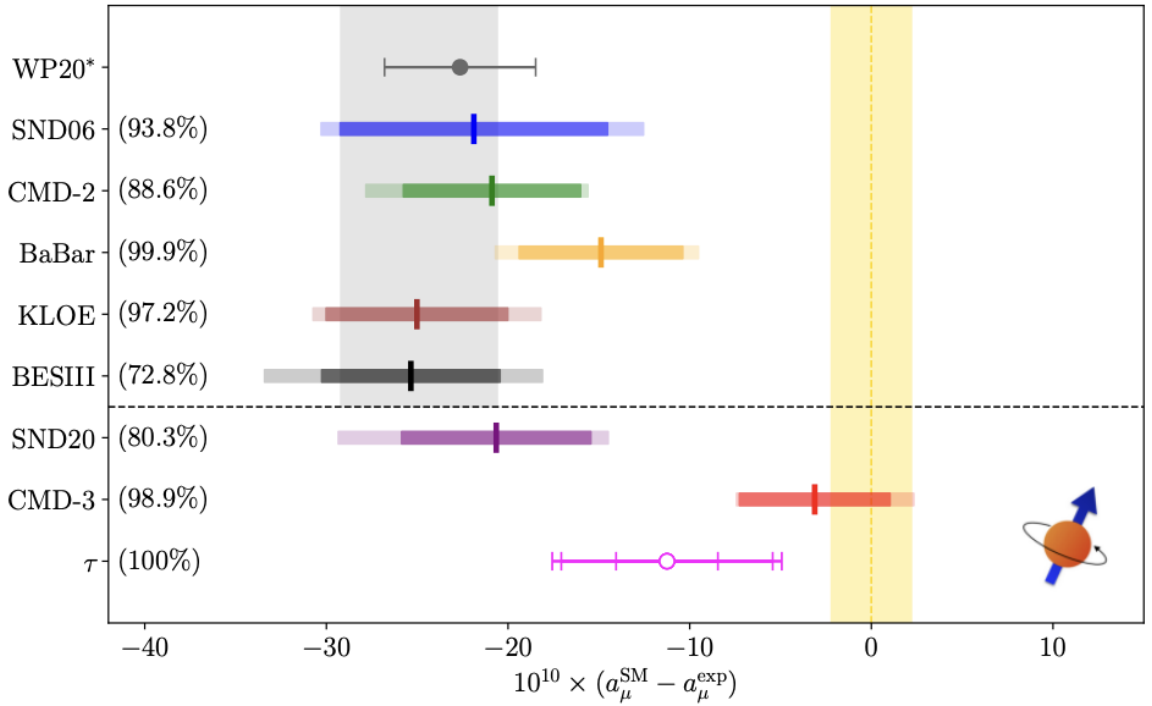

WP25 – dispersive

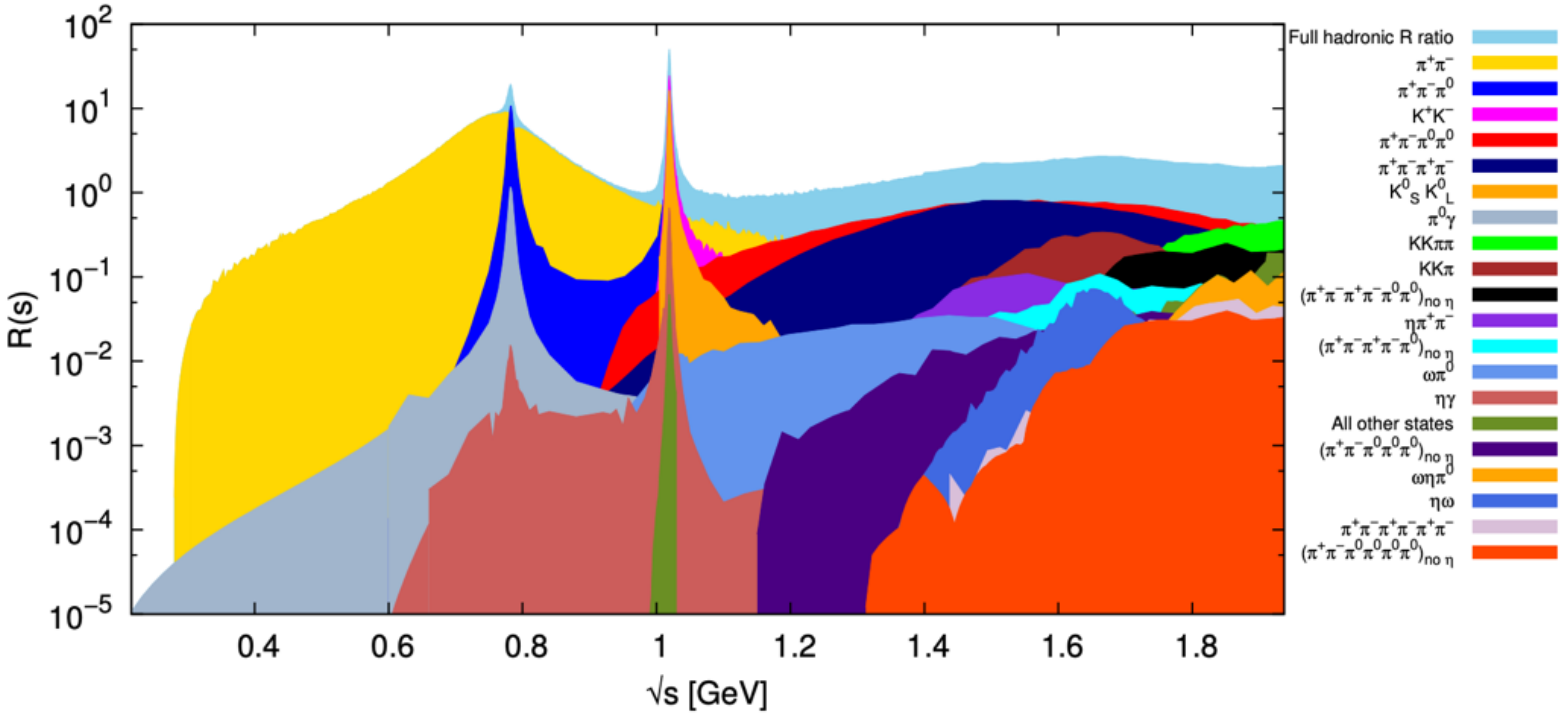

Figure 16: Contributions to the KNT data compilation of the total hadronic R-ratio from the different hadronic final states below 1.937 GeV [30, 265]. The full R-ratio is shown in light blue. Each final state is included as a new layer on top in decreasing order of the size of its contribution to $a_\mu^{\mathrm{HVP,\,LO}}$.

WP25 – lattice QCD

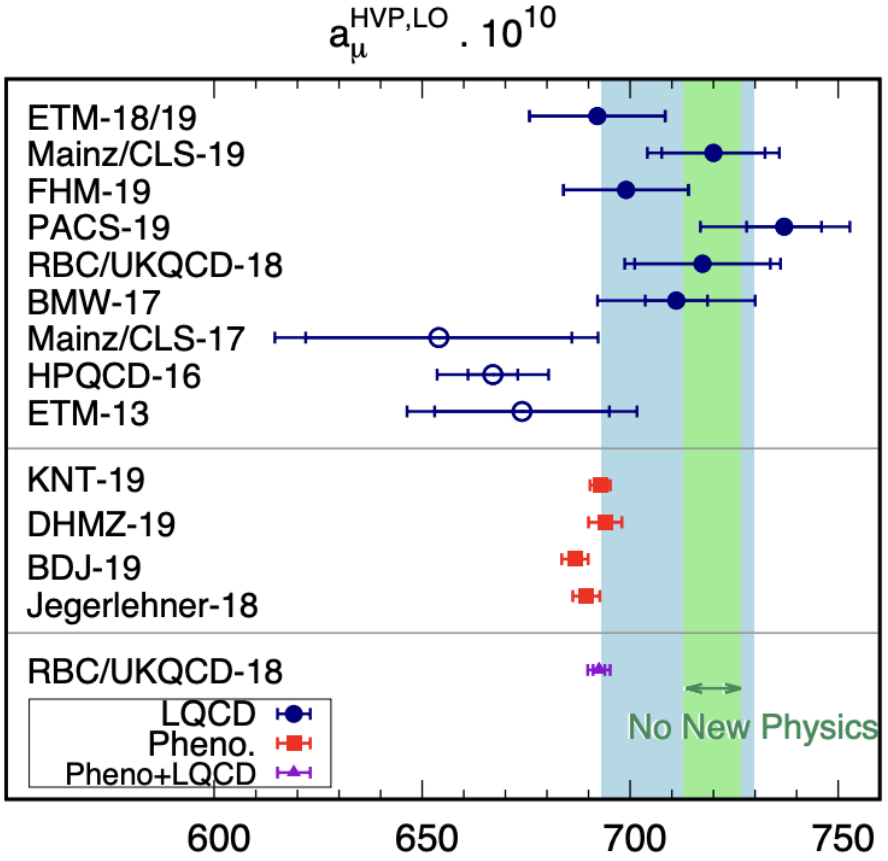

Figure 44: Compilation of recent results for $a_\mu^{\mathrm{HVP,\,LO}}$ in units of 10^{-10}. The filled dark blue circles are lattice results that are included in the "lattice world average". The average, which is obtained from a conservative averaging procedure in Sec. 3.5.1, is indicated by a light blue band, while the light-green band indicates the "no new physics" scenario, where $a_\mu^{\mathrm{HVP,\,LO}}$ results are large enough to bring the SM prediction of a_μ into agreement with experiment. The unfilled dark blue circles are lattice results that are older or superseded by more recent calculations. The red squares indicate results obtained from the data-driven methods reviewed in Sec. 2. See Table 8 for more information on the results included in the plot. Adapted from Ref. [443].